1970

Optimization and design of an axial flow turbine

Leslie Fielding
Lehigh University

OPTIMIZATION AND DESIGN OF AN AXIAL FLOW TURBINE

by

Leslie Fielding

A Thesis

Presented to the Graduate Faculty

of Lehigh University

in Candidacy for the Degree of

Master of Science

in

Mechanical Engineering

Lehigh University

1969

This thesis is accepted and approved in partial fulfillment of the requirements for the degree of Master of Science.

Sept 16 1969
date

Alan A Stevens
Professor-in-charge

Fredrick P. Keller
Chairman of Department

ACKNOWLEDGEMENTS

The author would like to thank Dr. Alan H. Stenning, Professor of Mechanical Engineering, for his helpful suggestions and constructive criticism during the writing of this thesis.

Thanks are also due to the Ingersoll-Rand Company for permission to publish the design and test data for a single stage turbine designed, by the author, in accordance with the methods described in this thesis.

TABLE OF CONTENTS

LIST OF FIGURES

LIST OF TABLES

All tables refer to design example.

Abstract

The basic problem in the aerodynamic design of an axial flow turbine is to obtain the maximum overall efficiency within the limitations imposed by stress, turbine matching, and economic considerations such as efficiency trade off versus number of stages.

To define exactly the flow conditions at all points in the flow field would require taking into account an extremely large number of variables in addition to solving the Navier Stokes equations for compressible, viscous, unsteady flow with turbulence. Any working method, therefore, must be a compromise between simplicity and accuracy.

In the optimization and design procedure the correlations of Ainley and Mathieson (Ref. 1) have been utilized, and since these correlations are based upon cascade mean flow path data, the method is essentially a mean diameter design procedure. The basic design procedure has been divided into three sequential steps, the first of which is the optimization and evaluation of the turbine major parameters with given limitations. After selection of major parameters the next step is the detailed thermodynamic calculation, the end result of which is the specifying of the temperature, pressure, velocity

and density throughout the flow field assuming a prescribed variation of peripheral velocity component with radius. The major simplifying assumption made, in addition to the usual boundary layer approximation that away from solid surfaces the flow is inviscid, is that in the solution of the Navier Stokes equation the flow may be considered to be the superimposition of two 2-dimensional solutions, i.e., the axisymmetrical flow solution and the blade to blade solution. The final step in the design procedure is the relating of the thermodynamic calculation to physical blade profiles in order to obtain the required amount of work.

The simplifying assumptions of this method have been found to greatly reduce the time required to design an axial flow turbine without incurring serious loss of accuracy. The accuracy, at the design point, that may be expected is in the order of $\pm$ 2% on efficiency and $\pm$ 3% on capacity.

In using the analysis of this report to predict part load operation, however, it has been found that while efficiency prediction remains reasonably good, the capacity prediction over estimates the flow by about 10% at quarter load. The probable reason for this is that at part load the

enthalpy and entropy gradients change such that the mean section is no longer an average representation of the flow conditions over the whole blade length.

In order to illustrate the use of the methods of this thesis, a design example is presented in Section 4. Since this example is of a turbine which has been built and tested, a comparison is made of the design prediction and test results.

SYMBOLS

A^1	Constant of integration
A	Area (ins^2)
A_n	Annulus Area (ins^2)
A_k	Leakage Area (ins^2)
A_t	Throat Area (ins^2)
$A_t{}^1$	Throat Area of row with zero tip clearance (ins^2)
a	Constant
B	Constant = .5 for row with radial tip clearance = .25 for row with shroud seal
C	Absolute velocity component (ft/sec)
C_B	Blade Chord (ft)
$\bar{C}$	Absolute velocity vector
C_m	Mean velocity (ft/sec)
C_L	Lift coefficient
C_{DS}	Secondary drag coefficient
C_{DK}	Leakage drag coefficient
c_1	Constant
c_2	Constant
C_p	Specific heat at constant pressure (Btu/lb/°F)
d	Diameter (ins)
D	Drag force (lb_f)

e	Blade Back Radius (ins)
$\bar{F}$	Force acting on gas particles by blade per unit Mass of time
F	Blade force (lb_f)
g	Acceleration of gravity (32.2 ft/sec^2)
g_c	Newton's Law Constant 32.2 (lbm/lbf) ft/sec^2
h	Enthalpy (Btu/lbm)
I.D.	Inside Diameter (ins)
i	Incidence (degrees)
i	Stalling incidence (degrees)
K_p	gJC_p
K	Blade Tip Clearance (ins)
k_1	Constant
k_2	Constant
L	Lift Force (lb_f)
M_n	Mach Number
N	RPM (revolutions/sec)
N_{Re}	Reynold's Number
O	Throat opening (ins)
O.D.	Outside diameter (ins)
P	Pressure (lb_f/ins^2)
R	Degree of reaction
R_G	Characteristic Gas Constant (ft.lbm/lb/°F)

R_c	Radius of Curvature (ft)
R_{hub}	Degree of reaction at hub diameter
r	Radius (ins)
S	Blade pitch (ins)
t_e	Trailing edge thickness (ins)
t_{max}	Blade maximum thickness (ins)
t	Time (seconds)
T	Temperature (°R)
U	Blade Speed (ft/sec)
W	Relative Blade Velocity (ft/sec)
W	Weight flow (lbm/sec)
X	Constant = .7 for row with shroud seal = 1.35 for row with radial tip clearance
$\bar{X}$	Radius Ratio
y_k	Leakage pressure loss coefficient
y_s	Secondary pressure loss coefficient
y_T	Total pressure loss coefficient
α	Absolute gas angles (degrees)
α^*	Stationary blade metal angle (degrees)
β	Relative gas metal angle (degrees)
β^*	Rotating blade metal angle
γ	Ratio of Specific Heats
η_T	Total to total turbine efficiency

η_s Total to static turbine efficiency

λ f (A_2, A, ID, OD)

μ Viscosity (lb_f/ft.sec.)

$\bar{\mu}$ f (C_L, S/C , Cos α_2 , Cos α_m)

ξ f (r_t, r_h, $K_p\Delta T$, U_m)

π Constant

ρ Density (lbm/ft^3)

σ Stress (lb_f/ins^2)

ϑ f (ξ, C_A, U_m)

ϕ Angle of streamline relative to axial direction

Ψ_A Aerodynamic load factor

Ω Angular velocity (radians/sec)

Subscripts

(a) Pressure, temperature, enthalpy

01	Total into stator
02	Total out of stator
02	Total relative to rotor inlet
03	Total relative to rotor outlet
03	Total absolute out of rotor
1	Static at stator inlet
2	Static at stator outlet
3	Static at rotor outlet

(b) Velocity diagrams

1	Inlet to stator
2	Outlet from stator, inlet to rotor
3	Outlet from rotor
M	Mean velocity component
θ	Tangential direction
θ_2	Tangential direction at outlet from stator
θ_3	Tangential direction at outlet from rotor
A	Axial
A_2	Axial at stator outlet
A_3	Axial at rotor outlet

(c) General

a	Axial
DP	Design Point
h	Hub
i	Inside
k	Leakage
M	Mean
O	Outside
t	Tip
1	Stator upstream station
2	Stator downstream, rotor upstream station
3	Rotor downstream station

INTRODUCTION

The purpose of this report is to present a complete method for the thermodynamic design of an axial flow turbine.

Today there are a multitude of text books and technical papers available which cover most completely the present state of the science and art of turbine design, and it is not proposed here to evaluate the advantages or disadvantages of any particular method. This paper rather gives a design method which the writer has found will permit the reliable prediction of capacity, efficiency, and part load operation of an axial flow turbine.

The basis of the thermodynamic design method is the Ainley and Mathieson report (1). This report does not use different relationships for rotating and stationary rows, and this simplification must involve errors since the flow in a rotating cascade is fundamentally different from that in a stationary cascade. As pointed out in the Ainley report in order to predict exactly the flow conditions at all points in the flow field, an exceedingly large number of variables would have to be taken into account.

In order to achieve a measure of simplicity the number of variables must be reduced to a minimum, and any working

method must be a compromise between simplicity and accuracy. A further major simplification throughout the treatment by Ainley is the one of considering the flow path through each stage at one diameter only. The reference diameter selected is the arithmetic mean of the rotor and stator inner and outer diameters. In adopting this procedure it is assumed that in any cross sectional plane of flow between adjacent rows the total pressure, temperature, and axial velocity are equal at all points in the flow field. In general this is far from the truth, however, the correct overall stage characteristics may be predicted if the efflux angles and pressure loss coefficients at the reference sections are equal to the mean values over the entire cross section. The accuracy of the performance calculations rests entirely upon the accuracy with which these values can be estimated. The correlations of Ainley and Mathieson do not permit the estimation of pressure loss coefficient for blades with negative inlet angles, and although negative blade angles may be expected at the blade tips, of a row with a high reaction mean section, since the overall blade loss is related to the mean section this should not present a problem. The estimation of optimum space chord ratio for tip sections

with negative inlet angles has been obtained by extrapolation of the correlations of Ainley and Mathieson with the aid of data from Traupel (2).

The methods of this thesis have been found to give accurate predictions for a large number of unchoked turbines of different sizes and horsepowers.

1. SELECTION OF PARAMETERS

The basic problem in the design of a turbine is to obtain the overall maximum efficiency within the limitations imposed by the matching of the turbine characteristics and stress. Turbines may be divided into two broad categories, one being the aircraft type turbine, the other being the industrial type turbine. The main differences between these two types are turbine inlet temperature, and last stage leaving conditions. In general aero engines tend to have higher turbine inlet temperatures in order to reduce size and weight, whereas in an industrial turbine these considerations are of less importance than blade life. Regarding last stage leaving conditions, the axial leaving velocity from the blading of an aircraft turbine is usually higher than that of an industrial type turbine. In the aircraft turbine further expansion takes place in the propelling nozzle after the fluid leaves the last blade row, however, in an industrial turbine the leaving velocity is lost except for that portion of kinetic energy recovered in the exhaust diffuser.

Approximate rules are required for the design of the most efficient turbines, with given limitations, so that the number of designs to be investigated are reduced to a minimum. This section of the paper outlines the principal factors affecting efficiency and puts forward a method of assessing it.

1.1 Blade Efficiency and Shaft Efficiency

Shaft efficiency is the efficiency based upon the horsepower delivered to the turbine shaft, and is the efficiency used in overall performance calculations. Blading efficiency is defined as the stage efficiency which would be measured in a fully shrouded and sealed turbine, and reflects only the profile and secondary losses. The difference between these two efficiencies is due to blade tip leakage, cooling air interference and other matters of a detail design nature, the effects of which can be minimized by careful design. The purpose of the distinction is to define an efficiency which is determined by the turbine design calculations alone and which can be attained, or very nearly so, if sufficient

care is taken in the detail design stage. This difference is very real and may be as much as 5%.

1.2 Work Parameter and Flow Coefficient

Referring to figure 1.1, Euler's equation may be written as follows:

$$\Delta h_o = \frac{1}{g_c J}\left[U_2 C_{\theta 2} - U_3 C_{\theta 3}\right]$$

or $$g_c J \Delta h_o = U_2 C_{\theta 2} - U_3 C_{\theta 3} \qquad \text{——— 1.1}$$

Now if $U_2 = U_3 = U$

Then $$g_c \frac{J \Delta h_o}{U} = C_{\theta 2} - C_{\theta 3} \qquad \text{——— 1.2}$$

Referring again to figure 1.1

$$\left.\begin{aligned} C_{\theta 2} &= C_{A_2} TAN\, \alpha_2 \\ C_{\theta 3} &= C_{A 3} TAN\, \alpha_3 \end{aligned}\right\} \qquad \text{——— 1.3}$$

$$\left.\begin{aligned} W_{\theta 2} &= C_{A_2} TAN\, \beta_2 \\ W_{\theta 3} &= C_{A 3} TAN\, \beta_3 \end{aligned}\right\} \qquad \text{——— 1.4}$$

Substituting (1.3) and (1.4) in (1.2), we get,

$$\frac{g_c J \Delta h_o}{U} = C_{A2} TAN\alpha_2 - C_{A3} TAN\alpha_3$$

in terms of absolute gas angles.

and

$$\frac{g_c J \Delta h_o}{U} = C_{A2} TAN\beta_2 - C_{A3} TAN\beta_3$$

in terms of relative gas angles.

if we now assume that $C_{A2} = C_{A3} = C_A$

Then
$$\left.\begin{aligned} \frac{g_c J \Delta h_o}{U} &= C_A \left[TAN\alpha_2 - TAN\alpha_3\right] \\ &= C_A \left[TAN\beta_2 - TAN\beta_3\right] \end{aligned}\right\} \quad 1.5$$

Dividing both sides by U in order to make the above equation dimensionless, we get

$$\left.\begin{aligned} \frac{g_c J \Delta h_o}{U^2} &= \frac{C_A}{U} \left[TAN\alpha_2 - TAN\alpha_3\right] \\ &= \frac{C_A}{U} \left[TAN\beta_2 - TAN\beta_3\right] \end{aligned}\right\} \quad 1.6$$

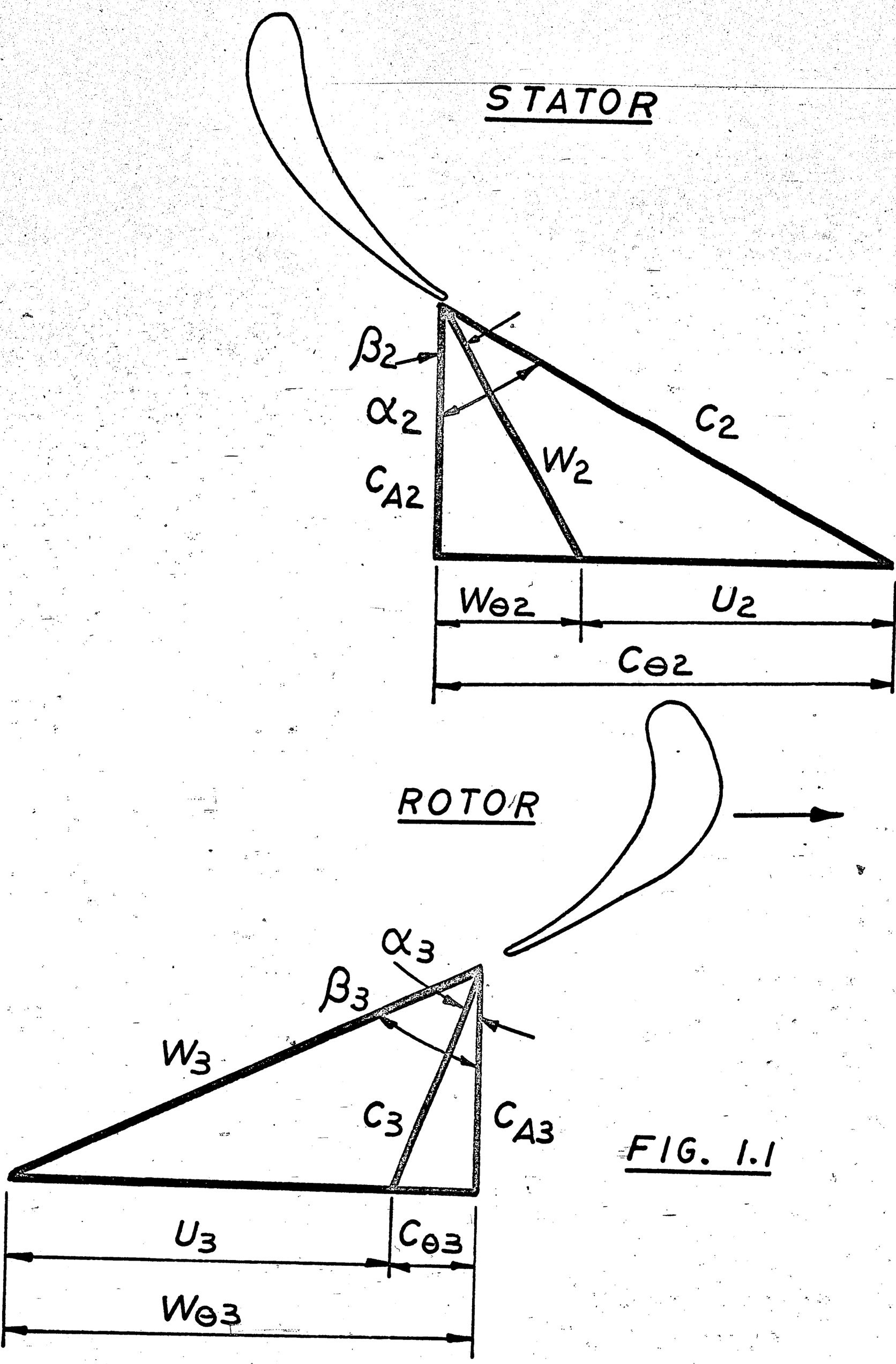
STATOR
β_2
α_2
c_{A2}
W_2
c_2
$W_{\theta 2}$
U_2
$c_{\theta 2}$
ROTOR
α_3
β_3
W_3
c_3
c_{A3}
U_3
$c_{\theta 3}$
$W_{\theta 3}$

FIG. 1.1

Let $K_p = g_c J C_p$, and equation (1.6) may be written

$$\frac{K_p \Delta T}{U^2} = \left.\begin{array}{l} \frac{C_A}{U}\left[TAN\alpha_2 - TAN\alpha_3\right] \\ \frac{C_A}{U}\left[TAN\beta_2 - TAN\beta_3\right] \end{array}\right\} \quad 1.7$$

In equation (1.7) $\frac{K_p \Delta T}{U^2}$ is defined as the <u>work parameter</u> and $\frac{C_A}{U}$ as the <u>flow coefficient</u>. Examination of this equation shows that the work parameter is a function of flow coefficient and blade geometry. Further, it may be shown that a condition such as 50% reaction or zero exit swirl is sufficient to determine blade geometry for a given value of work parameter and flow coefficient. In order to determine efficiency for a given configuration then, it is only necessary to specify the above conditions. Initially an attempt was made to obtain a correlation between efficiency and blade geometry, for a given value of work parameter and flow coefficient, by assuming blade geometry could be defined by deflection only (i.e. $\alpha_1 - \alpha_2$ OR $\beta_2 - \beta_3$). It was subsequently found, however, that this is only possible

if the inlet area to the row is large compared with the outlet area. (i.e. far away from impulse).

Figure 1.2 is a cross plot of data from the Ainley and Mathieson report. Examination of this curve shows that below an area ratio about 1.5 the profile loss coefficient increases sharply, and it is no longer permissible to assume that deflection alone determines its magnitude. For preliminary estimates of the variation of efficiency with work parameter and flow coefficient the following cases were found sufficient to enable a reasonable estimate to be made prior to a detail design.

(1) First stage, axial inlet, 50% reaction.

(2) Internal stage, $\alpha_1 = \beta_2$, 50% reaction.

(3) Last stage, $\alpha_1 = 20^\circ$, $\alpha_3 = 0$

(4) Single stage $\alpha_1 = \alpha_3 = 0$

For the first two cases only the total to total efficiency was calculated, for the last two cases total to total and total to static efficiencies were calculated.

FIGURE 1·2

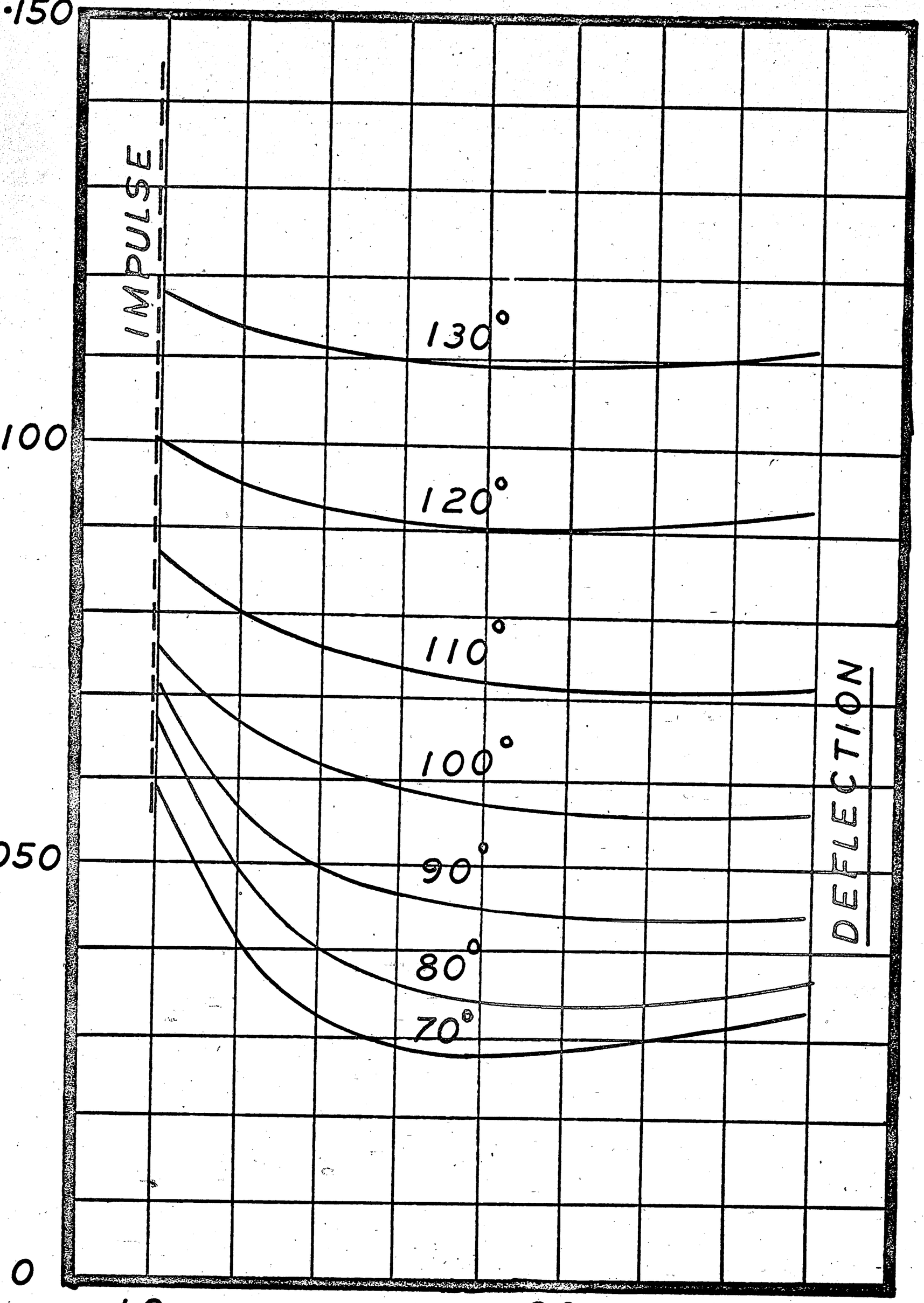
·150
·100
·050
0
PROFILE LOSS COEFFICIENT Y_P
IMPULSE
130°
120°
110°
100°
90°
80°
70°
DEFLECTION
1·0
2·0
AREA RATIO

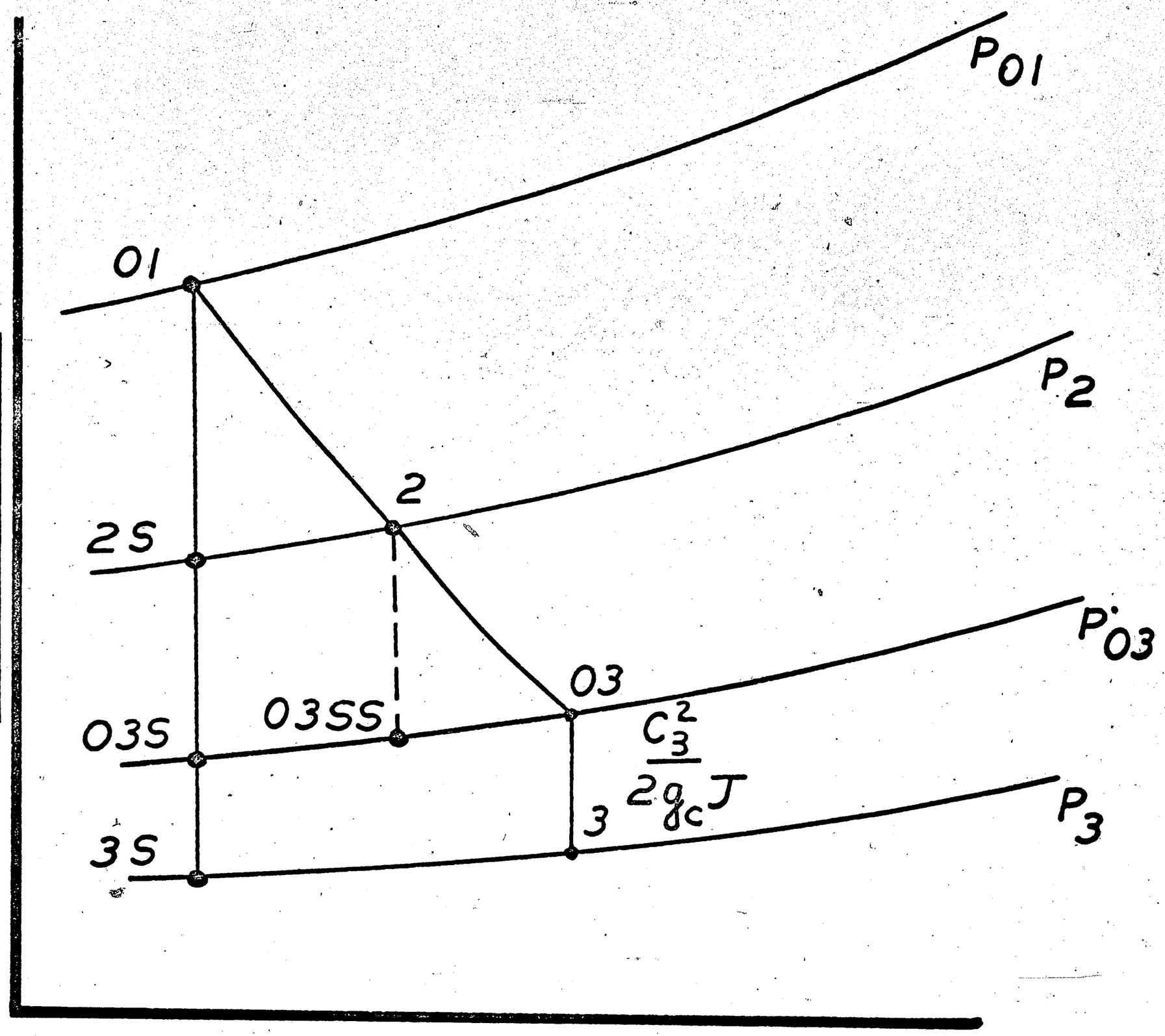

FIG. 1.3

Referring to figure 1.3 the total to total efficiency is defined as follows:

$$\eta_T = \frac{h_{01} - h_{03}}{h_{01} - h_{03S}}$$

For the last stage of a multistage turbine, or a single stage turbine, much of the kinetic energy is not recoverable and there is an additional enthalpy loss. If no exit diffuser is used then the loss is equal to

$$\frac{C_3^2}{2 g_c J}$$

Defining the total to static efficiency as the ratio of actual turbine work to the work that would be obtained from an isentropic expansion from P_{01} to P_3 with zero kinetic energy at 3

$$\eta_s = \frac{h_{01} - h_{03}}{h_{01} - h_{3s}}$$

If we assume a perfect gas the above equation becomes

$$\eta_s = \frac{T_{01} - T_{03}}{T_{01} - T_{3s}}$$

$$= \frac{1 - \frac{T_{03}}{T_{01}}}{1 - \frac{T_{3s}}{T_{01}}}$$

$$\eta_S = \frac{1 - \frac{T_{03}}{T_{01}}}{1 - \left(\frac{P_3}{P_{01}}\right)^{\frac{\gamma-1}{\gamma}}} \qquad 1.8$$

Similarly

$$\eta_T = \frac{1 - \frac{T_{03}}{T_{01}}}{1 - \left(\frac{P_{03}}{P_{01}}\right)^{\frac{\gamma-1}{\gamma}}} \qquad 1.9$$

A computer program was written to perform the above calculations, which includes the following assumptions.

(1) Profile and secondary losses are those taken from the Ainley and Mathieson report.

(2) Blades are fully shrouded and sealed.

(3) Blades are at the optimum space/chord ratio.

(4) $\gamma = 1.350$

(5) Hub/tip ratio = .75

(6) Area Ratio = $\frac{\cos\alpha_3}{\cos\alpha_2} = \frac{\cos\beta_3}{\cos\beta_2}$

(7) $C_{A2} = C_{A3} = C_A$

(8) $t_e/S = .02$

(9) $t/C = .2$

With the above assumptions it is considered that the results obtained are sufficient to enable the best velocity triangles to be drawn for optimum heat drop distribution. For reasons explained in Section 1.1 the efficiencies calculated are blading efficiencies and corrections have to be made for leakage losses and cooling air interference, etc. Curves of total and static efficiencies have been plotted, the examination of which permits the following general observations.

(1) In the first and internal stages of a multistage turbine the efficiency will be maximum when the flow coefficient lies between .6 and .9. The optimum value within this range is a function of work coefficient.

(2) In the last stage of a multistage turbine or in a single stage turbine, if the exit

kinetic energy is utilized, such as in the propelling nozzle of an aircraft engine, then a value of flow coefficient which lies between .6 and .9 is desirable. The optimum value within this range is a function of work coefficient. However, in an industrial turbine the value of flow coefficient should not be greater than .5 for a high efficiency turbine, since the kinetic energy of the leaving velocity is lost except for that portion recovered in the exhaust diffuser. Further, the curves enable the formulation of a set of design rules for high efficiency turbines as follows:-

Design Rules

Rule 1

For the first stage of a multistage turbine,

$$2{\cdot}0 \geqslant \frac{K_p \Delta T}{U^2} \geqslant 1{\cdot}0$$

$$0{\cdot}9 \geqslant \frac{C_A}{U} \geqslant 0{\cdot}6$$

Rule 2

For the internal stages of a multistage turbine,

$$1.6 \geqslant \frac{K_p \Delta T}{U^2} \geqslant 1.0$$

$$0.9 \geqslant \frac{C_A}{U} \geqslant 0.6$$

Rule 3

For the last stage of a multistage turbine, or a single stage turbine,

$$1.5 \geqslant \frac{K_p \Delta T}{U^2} \geqslant 1.0$$

$\frac{C_A}{U}$ should lie between 0.9 and 0.6 in turbines where the exhaust velocity is utilized, but in industrial turbines where the exhaust velocity is lost $\frac{C_A}{U}$ should be made as small as possible, and for high efficiency should not exceed 0.5.

FIGURE 1.4

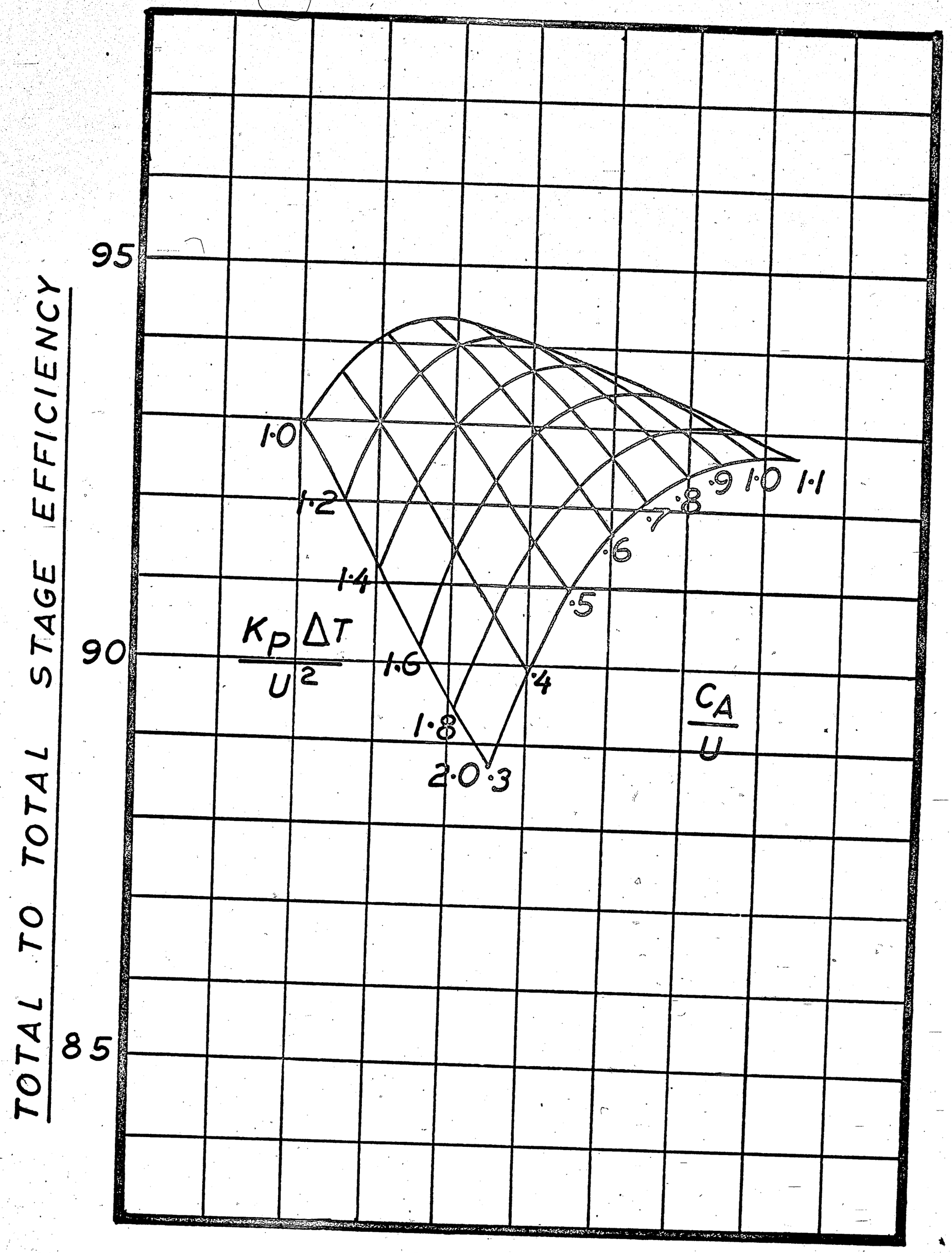

FIRST STAGE — AXIAL INLET
50% REACTION

FIGURE 1·5

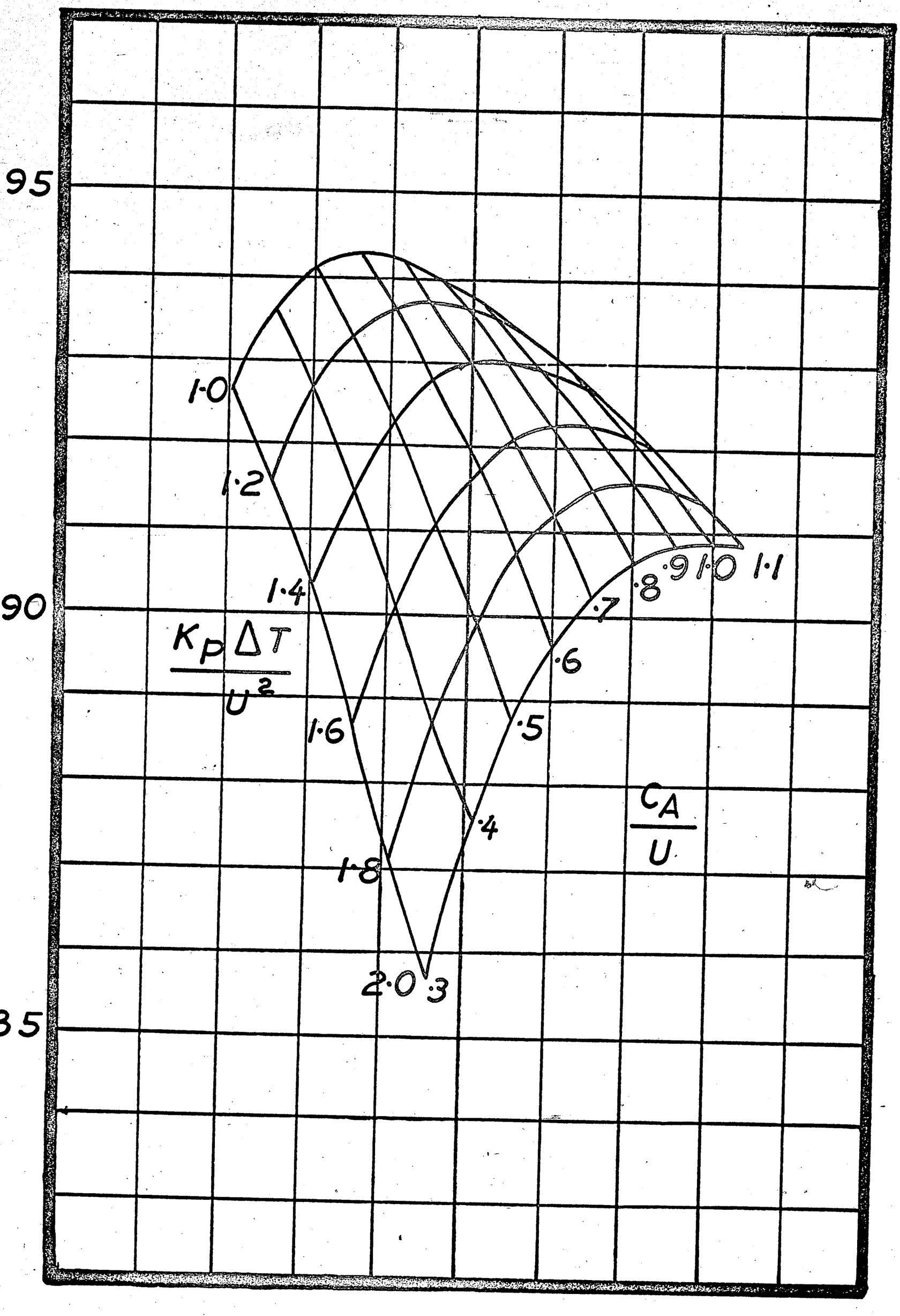

INTERNAL STAGE $\alpha_1 = \beta_2$ — 50% REACTION

FIGURE 1·6

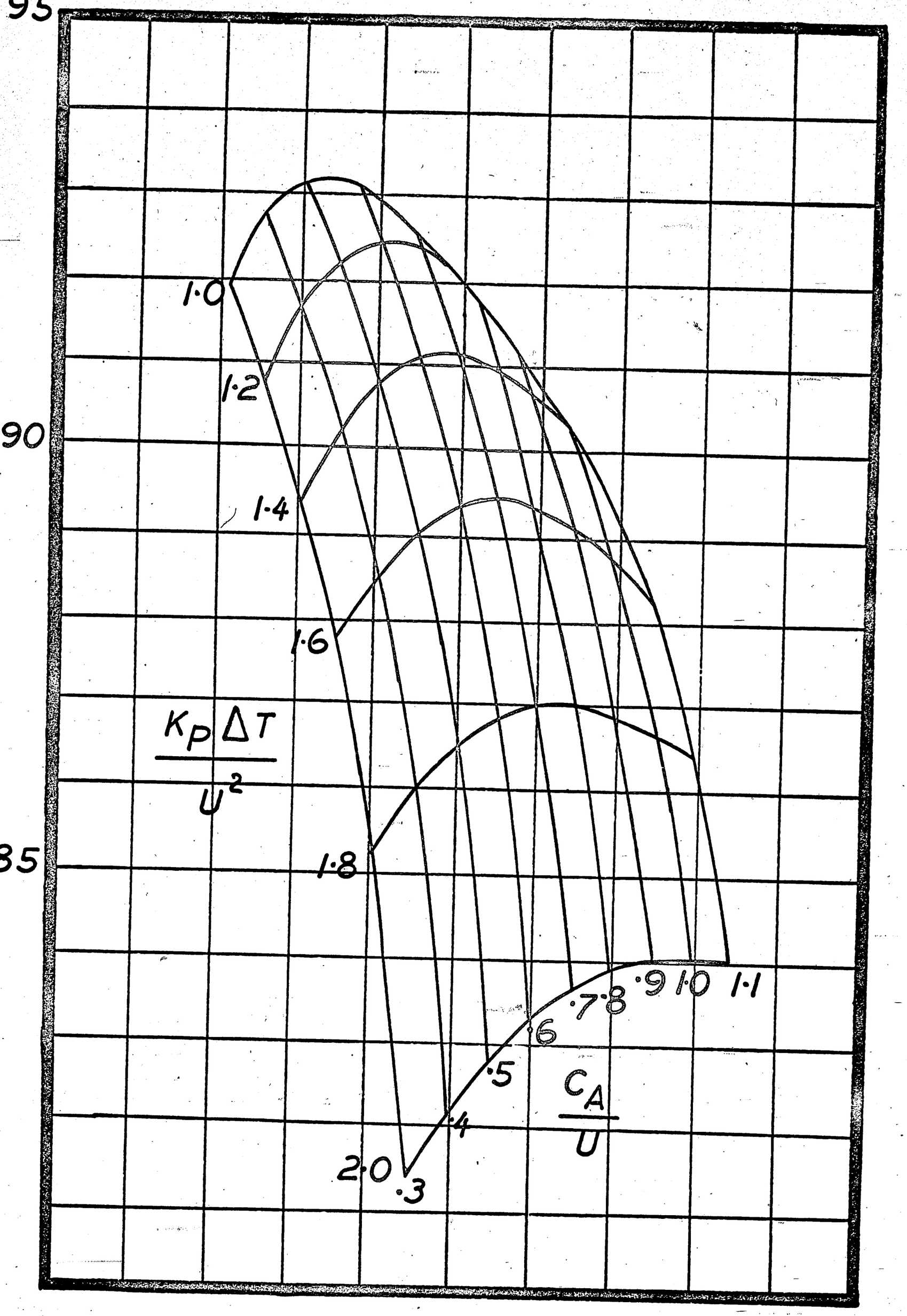

LAST STAGE $\alpha_1 = 20^\circ$, $\alpha_3 = 0$

FIGURE 1·7

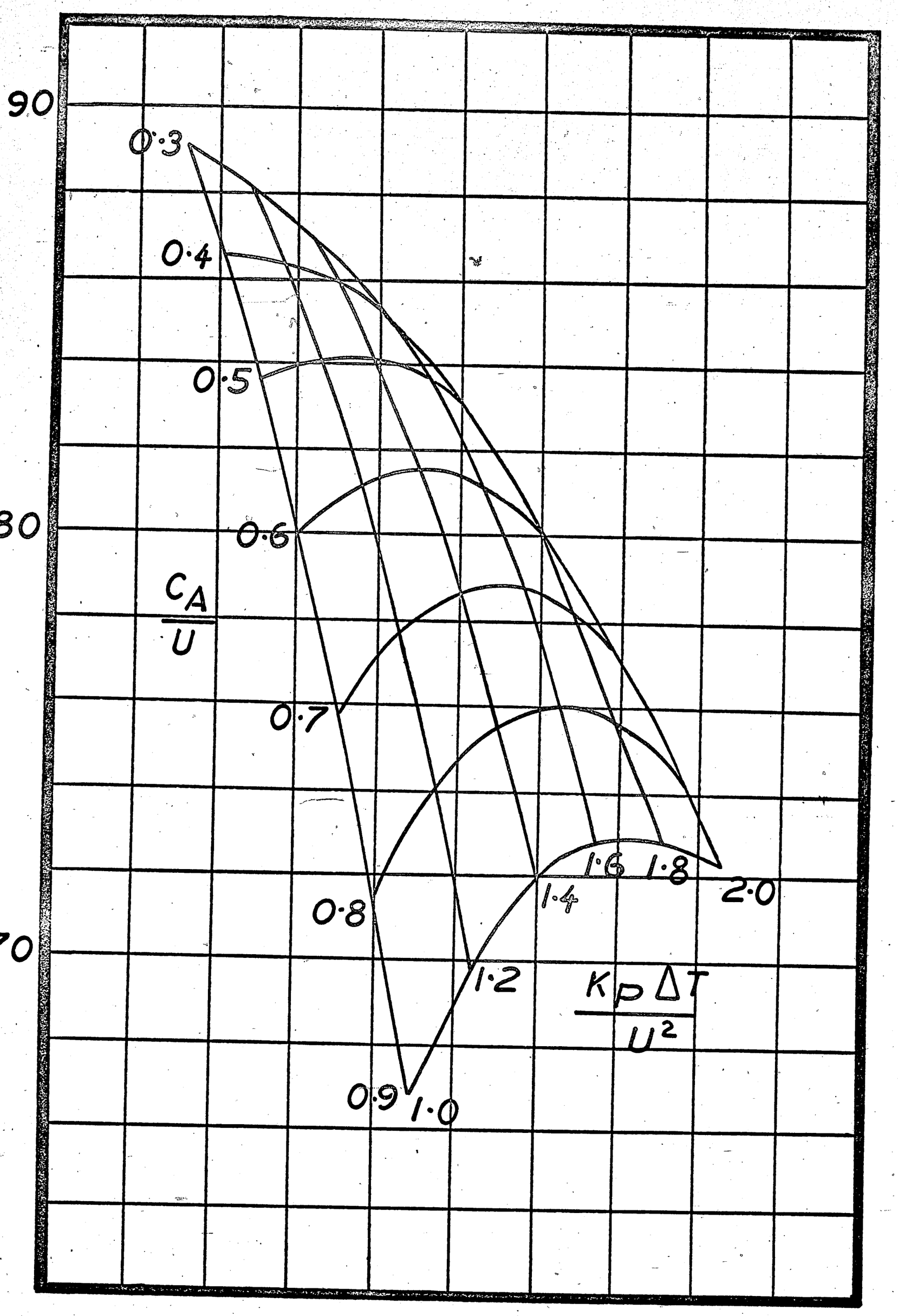

LAST STAGE $\alpha_1 = 20^\circ, \alpha_2 = 0$

FIGURE 1·8

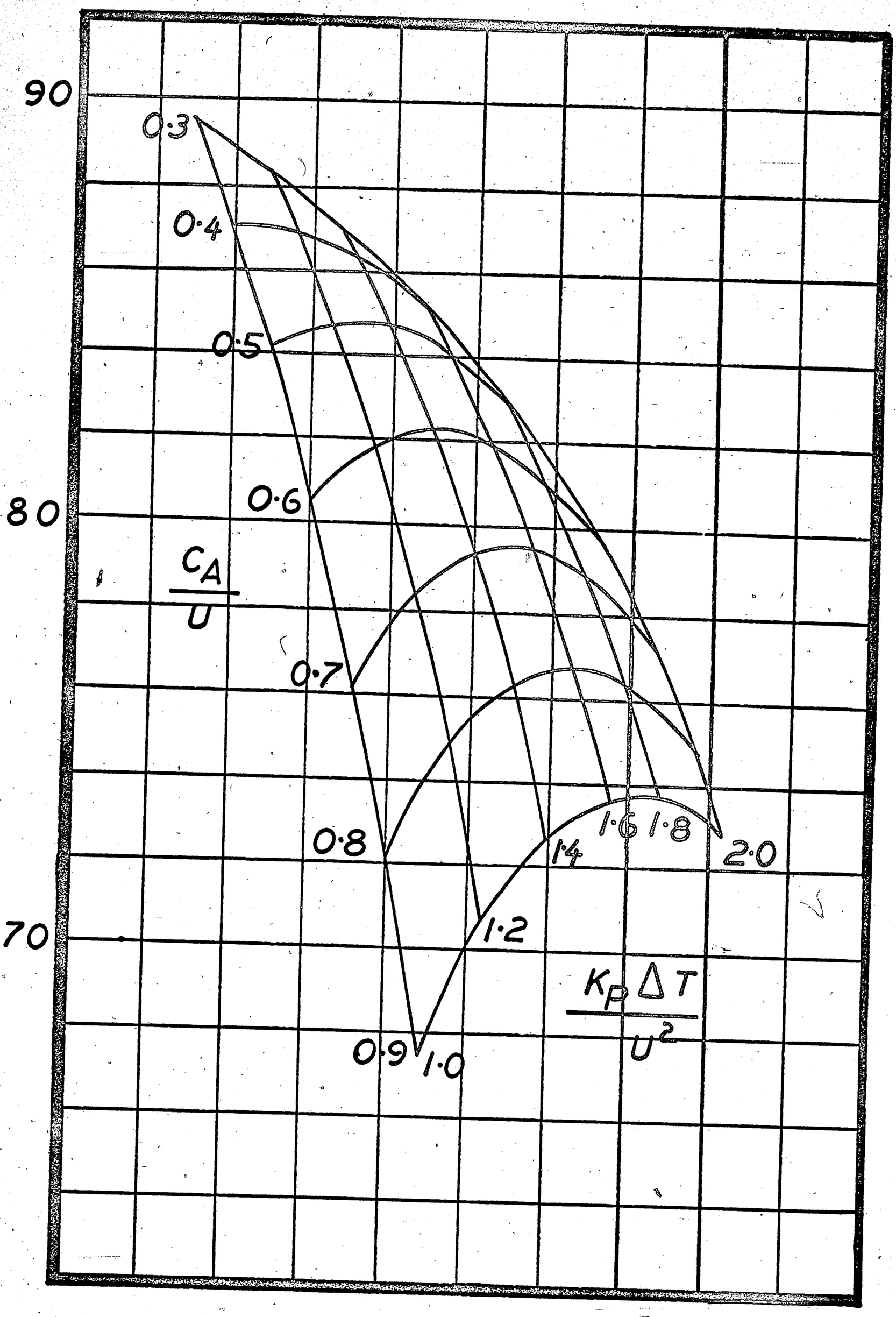

SINGLE STAGE $\alpha_1 = \alpha_3 = 0$

FIGURE 1·9

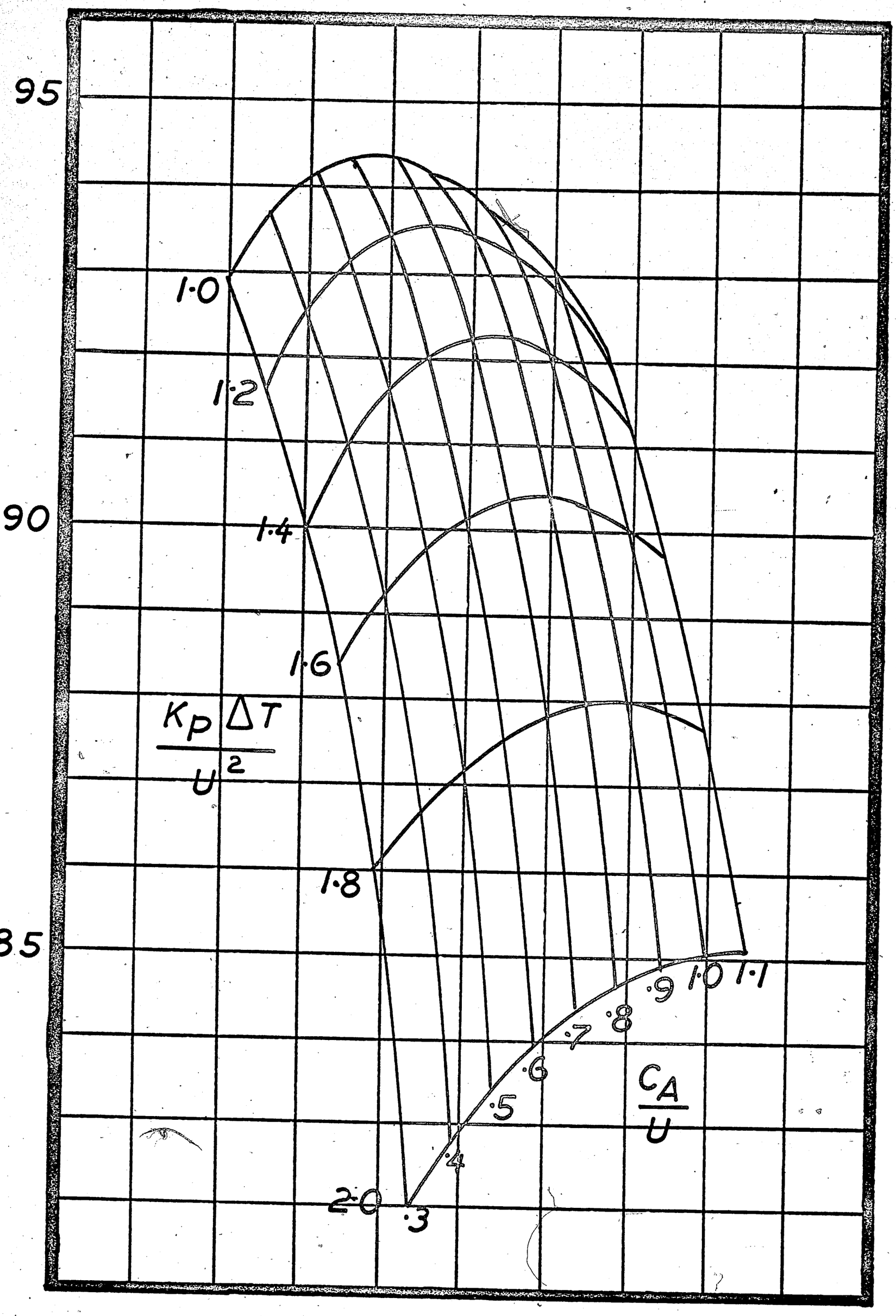

SINGLE STAGE $\alpha_1 = \alpha_3 = 0$

1.3 Degree of Reaction

Degree of reaction is defined as follows:

$$R = \frac{h_2 - h_3}{h_{o2} - h_{o3}} \qquad \text{---------- 1.10}$$

Now

$$\left.\begin{aligned} h_{o2r} &= h_2 + \frac{W_2^2}{2 g_c J} \\ &= h_{o3r} \\ &= h_3 + \frac{W_3^2}{2 g_c J} \end{aligned}\right\} \qquad \text{---------- 1.11}$$

From (1.11) it follows that:

$$h_2 - h_3 = \frac{W_3^2 - W_2^2}{2 g_c J} \qquad \text{---------- 1.12}$$

Substituting (1.12) in equation (1.10), we get:

$$R = \frac{\dfrac{W_3^2 - W_2^2}{2 g_c J}}{h_{o2} - h_{o3}} \qquad \text{---------- 1.13}$$

Now $$h_{o2} - h_{o3} = \frac{U \Delta C_\theta}{g_c J}$$

$$= \frac{U(C_{\theta 2} - C_{\theta 3})}{g_c J} \qquad \text{---------- 1.14}$$

Substituting (1.14) into equation (1.13), we get:

$$R = \frac{1}{2} \cdot \frac{W_3^2 - W_2^2}{U(C_{\theta 2} - C_{\theta 3})} \qquad \text{---------- 1.15}$$

Now from figure 1.1 it can be seen that:

$$\left.\begin{aligned} C_{\theta 2} &= W_{\theta 2} + U \\ C_{\theta 3} &= W_{\theta 3} + U \\ W_3^2 &= W_{\theta 3}^2 + C_{A3}^2 \\ W_2^2 &= W_{\theta 2}^2 + C_{A2}^2 \end{aligned}\right\} \qquad \text{---------- 1.16}$$

Substituting equation (1.16) into (1.15), and assuming $C_{A3} = C_{A2}$

$$R = -\frac{1}{2} \frac{(W_{\theta 3} + W_{\theta 2})}{U} \qquad \text{---------- 1.17}$$

Examination of figure 1.2 shows that the most efficient turbines are those with a high degree of reaction, and as a

general rule 50% reaction, at the mean section should be aimed at on all designs. Although it theoretically is possible to obtain higher efficiencies by increasing the mean section reaction beyond 50%, in practice this presents stressing problems, particularly in high temperature turbines where minimum stress requirements demand high taper ratios i.e., maximum blade root section area and minimum blade tip section area. In applying the recommended radial equilibrium of section 2.3 it will be seen that the degree of reaction varies along the blade length. The limitations on degree of reaction are 100% reaction and zero reaction, and because of reaction variation with blade length it may not be possible, in all cases, to obtain 50% reaction at the mean section. The limitations imposed by reaction variation with blade length are discussed in section 1.4. Returning to the mean section design, two cases will now be considered, as follows:

(1) <u>50% Reaction Design</u>

From examination of Figure 1.1 it can be seen that:

$$W_{\theta 2} = C_{\theta 2} - U$$
$$W_{\theta 3} = C_{\theta 3} - U \qquad \text{---------- 1.18}$$

Substituting equation (1.18) in equation (1.17), we get:

$$R = \left| - \frac{1}{2} \frac{C_{\theta 2} + C_{\theta 3}}{U} \right| \qquad \text{---------- 1.19}$$

Now

$$C_{\theta 2} = C_A \, TAN \, \alpha_2$$
$$C_{\theta 3} = C_A \, TAN \, \alpha_3 \qquad \text{---------- 1.20}$$

Substituting equation (1.20) in (1.19), we get:

$$R = \left| - \frac{1}{2} \frac{C_A}{U} \left(TAN \, \alpha_2 + TAN \, \alpha_3 \right) \right| \qquad \text{---------- 1.21}$$

Referring again to Figure 1.1

$$\left.\begin{aligned} \frac{C_A}{U} &= \frac{1}{TAN\alpha_2 - TAN\beta_2} \\ &= \frac{1}{TAN\alpha_3 - TAN\beta_3} \end{aligned}\right\} \quad 1.22$$

Substituting equation (1.22) in (1.21), we get:

$$\left.\begin{aligned} R &= 1 - \frac{1}{2}\,\frac{TAN\alpha_2 + TAN\alpha_3}{TAN\alpha_2 - TAN\beta_2} \\ &= 1 - \frac{1}{2}\,\frac{TAN\alpha_2 + TAN\alpha_3}{TAN\alpha_3 - TAN\beta_3} \end{aligned}\right\} \quad 1.23$$

Now for 50% reaction, i.e, R = .5, equation (1.23) gives:

$$TAN\alpha_2 - TAN\beta_2 = TAN\alpha_2 + TAN\alpha_3$$

$$I.E. \quad \beta_2 = -\alpha_3 \qquad 1.24$$

$$TAN\alpha_3 - TAN\beta_3 = TAN\alpha_2 + TAN\alpha_3$$

$$I.E. \quad -\beta_3 = \alpha_2 \qquad 1.25$$

(2) Zero Exit Swirl Design

The zero exit swirl design is important since the condition of zero exit swirl is desirable for the

last stage of a multistage turbine, or a single stage turbine,

Now for zero exit swirl, $C_{\theta 3} = 0$

From equation (1.2), $$\frac{K_p \Delta T}{U} = \Delta C_\theta$$

or $$\frac{K_p \Delta T}{U^2} = \frac{\Delta C_\theta}{U}$$

and since $C_{\theta 3} = 0$

$$\frac{K_p \Delta T}{U^2} = \frac{C_{\theta 2}}{U} \qquad 1.26$$

From equation (1.19), for $C_{\theta 3} = 0$

$$R = 1 - \frac{1}{2} \frac{C_{\theta 2}}{U} \qquad 1.27$$

Substituting (1.26) into (1.27)

$$R = 1 - \frac{1}{2} \frac{K_p \Delta T}{U^2} \qquad 1.28$$

Examination of equation (1.28) reveals the following:

(a) A 50% reaction design can only be obtained for a value of $\frac{K_P \Delta T}{U^2} = 1.0$

(b) The value of $\frac{K_P \Delta T}{U^2}$ varies linearly with reaction from a value of two at zero reaction, to zero at 100% reaction.

(c) The maximum value of work parameter that can be used is two. To increase the work parameter above two requires the introduction of exit swirl if the condition of rotor diffusion is to be avoided.

1.4 Minimum Permissible Hub/Tip Ratio

At the preliminary design stage it is important to know what restrictions, if any, hub/tip ratio will impose upon a selected design. In accordance with the comments made in section 1.3 relating to mean section design, three cases will be considered, as follows:

(a) 50% reaction mean section design.

(b) Impulse root design.

(c) Zero exit swirl design.

In the following analysis simple radial equilibrium will be assumed. Although the application of the simplified radial equilibrium equation may not give an exact solution to the particular design under consideration, it is sufficiently accurate to enable the limiting hub/tip ratio to be determined at the preliminary design stage.

In section 2.3 it is shown that if in a turbine stage the tangential velocity distribution behind the stator and rotor row are both free vortex, then

$$\left.\begin{aligned} r\,C_{\theta 2} &= \text{constant} \\ r\,C_{\theta 3} &= \text{constant} \end{aligned}\right\} \qquad 1.29$$

Further, if the enthalpy drop and entropy increase are constant at all radii then a complete solution to the flow is as follows:

$$C_{A2} = \text{CONSTANT}\ , \quad C_{\theta 2} = \frac{K_2}{r}$$

$$C_{A3} = \text{CONSTANT}\ , \quad C_{\theta 3} = \frac{K_3}{r}$$

$$TAN\alpha_2 = \frac{K_2}{rC_{A2}} \quad , \quad TAN\beta_2 = \frac{K_2}{rC_{A_2}} - \frac{\Omega r}{C_{A2}}$$

$$TAN\alpha_3 = \frac{K_3}{rC_{A3}} \quad , \quad TAN\beta_3 = \frac{K_3}{rC_{A3}} - \frac{\Omega r}{C_{A3}} \qquad \} \; 1.30$$

Where K_2 and K_3 are constants determined from the mean section design.

Now from equation (1.19)

$$R = | - \frac{1}{2} \frac{C_{\theta 3} + C_{\theta 2}}{U}$$

Substituting $C_{\theta 2}$ and $C_{\theta 3}$ from equation (1.30), we get,

$$R = | - \frac{1}{2U}\left[\frac{K_2}{r} + \frac{K_3}{r} \right]$$

and if $U = \Omega r$

$$R = | - \frac{1}{2\Omega}\left[\frac{K_2 + K_3}{r^2} \right] \qquad 1.31$$

The limit on permissible hub/tip ratio is assumed to be impulse root, since high losses result from recompression in the rotor. Thus if the reaction at the root r_h is zero,

$$\frac{1}{2\Omega}\left[\frac{K_2 + K_3}{r_h^2} \right] = | \qquad 1.32$$

Substituting equation (1.32) into (1.31) we find that the reaction at any radius r is given by,

$$R = 1 - \frac{r_h^2}{r^2} \qquad 1.33$$

For cases (a) and (b) the application of equation (1.33) gives the following results:

(a) 50% reaction mean section design

Let r_m = mean radius.

r_t = tip radius.

r_h = root radius.

Then

$$r_m = \frac{r_h + r_t}{2} \qquad 1.34$$

Now substituting equation (1.34) into (1.33), we get

$$\frac{r_h}{r_t} = \frac{1}{2\sqrt{2}-1} \simeq .55 \qquad 1.35$$

Therefore for 50% reaction at the mean section the limiting hub/tip ratio is .55 independent of all other considerations.

(b) Impulse root radius design.

The radius where the reaction is 50%, for impulse root design, is given by substituting equation (1.34) into (1.33) as follows:

$$\frac{r_h}{r_t} = \frac{1}{\sqrt{2}} \simeq .707 \qquad 1.36$$

Therefore in a machine with a hub/tip ratio of less than .707, if impulse root conditions are selected, the reaction will exceed 50% towards the tip.

(c) Zero exit swirl design.

From equation (1.27)

$$R = | - \frac{1}{2} \frac{C_{\theta 2}}{U}$$

Substituting $C_{\theta 2}$ from equation (1.30), the flow solution for simple radial equilibrium, we get

$$R = | - \frac{1}{2} \frac{K_2}{r^2 \Omega} \qquad 1.37$$

Where $U = \Omega r$, and $C_{\theta 3} = 0$ (i.e. zero exit swirl)

Now for impulse root conditions,

$$\frac{K_2}{2\Omega r_h^2} = 1 \qquad \text{1.38}$$

Substituting (1.38) into (1.37), we get

$$R = 1 - \frac{r_h^2}{r^2} \qquad \text{1.39}$$

This equation is identical to equation (1.33), and could have been anticipated.

Now from equation (1.28)

$$R = 1 - \frac{1}{2}\frac{K_p \Delta T}{U^2} \qquad \text{1.28}$$

If U_m is the mean section blade speed, then equating equations (1.28) and (1.39), we get

$$\frac{K_p \Delta T}{U_m^2} = \frac{2 r_h^2}{r_m^2} \qquad \text{1.40}$$

and since

$$r_m = \frac{r_h + r_t}{2}$$

equation (1.40) becomes

$$\frac{K_p \Delta T}{U_m^2} = \frac{8\left[\frac{r_h}{r_t}\right]^2}{\left[\frac{r_h}{r_t} + 1\right]^2} \qquad \text{1.41}$$

Equation (1.41) gives the condition for a zero exit swirl design with impulse root. To obtain rotor root convergence the left hand side of the equation must always be less than the right hand side. Because of the importance of determining the limiting hub/tip ratio at the preliminary design stage, equation (1.41) has been plotted on Figure 1.10 to enable rapid assessment of root condition.

1.5 Minimum Exit Mach Number and Effect of Reynolds Number

In general for high area ratio passages low entry Mach numbers will be inevitable. For high efficiency subsonic turbines .5 should be considered as the minimum permissible exit Mach number from a row since below this value losses increase rapidly. Mach number and Reynolds number are considered here together since part of the reason for avoiding low Mach numbers is the accompanying low Reynolds number. Based on blade chord length the minimum permissible Reynolds number for high efficiency turbines is considered to be 10^5. Ainley suggests that the losses in a turbine vary as the ratio

$$\left[\frac{2\times10^5}{N_{RE}}\right]^{\frac{1}{5}}$$

FIGURE 1.10

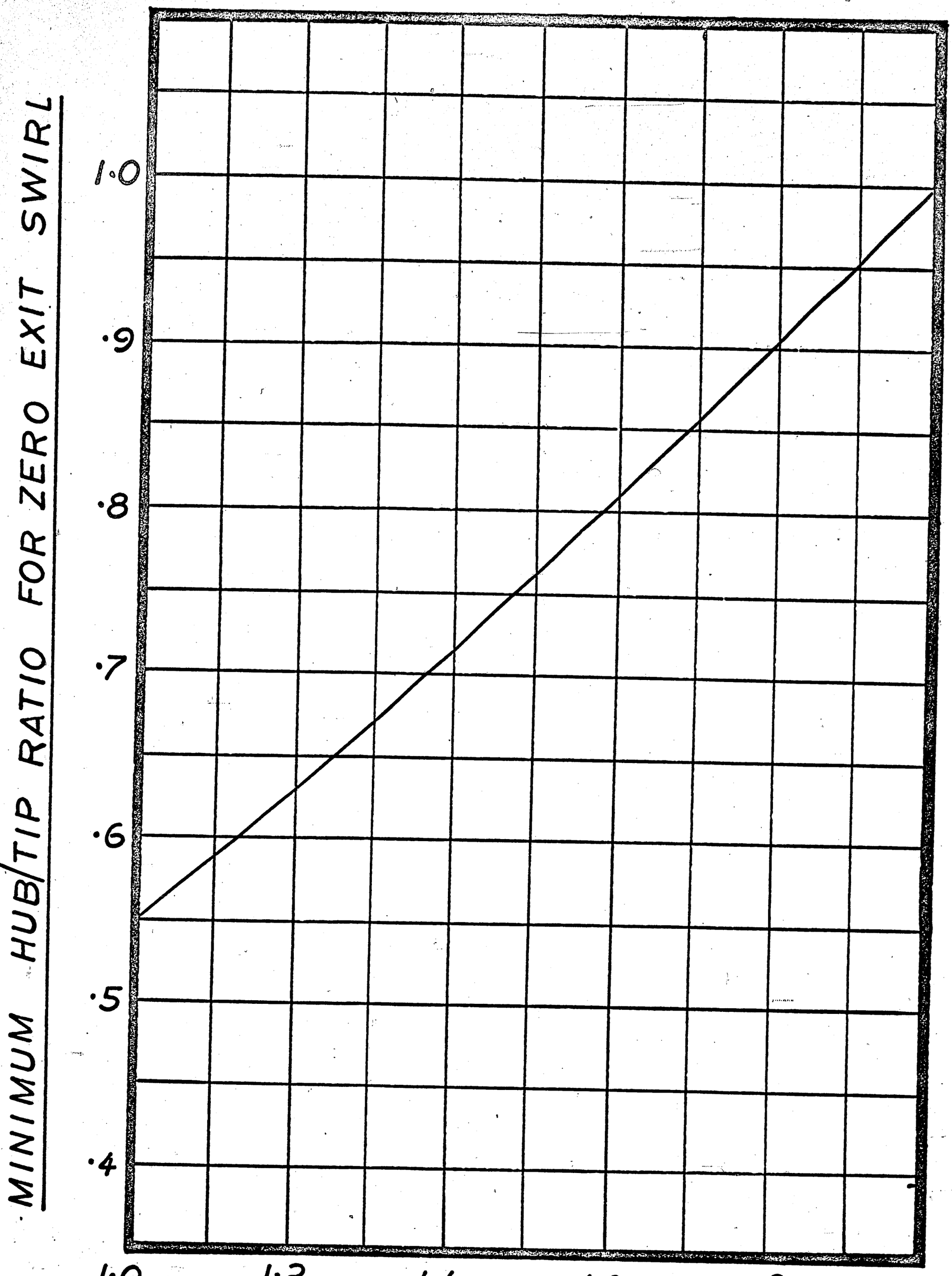
MINIMUM HUB/TIP RATIO FOR ZERO EXIT SWIRL
1.0
.9
.8
.7
.6
.5
.4
1.0
1.2
1.4
1.6
1.8
2.0
$\frac{K_p \Delta T}{U_m^2}$

It has been the writers experience, however, that efficiency increases little with increased Reynolds number, however, high Reynolds number does appear to effect capacity due to decreased boundary layer displacement thickness. For a Reynolds number of 10^6 the capacity appears to increase by 3 to 5% from that calculated by the Ainley method. The Reynolds number based on blade chord is obtained as follows:

$$N_{RE} = \frac{C\, C_B\, P_S}{\mu\, R_G\, T_S} \qquad 1.42$$

Where C = velocity in ft/sec.

C_B = blade chord in ft.

P_S = static pressure in lb/sq.ft.

T_S = static temperature in degrees Rankine

R_G = characteristic gas constant in ft.lb./lb./°F.

μ = dynamic viscosity in lb./ft.sec.

For air the variation of viscosity with temperature may be represented by the following equation:

$$\mu = 2.85 \left[\frac{T}{1800}\right]^{.68} \times 10^{-5} \qquad 1.43$$

FIGURE 1·11

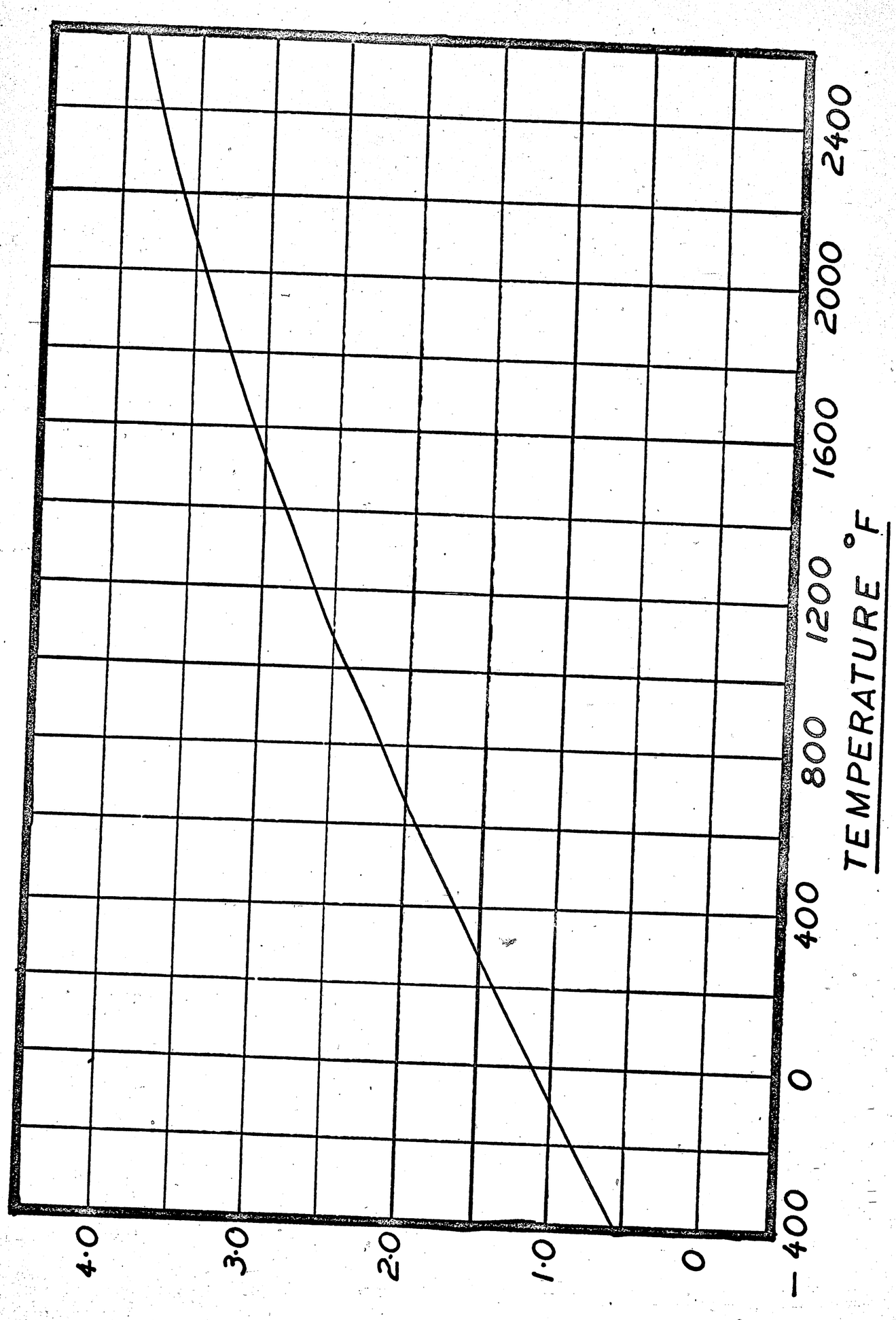
μ [LB/FT SEC]
4.0
3.0
2.0
1.0
0
-400
0
400
800
1200
1600
2000
2400
TEMPERATURE °F

Figure 1.11 is a plot of equation 1.43, which although for air, is considered sufficiently accurate for the estimation of the variation of viscosity with temperature for normal gas turbine combustion products. At the preliminary design stage a knowledge of the maximum Mach number is essential in order to evaluate the proposed design. The two cases to be considered in this section are a 50% reaction mean section design and a zero exit swirl design. As for the determination of minimum hub/tip ratio of section 1.4 simple radial equilibrium is considered sufficiently accurate at the preliminary design stage to estimate critical Mach numbers. For the two cases to be considered the maximum Mach number occurs at the stator root and may be estimated as follows:

(a) 50% reaction mean section design

From equation (1.31)

$$R = 1 - \frac{1}{2\Omega}\left[\frac{K_2 + K_3}{r^2}\right]$$

$$= 1 - \frac{1}{2U}\left[\frac{K_2 + K_3}{r}\right] \qquad 1.44$$

Where $U = \Omega r$

For 50% reaction at the mean section

$$K_2 + K_3 = U_m r_m \qquad 1.45$$

Substituting equation (1.45) into (1.44), we get:

$$R = 1 - \frac{1}{2}\frac{U_m r_m}{U r}$$

and since $\frac{U_m}{U} = \frac{r_m}{r}$

$$R = 1 - \frac{r_m^2}{r^2} \qquad 1.46$$

Now $r_m = \frac{r_h + r_t}{2}$

or $$r_h = \frac{2r_m}{\left[\frac{r_t}{r_h} + 1\right]} \qquad 1.47$$

Substituting equation (1.47) into (1.46), we get:

$$R_{hub} = 1 - \frac{1}{8}\left[\frac{r_t}{r_h} + 1\right]^2 \qquad 1.48$$

From equation (1.19)

$$R_{hub} = 1 - \frac{1}{2}\left[\frac{C_{\theta 3 hub} + C_{\theta 2 hub}}{U_{hub}}\right] \qquad 1.49$$

Equating equations (1.48) and (1.49), we get:

$$\frac{1}{8}\left[\frac{r_t}{r_h}+1\right]^2 = \frac{1}{2}\left[\frac{C_{\theta 3hub}+C_{\theta 2hub}}{U_{hub}}\right]$$

or

$$C_{\theta 3hub}+C_{\theta 2hub} = \frac{U_{hub}}{4}\left[\frac{r_t}{r_h}+1\right]^2 \qquad 1.50$$

From equation (1.2)

$$\frac{K_P \Delta T}{U_{hub}} = C_{\theta 2hub} - C_{\theta 3hub} \qquad 1.51$$

adding equations (1.51) and (1.50), we get:

$$2\,C_{\theta 2hub} = \frac{U_{hub}}{4}\left[\frac{r_t}{r_h}+1\right]^2 + \frac{K_P \Delta T}{U_{hub}}$$

and since $U_{hub} = U_m \cdot \frac{r_h}{r_m}$

$$C_{\theta 2hub} = \frac{U_m}{8}\cdot\frac{r_h}{r_m}\left[\frac{r_t}{r_h}+1\right]^2 + \frac{1}{2}\frac{K_P \Delta T}{U_m}\frac{r_m}{r_h}$$

and since $r_m = \frac{r_h + r_t}{2}$

$$c_{\theta 2hub} = \frac{U_m}{4}\left[\frac{r_t}{r_h} + 1\right] + \frac{1}{4} \cdot \frac{K_p \Delta T}{U_m}\left[\frac{r_t}{r_h} + 1\right]$$

and dividing by U_m

$$\frac{c_{\theta 2hub}}{U_m} = \frac{1}{4}\left[\frac{r_t}{r_h} + 1\right]\left[\frac{K_p \Delta T}{U_m^2} + 1\right] \qquad 1.52$$

Let $$\xi = \left[\frac{r_t}{r_h} + 1\right]\left[\frac{K_p \Delta T}{U_m^2} + 1\right] \qquad 1.53$$

Then $$\frac{c_{\theta 2hub}}{U_m} = \frac{\xi}{4} \qquad 1.54$$

At the root the maximum Mach number is that related to C2, the nozzle efflux velocity.

Now

$$c_{2hub}^2 = c_{\theta 2hub}^2 + c_{Ahub}^2 \qquad 1.55$$

Dividing by U_m^2, and since for simple radial equilibrium

$C_{A\ hub} = C_{A\ m} = C_{A\ tip} = C_A$, equation (1.54) becomes:

$$\frac{C_{2hub}^2}{U_m^2} = \frac{C_{\theta 2hub}^2}{U_m^2} + \left[\frac{C_A^2}{U_m^2}\right] \qquad 1.56$$

Substituting equation (1.54) into (1.56), and dividing by $\sqrt{T_{01}}$, we get:

$$\frac{C_{2hub}}{\sqrt{T_{01}}} = \frac{U_m}{\sqrt{T_{01}}}\sqrt{\xi^2/16 + \left(\frac{C_A}{U_m}\right)^2} \qquad 1.57$$

The Mach number related to the value of $\frac{C_{2\ hub}}{\sqrt{T_{01}}}$ can be found from figure 1.14.

Equation (1.57) therefore relates the maximum root Mach number to the mean blade speed, $\frac{C_A}{U}$, the stage inlet temperature, the work parameter and the hub/tip ratio.

If $\sqrt{\xi^2/16 + \left|\frac{C_A}{U_m}\right|^2} = \vartheta$

Then $$\frac{C_{2hub}}{\sqrt{T_{01}}} = \frac{U_m}{\sqrt{T_{01}}}\vartheta \qquad 1.59$$

Figure 1.12 is a plot of ξ against υ and C_{A_U}.

In order to estimate the root Mach number ξ is first obtained from equation (1.53). From figure 1.12 the factor υ may then be found, which, together with $\frac{U_m}{\sqrt{T_{01}}}$ gives a value for $\frac{C_2}{\sqrt{T_{01}}}$, and hence Mach number.

(b) Zero Exit Swirl Design

From equation (1.37), for zero exit swirl

$$R = 1 - \frac{1}{2\Omega}\frac{K_2}{r^2}$$

$$= 1 - \frac{1}{2U}\frac{K_2}{r} \qquad 1.59$$

Where $U = \Omega r$

The degree of reaction at the mean section is given by

$$R_m = 1 - \frac{1}{2U_m}\frac{K_2}{r_m}$$

Therefore

$$K_2 = 2U_m r_m (1 - R_m) \qquad 1.60$$

Substituting equation (1.60) into (1.59) we get:

$$R = 1 - \frac{U_m}{U}\frac{r_m}{r}(1 - R_m)$$

and since $\frac{U_m}{U} = \frac{r_m}{r}$

$$R = 1 - \frac{r_m^2}{r^2}(1 - R_m) \qquad 1.61$$

From equation (1.28)

$$R_m = 1 - \frac{1}{2}\frac{K_p \Delta T}{U_m^2} \qquad 1.62$$

Substituting equation (1.62) into (1.61), we get:

$$R = 1 - \frac{1}{2}\frac{r_m^2}{r^2}\frac{K_p \Delta T}{U_m^2}$$

or

$$R_{hub} = 1 - \frac{1}{2}\frac{r_m^2}{r_{hub}^2}\frac{K_p \Delta T}{U_m^2} \qquad 1.63$$

Substituting equation (1.47) into (1.63), we get:

$$R_{hub} = 1 - \frac{1}{8}\left(\frac{r_t}{r_h} + 1\right)^2 \frac{K_p \Delta T}{U_m^2} \qquad 1.64$$

Now from equation (1.27)

$$R_{hub} = 1 - \frac{1}{2}\frac{C_{\theta 2\,hub}}{U_{hub}} \qquad 1.65$$

Equating equations (1.64) and (1.65), we get:

$$\frac{1}{8}\left(\frac{r_t}{r_h}+1\right)^2 \frac{K_p \Delta T}{U_m^2} = \frac{1}{2}\frac{C_{\theta 2 hub}}{U_{hub}}$$

or

$$\frac{C_{\theta 2 hub}}{U_{hub}} = \frac{1}{4}\left(\frac{r_t}{r_h}+1\right)^2 \frac{K_p \Delta T}{U_m^2}$$

and since $U_{hub} = U_m \cdot \frac{r_h}{r_m}$

$$\frac{C_{\theta 2 hub}}{U_m}\frac{r_m}{r_h} = \frac{1}{4}\left(\frac{r_t}{r_h}+1\right)^2 \frac{K_p \Delta T}{U_m^2} \qquad \text{——— 1.66}$$

Substituting equation (1.47) into (1.66), we get:

$$\frac{C_{\theta 2 hub}}{U_m} \cdot \frac{1}{2}\left(\frac{r_t}{r_h}+1\right) = \frac{1}{4}\left(\frac{r_t}{r_h}+1\right)^2 \frac{K_p \Delta T}{U_m^2}$$

or $$\frac{C_{\theta 2 hub}}{U_m} = \frac{1}{2}\left(\frac{r_t}{r_h}+1\right) \frac{K_p \Delta T}{U_m^2} \qquad \text{——— 1.67}$$

Let $$\xi_2 = \left(\frac{r_t}{r_h}+1\right) \frac{K_p \Delta T}{U_m^2} \qquad \text{——— 1.68}$$

Then

$$\frac{C_{e2\,hub}}{U_m} = \frac{\xi_2}{2} \qquad 1.69$$

Substituting equation (1.69) into (1.56), we get:

$$\frac{C_{2\,hub}^2}{U_m^2} = \frac{\xi_2^2}{4} + \left(\frac{C_A}{U_m}\right)^2 \qquad 1.70$$

or

$$\frac{C_{2\,hub}}{\sqrt{T_{01}}} = \frac{U_m}{\sqrt{T_{01}}}\left(\sqrt{\frac{\xi_2^2}{4} + \left(\frac{C_A}{U_m}\right)}\right) \qquad 1.71$$

The comments relating to the 50% reaction mean section design on page 36 also apply here.

If

$$J_2 = \sqrt{\frac{\xi_2^2}{4} + \left(\frac{C_A}{U}\right)^2}$$

Then

$$\frac{C_{2\,hub}}{\sqrt{T_{01}}} = \frac{U_m}{\sqrt{T_{01}}} \cdot J_2 \qquad 1.72$$

Figure 1.13 is a plot of ξ_2 against J_2 and $\frac{C_A}{U}$.

In order to estimate the root Mach Number, ξ_2 is first obtained from equation (1.68). From figure 1.13 the factor J_2 may then be found, which, together with $\frac{U_m}{\sqrt{T_{01}}}$ gives a value for $\frac{C_2}{\sqrt{T_{01}}}$, and hence Mach number.

1.6 General Parameters

(a) Flare

Because of compressibility effects the density of the working fluid decreases as it passes through the blade rows, which is usually compensated for by increase of annulus area. This change of area is usually continuous through the turbine, and introduces radial velocities of the same order of magnitude as the axial velocity. The implications of this are dealt with in section 2.3. In general, there is no evidence that flare has any detrimental effect upon turbine efficiency, and up to an included angle of 30° no special consideration is necessary. This conclusion is based upon the design and testing of several turbines of varying horsepowers.

(b) Aspect Ratio

Aspect ratio is defined as the ratio $\frac{\text{axial blade chord}}{\text{blade height}}$

FIGURE 1.12

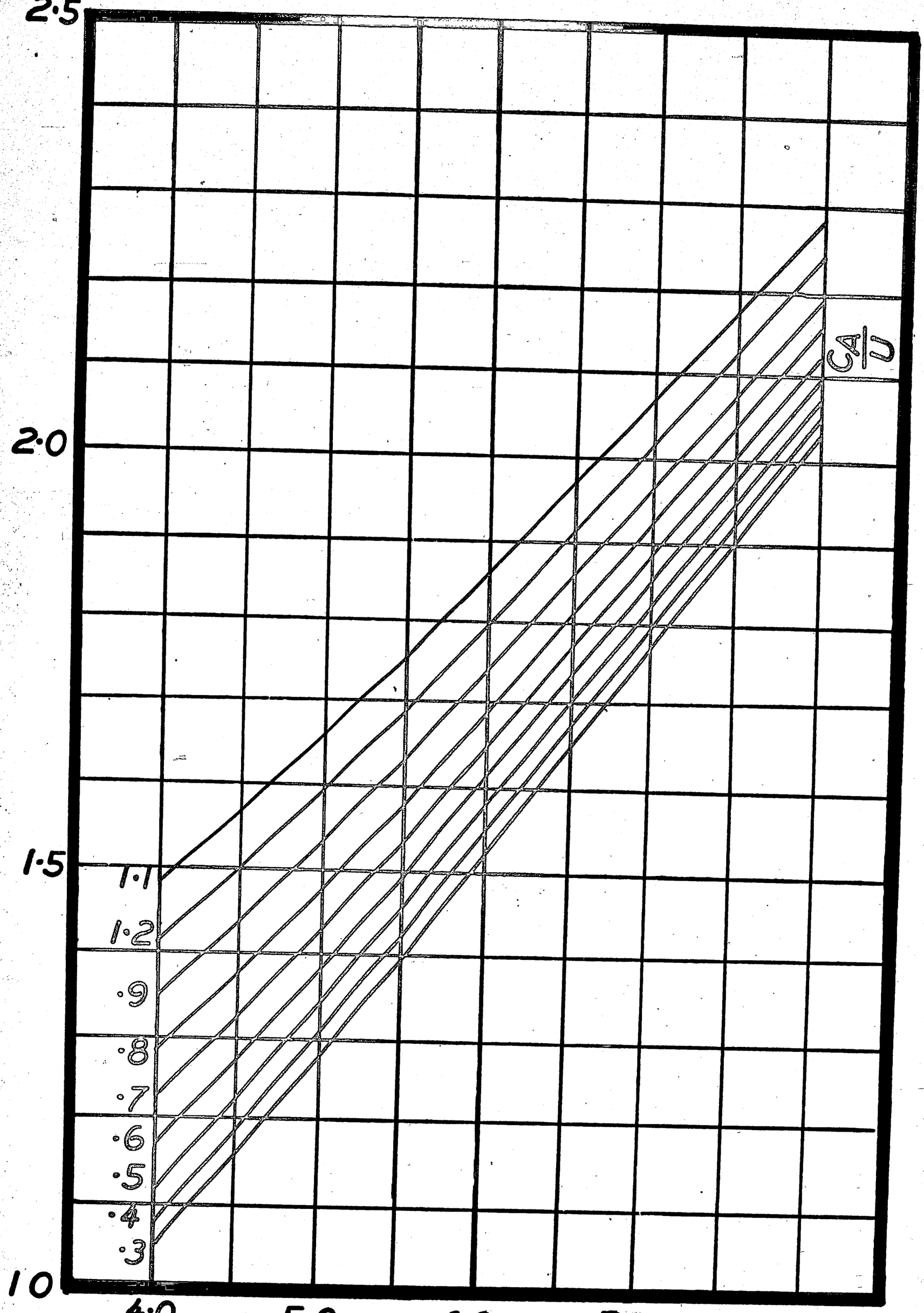
50% REACTION MEAN SECTION
2.5
2.0
1.5
1.1
1.2
.9
.8
.7
.6
.5
.4
.3
10
4.0
5.0
6.0
7.0
8.0
ξ
CA/U

FIGURE 1·13

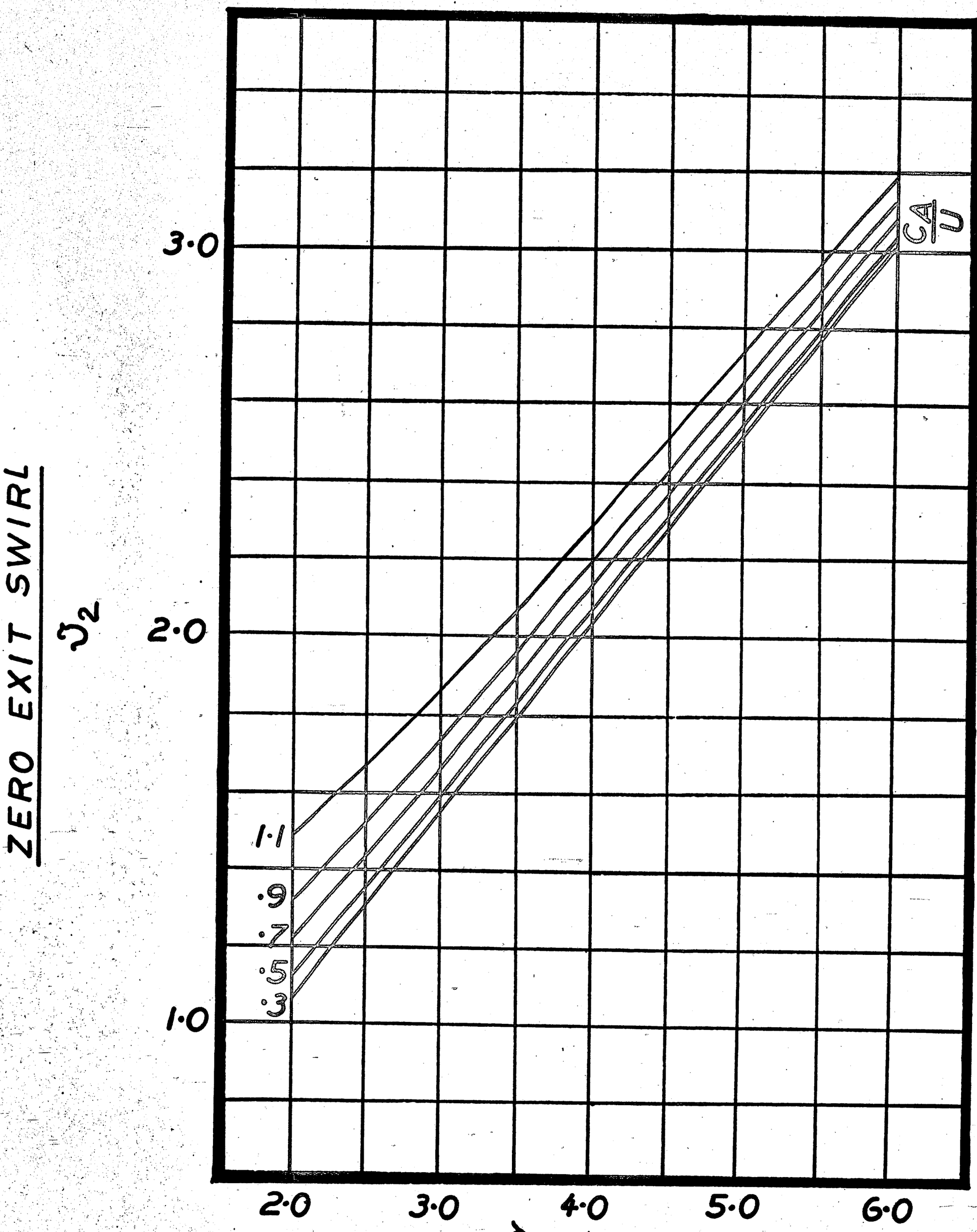
ZERO EXIT SWIRL
ϑ_2
3·0
2·0
1·1
·9
·7
·5
·3
1·0
CA
U
2·0
3·0
4·0
5·0
6·0
ξ_2

FIGURE 1.14

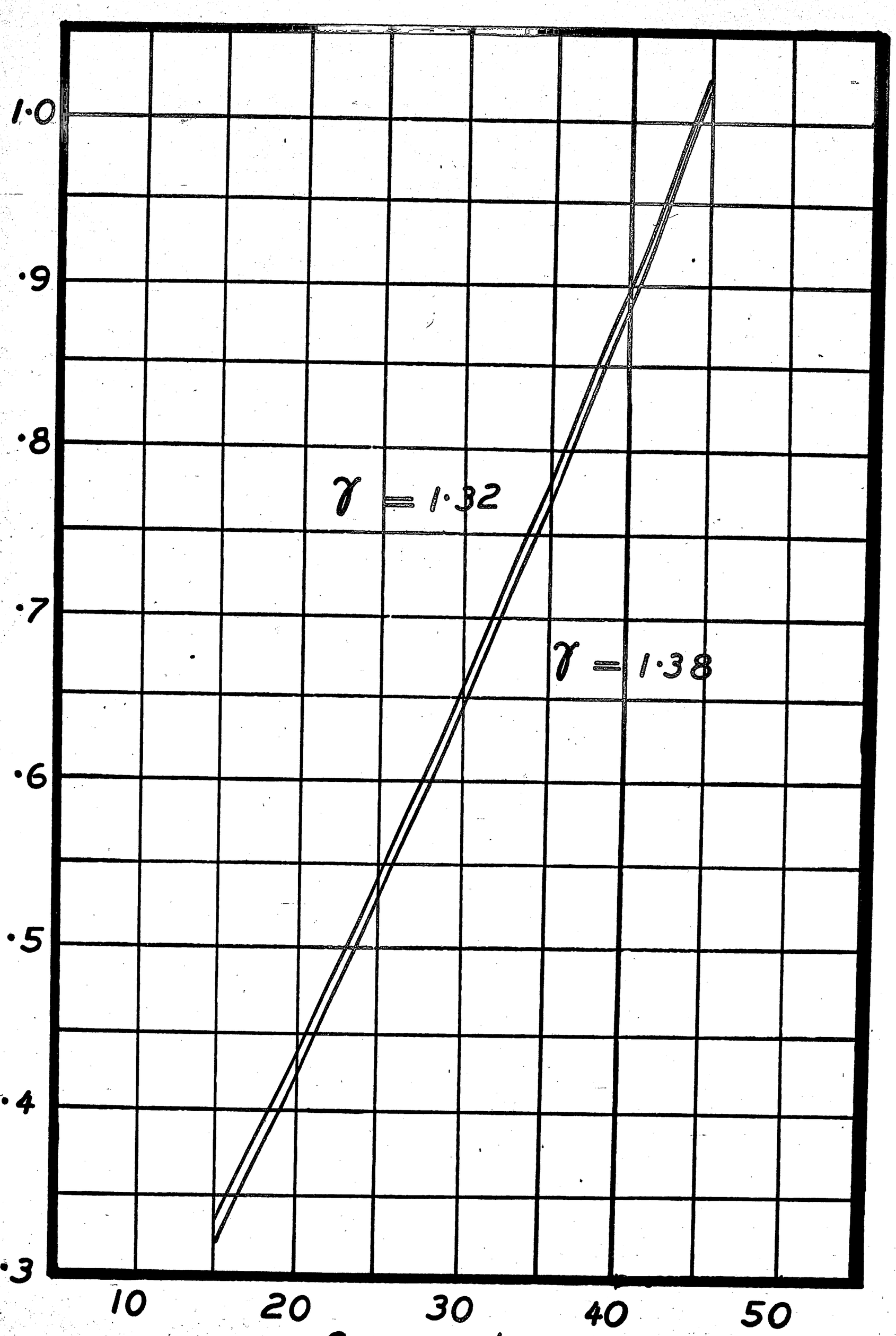

The effect of aspect ratio on secondary loss is inconclusive. Ainley's correlation includes the effect of aspect ratio in the parameter λ which increases with reduced aspect ratio, and within the writers experience this appears to give valid results. In general it is recommended that the minimum value assigned to aspect ratio be three, and for high efficiency turbines certainly no less than two and a half.

1.7 Effect of Stress on Turbine Efficiency

In section 1.2 the effect of axial velocity on turbine efficiency was discussed. Now the axial velocity in a turbine is determined by the magnitude of the annulus area which is related to the centrifugal stress as follows:

$$\text{C F stress} \propto RPM^2 \times \text{annulus area.}$$

The constant of proportionality is a function of blade taper ratio.

If the turbine designer has a free choice in selecting the RPM it is possible to choose a blade speed to give the desired value of $\frac{K_p \Delta T}{U^2}$ and an annulus area to give the desired value of C_A/U. The RPM would then be selected to give an acceptable stress. Any difficulty with the

root section could be dealt with by using less than the permissible RPM, which in turn would give a stress less than the maximum permissible. The effect of this would be large diameter turbines with large hub/tip ratios for a given duty. However, it is usually the case that the RPM is determined by other considerations. In this case there exists a maximum value of annulus area from stress considerations which in turn puts a limit on the minimum axial velocity attainable. There is then only one variable left, i.e., U_m to satisfy the two parameters $\frac{K_p \Delta T}{U^2}$ and C_A/U. A limit may therefore be set on the maximum efficiency attainable, in this case. It is clear, then, that the permissible stress level must be determined early in the design.

The stress in a blade with a linear taper from the outer to inner radius may be approximated by the following formula, for a material density of .283 lbm/cubic ins.

$$\sigma = \frac{N^2 An}{1.14} \times 10^{-6} \qquad 1.73$$

Equation (1.73) is considered accurate enough to enable a reasonable estimation to be made of the blade root stress

at the preliminary design stage. This in turn will enable the limitations imposed on efficiency, by stress, to be determined.

2.0 DETAILED STAGE CALCULATIONS

Section 1.0 is concerned with the selection of the optimum stage velocity triangles within the limitations imposed by stress and matching. Further, formulae have been developed to enable the validity of a proposed design to be checked at the root for limiting hub/tip ratio conditions and critical Mach number. The purpose of section 1.0 is to reduce to a minimum the number of designs that have to be investigated in detail in order to arrive at a satisfactory solution. In contrast to section 1.0 this section is concerned with the detailed thermodynamic design, assuming that the basic design parameters have been previously optimized and selected. Further only design point calculations will be considered. Finally, in calculating losses at the design point, zero incidence will be assumed at the inlet to the stator and rotor. In order to increase efficiency at expansion ratios higher than design it is usual practice to design blades with five or ten degrees negative incidence (see figure 2.1). The reason for this is apparent from examination of figure 2.2 which is a plot of the variation

of total pressure loss coefficient with incidence for a typical turbine blade. From this plot it can be seen that the loss coefficient increases rapidly for quite a modest increase in positive incidence, while for negative incidence the loss coefficient remains substantially constant over a large range.

The design incidence selected must of necessity be small since increasing the negative incidence at design point also increases blade turning angle, which in turn reduces blade stalling incidence and range. In view of this it is considered justified to assume zero incidence for design point calculations, since the permissible value of incidence selected at design point is such that the loss coefficient will be substantially that at zero incidence.

2.1 Profile loss and optimum space/chord ratio

The profile loss at zero incidence is assumed by Ainley to be a function of

$$\alpha_2, \quad \alpha_1^*/\alpha_2, \quad s/c, \quad \& \quad \frac{t_{max}}{c}$$

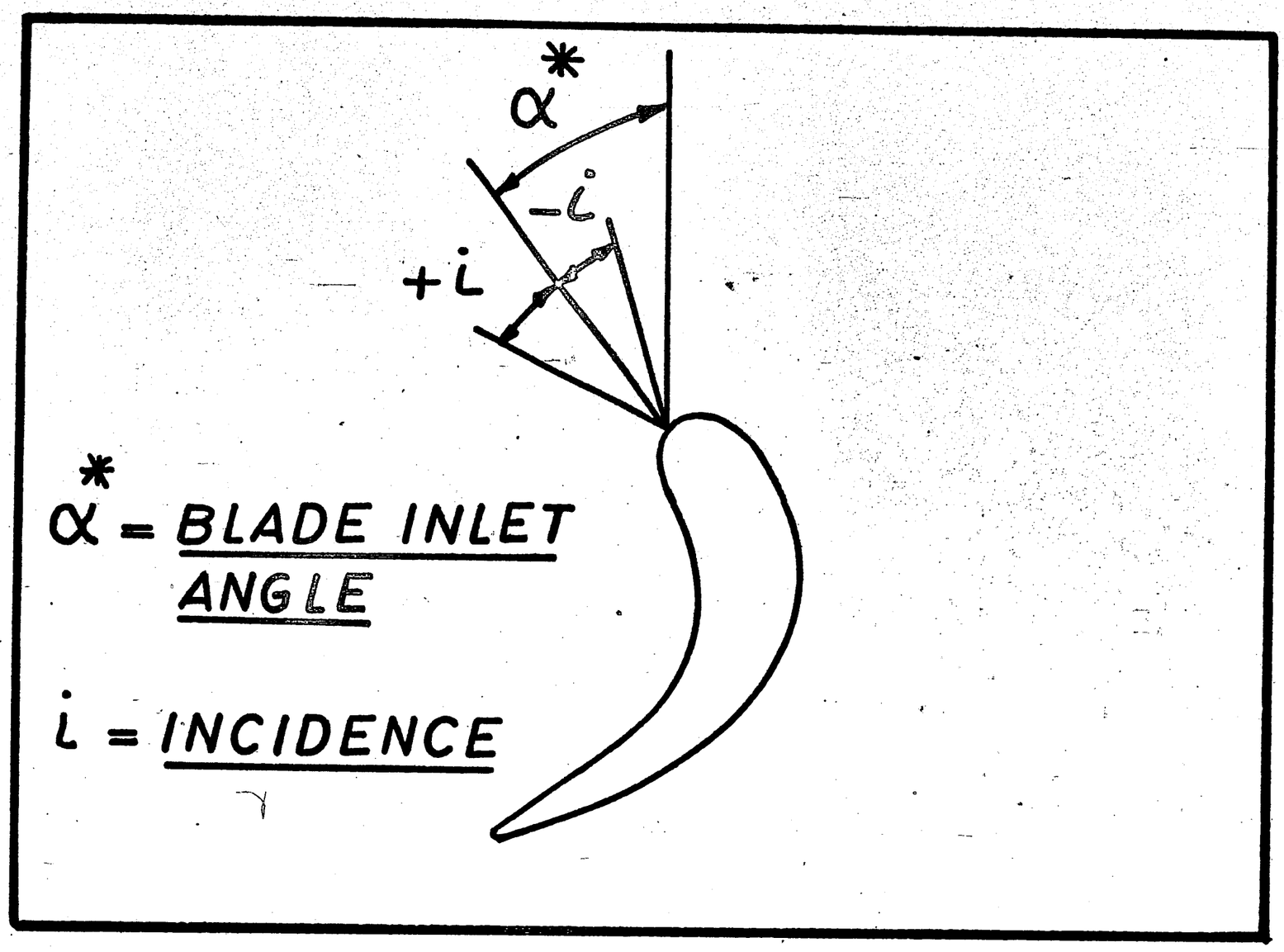

FIGURE 2·1

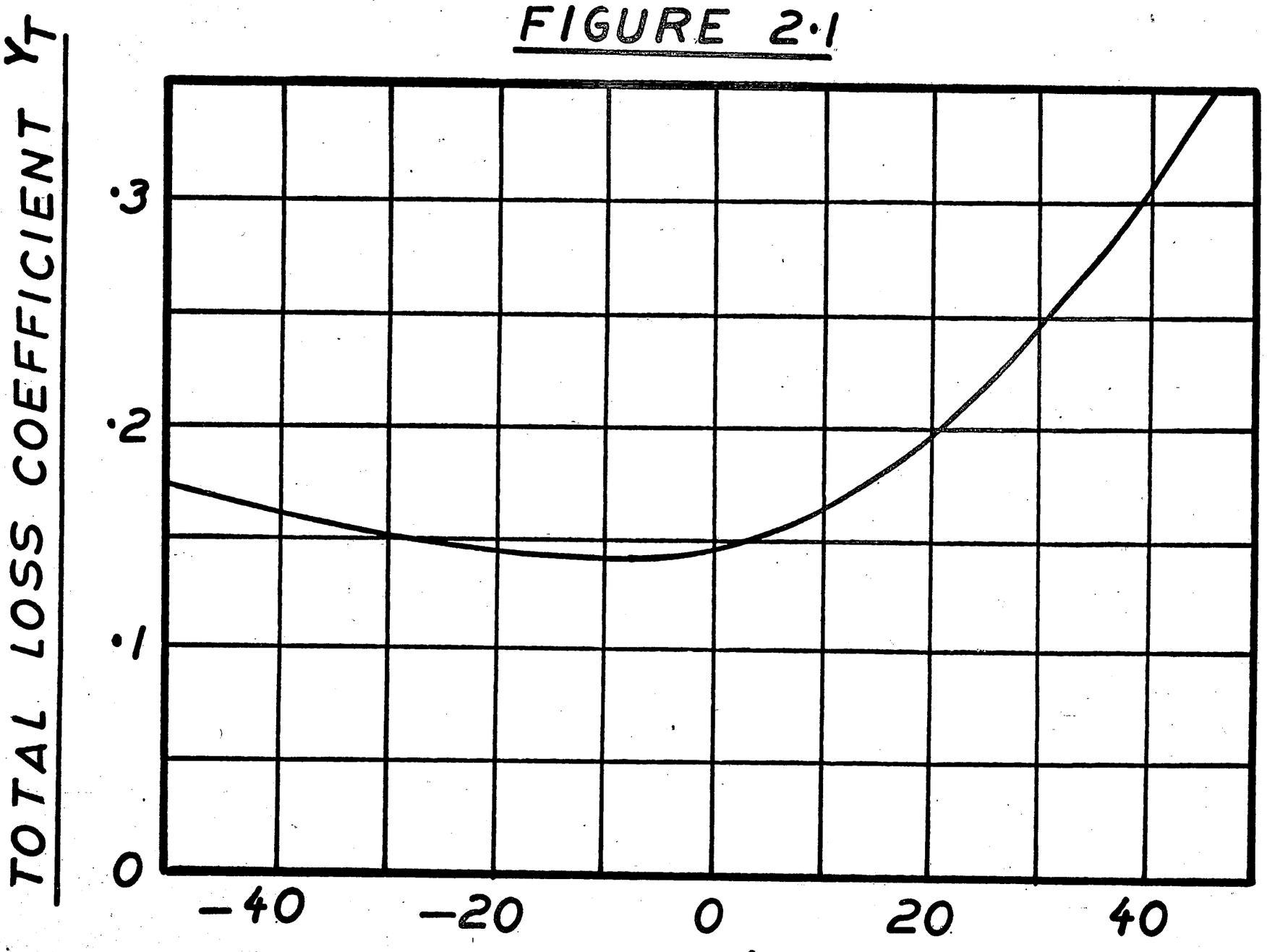

FIGURE 2·2

Where α_2 = gas outlet angle

α_1^* = blade inlet angle, which equals the gas inlet angle at zero incidence

$\frac{S}{C}$ = space/chord ratio

$\frac{t}{C}$ = maximum blade thickness/chord ratio

The correlation given by Ainley for the profile loss coefficient is as follows:

$$Y_{P(i=0)} = \left(Y_P(\alpha_1^*=0) + \left|\frac{\alpha_1^*}{\alpha_2}\right| \left[Y_P(\alpha_1^*=-\alpha_2) - Y_P(\alpha_1^*=0) \right] \right) \left(\frac{t}{C}\right)^{-\frac{\alpha_1^*}{\alpha_2}}$$

Where i = incidence

$Y_{P(i=0)}$ = profile loss coefficient of a blade having $\alpha_1^* = 0$ and the same α_2 and S/C as the actual blade.

$Y_{P(\alpha_1^*=-\alpha_2)}$ = profile loss coefficient of a blade having $\alpha_1^* = -\alpha_2$ and the same α_2 and S/C as the actual blade (i.e. impulse blade).

Figure 2.3 and 2.4 are taken from figure 4 of Ainley's report. These plots are used to obtain the data for substitution into the above equation for Y_p. In order

to obtain a more rapid assessment of the profile loss for a particular design it was found convenient to replot the data given by Ainley. Accordingly a set of curves have been produced which are plots of the profile loss coefficient against gas inlet angle and outlet angle, for constant values of S/C (figures 2.5 to 2.11). These curves were drawn assuming a value of blade maximum thickness to chord ratio of .2. For values other than .2, figure 2.12 provides a correction factor. At the preliminary design stage .2 is a good average number to use. In estimating profile and secondary losses all curves assume that the trailing edge thickness is 2% of the blade pitch. Figure 2.19 provides a correction factor to be applied to the total loss coefficient Y_T where the trailing edge thickness of the blade is other than that given above. At the preliminary design stage 2% is a good average number to use.

The total loss coefficient is defined as

$$Y_T = Y_p = Y_S + Y_K$$

Where Y_p = profile loss coefficient

Y_S = secondary loss coefficient

Y_K = leakage loss coefficient

The estimation of $Y_S + Y_K$ is given in section 2.2.

FIGURE 2·3

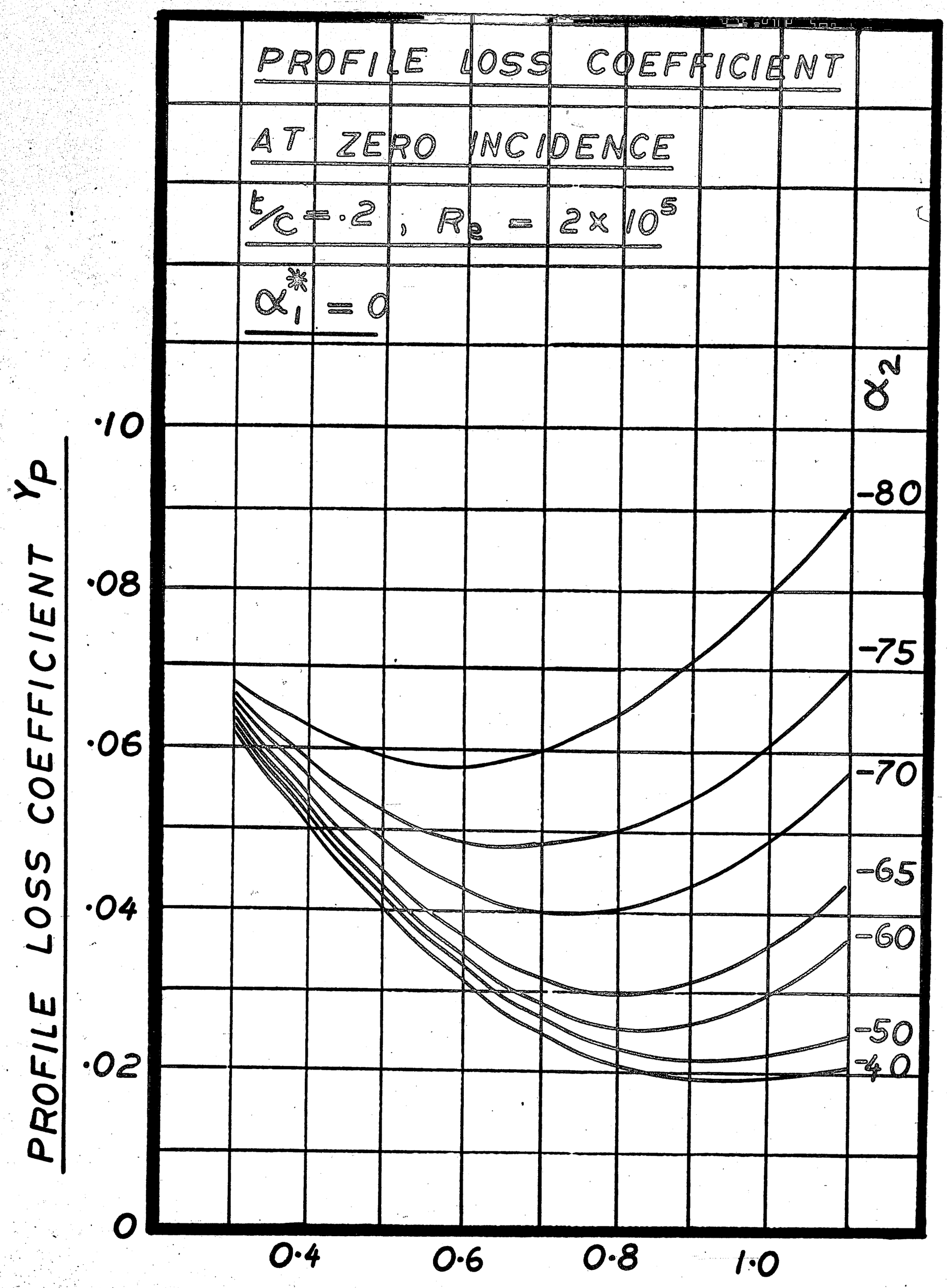
PROFILE LOSS COEFFICIENT
AT ZERO INCIDENCE
t/c = .2 , Re = 2 x 10^5
α1* = 0
PROFILE LOSS COEFFICIENT Yp
.10
.08
.06
.04
.02
0
0·4
0·6
0·8
1·0
PITCH / CHORD RATIO
α2
-80
-75
-70
-65
-60
-50
-40

FIGURE 2·4

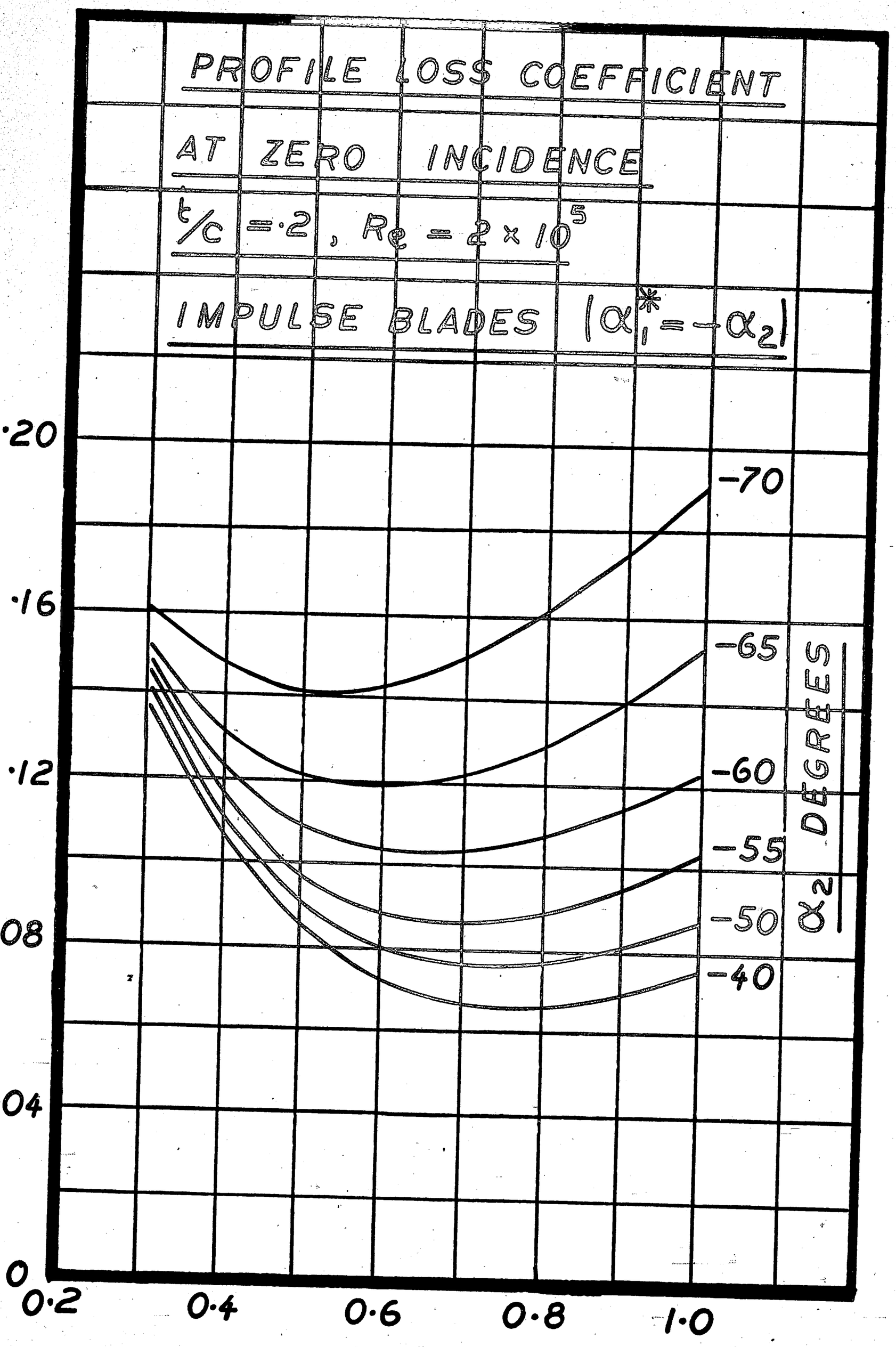
PROFILE LOSS COEFFICIENT
AT ZERO INCIDENCE
t/c = ·2, Re = 2 × 10^5
IMPULSE BLADES |α1* = −α2|
PROFILE LOSS COEFFICIENT Yp
·20
·16
·12
·08
·04
0
0·2
0·4
0·6
0·8
1·0
PITCH/CHORD RATIO
−70
−65
−60
−55
−50
−40
α2 DEGREES

FIGURE 2.5

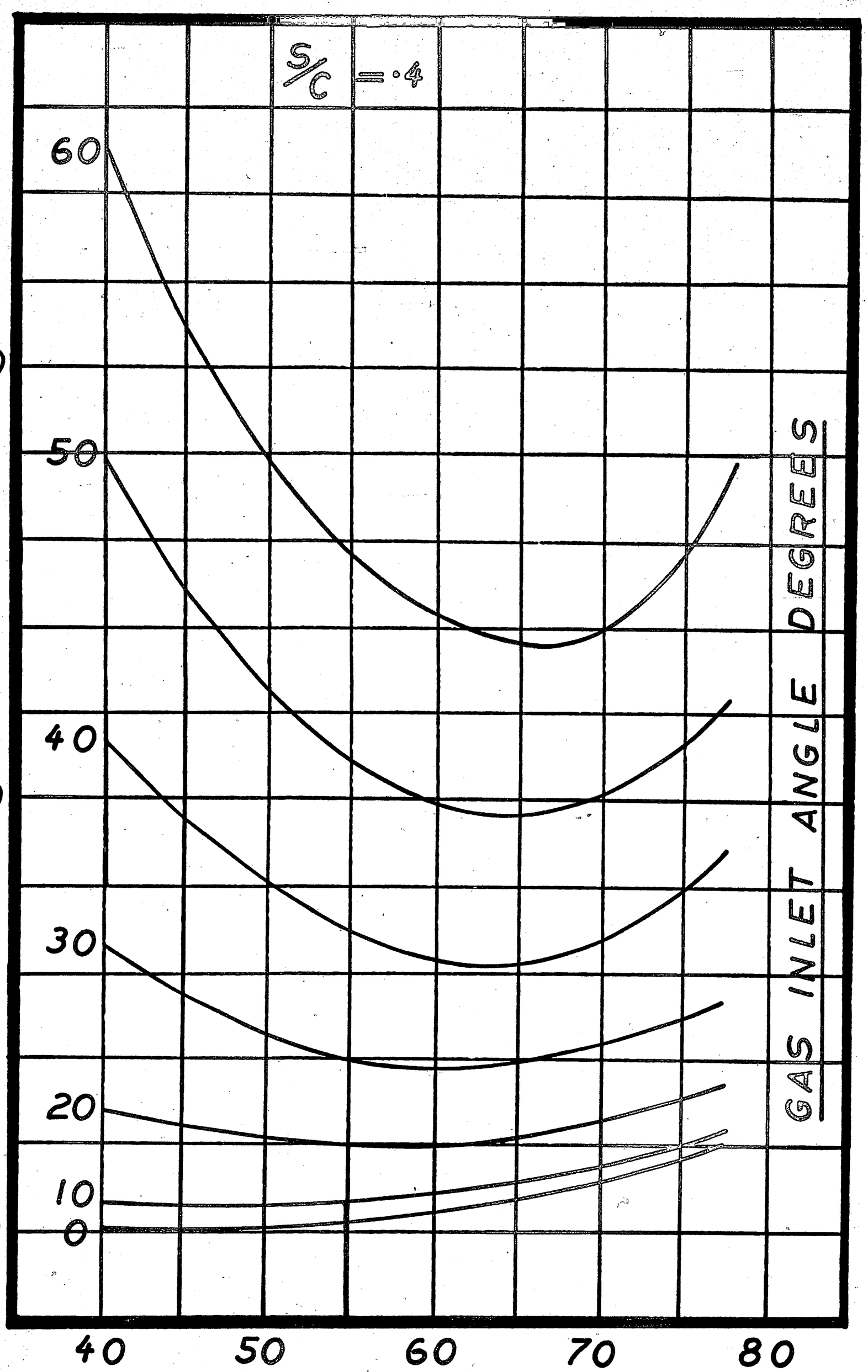
S/C = .4
60
50
40
30
20
10
0
.150
.100
.050
PROFILE LOSS COEFFICIENT, Y_P
40
50
60
70
80
GAS INLET ANGLE DEGREES
GAS OUTLET ANGLE DEGREES

FIGURE 2·6

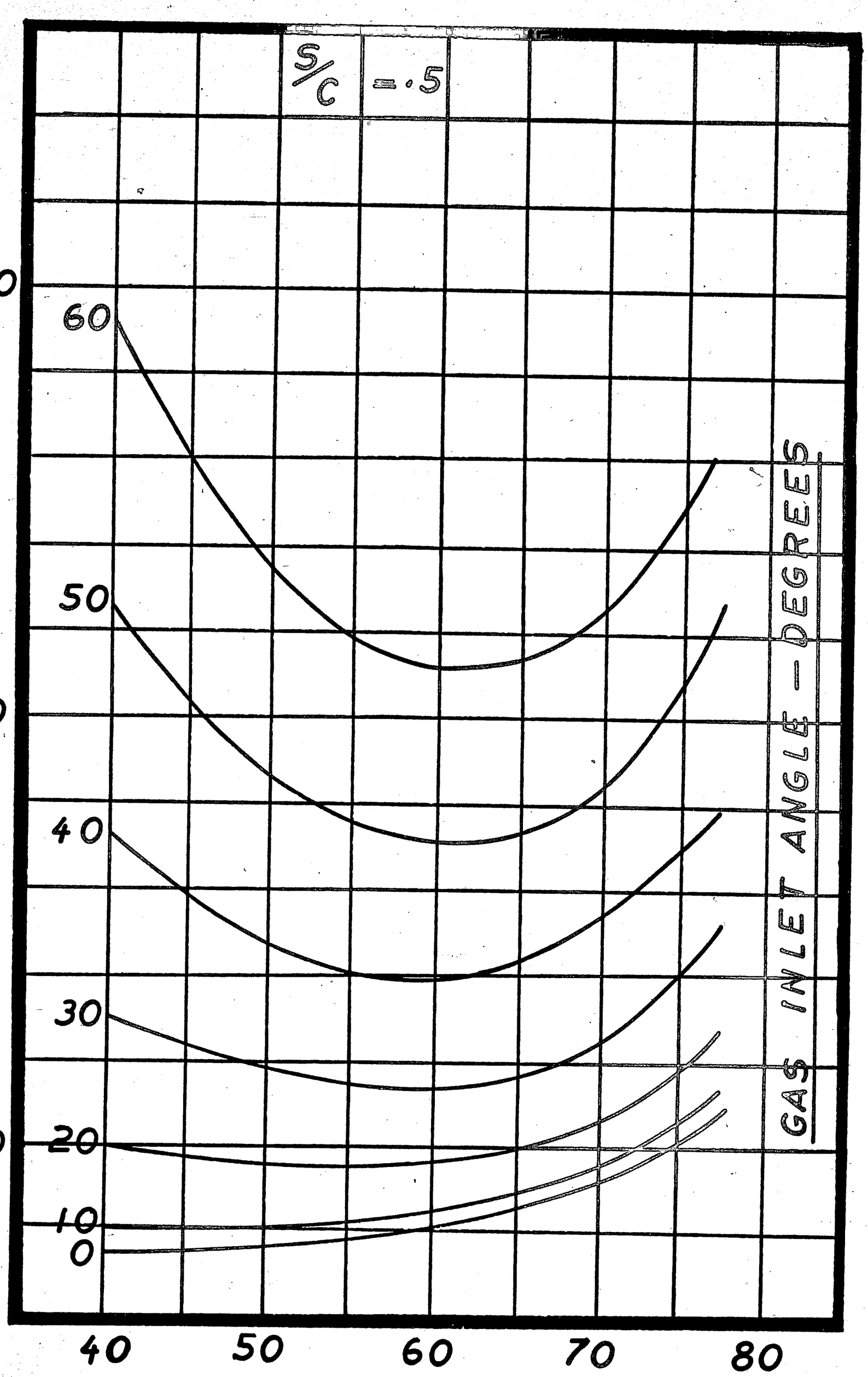
S/C = .5
.150
.100
.050
PROFILE LOSS COEFFICIENT Yp
60
50
40
30
20
10
0
GAS INLET ANGLE - DEGREES
40
50
60
70
80
GAS OUTLET ANGLE DEGREES

FIGURE 2·7

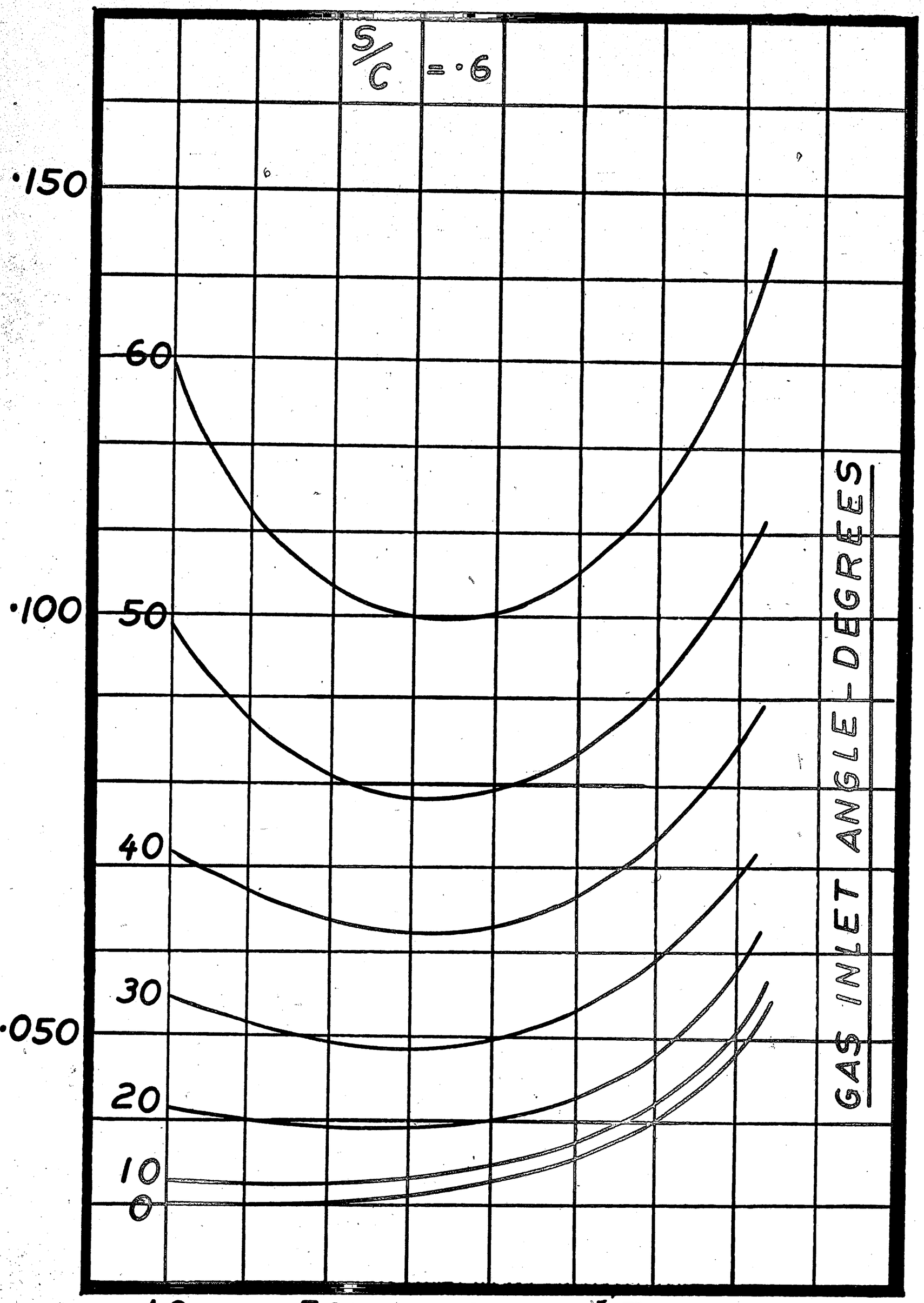
S/C = ·6
·150
·100
·050
PROFILE LOSS COEFFICIENT Y_P
60
50
40
30
20
10
0
GAS INLET ANGLE - DEGREES
40
50
60
70
80
GAS OUTLET ANGLE DEGREES

FIGURE 2·8

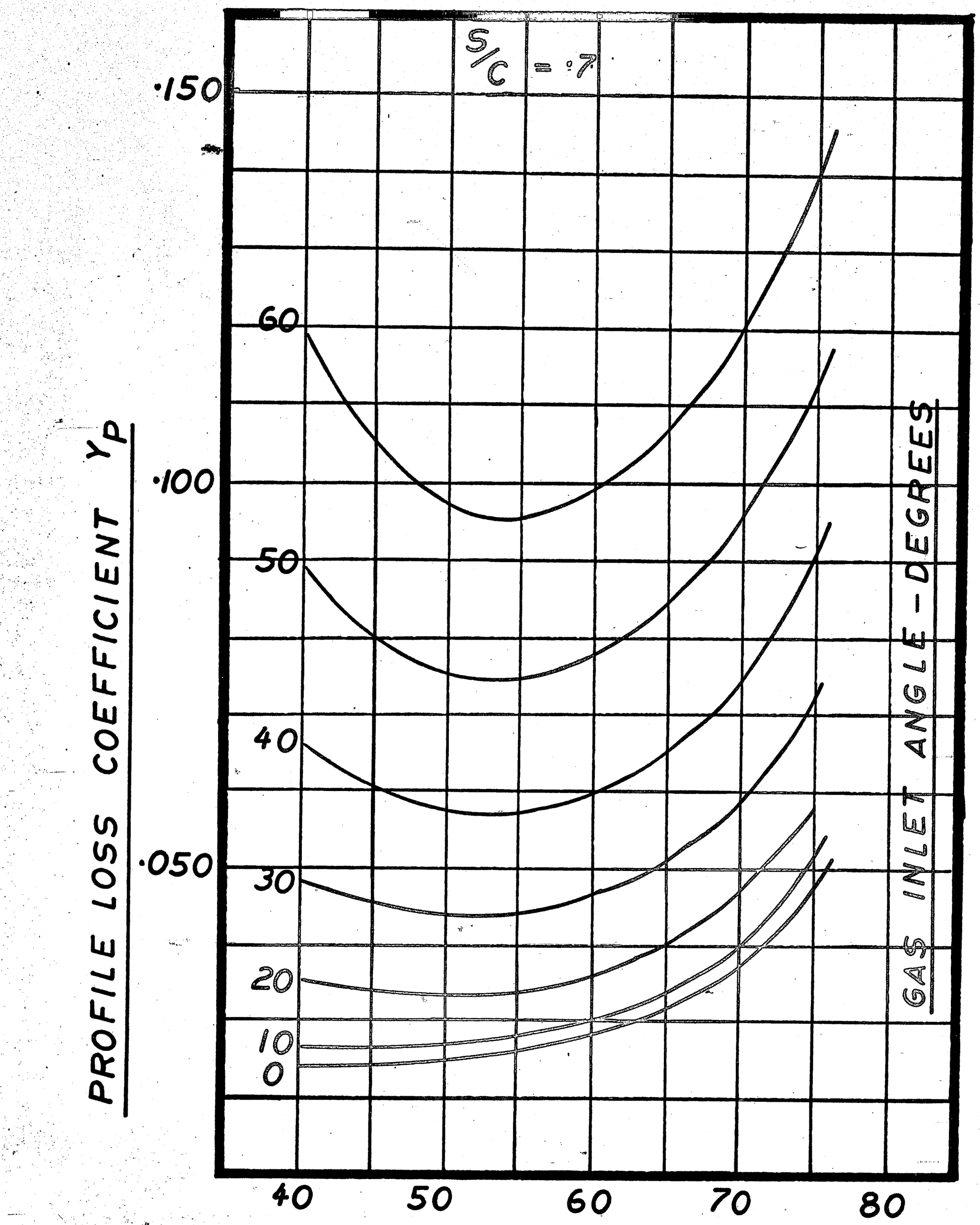
S/C = 0.7
·150
·100
·050
60
50
40
30
20
10
0
40
50
60
70
80
PROFILE LOSS COEFFICIENT Y_P
GAS INLET ANGLE - DEGREES
GAS OUTLET ANGLE. DEGREES

FIGURE 2·9

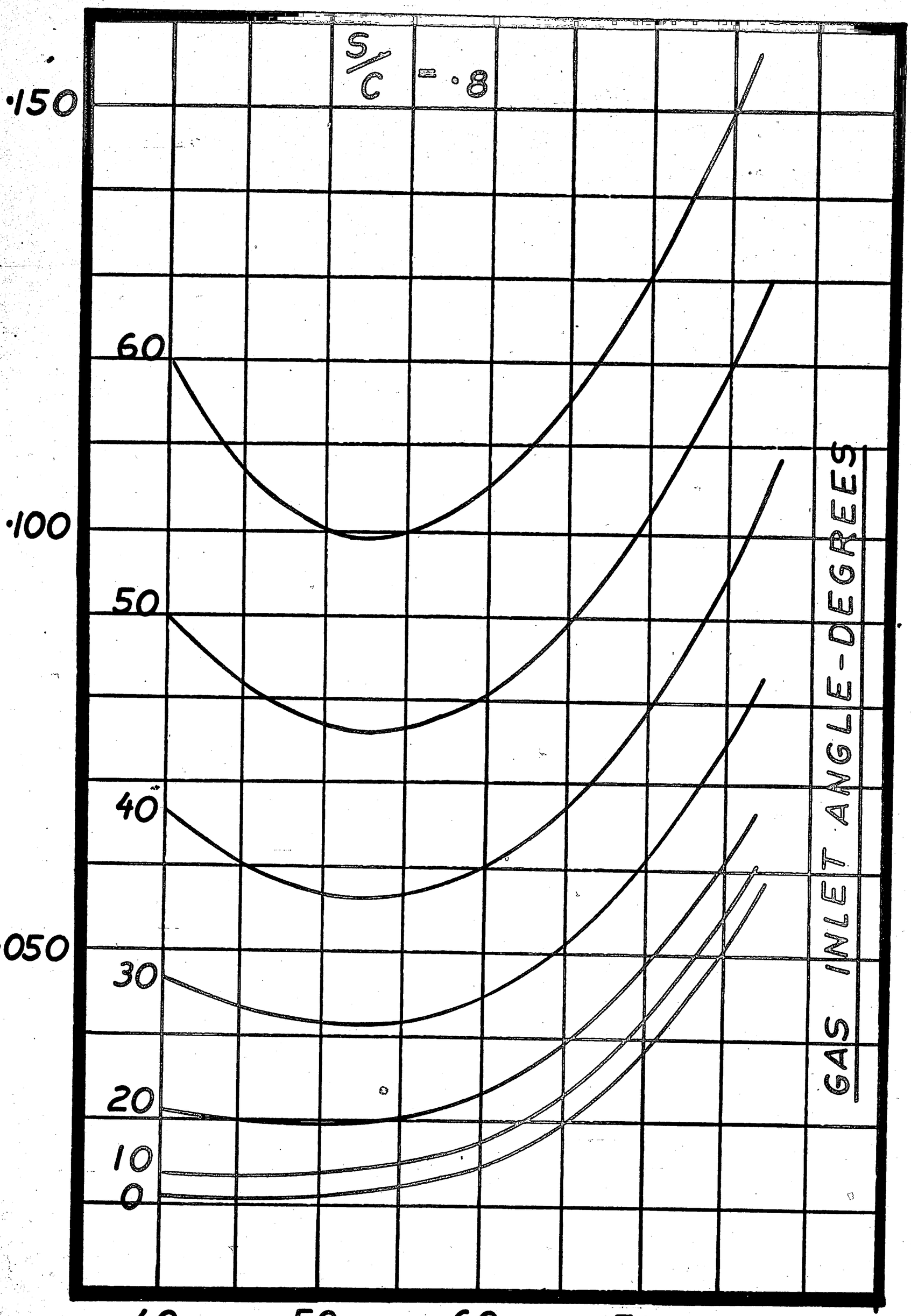
S/C = ·8
·150
·100
·050
60
50
40
30
20
10
0
PROFILE LOSS COEFFICIENT Y_P
GAS INLET ANGLE-DEGREES
40
50
60
70
80
GAS OUTLET ANGLE-DEGREES

FIGURE 2·10

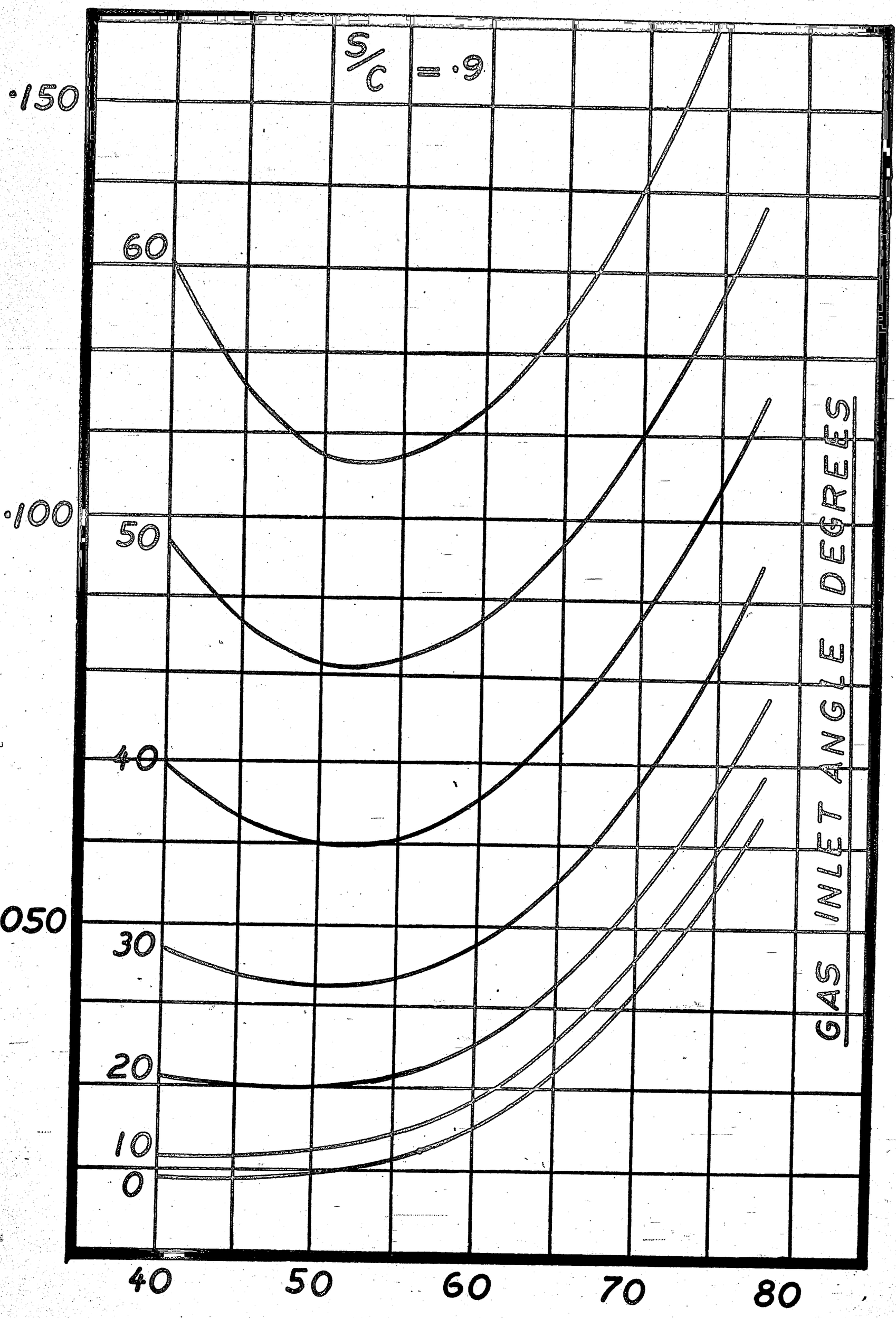
S/C = ·9
·150
·100
·050
PROFILE LOSS COEFFICIENT Y_P
60
50
40
30
20
10
0
40
50
60
70
80
GAS INLET ANGLE DEGREES
GAS OUTLET ANGLE DEGREES

FIGURE 2·11

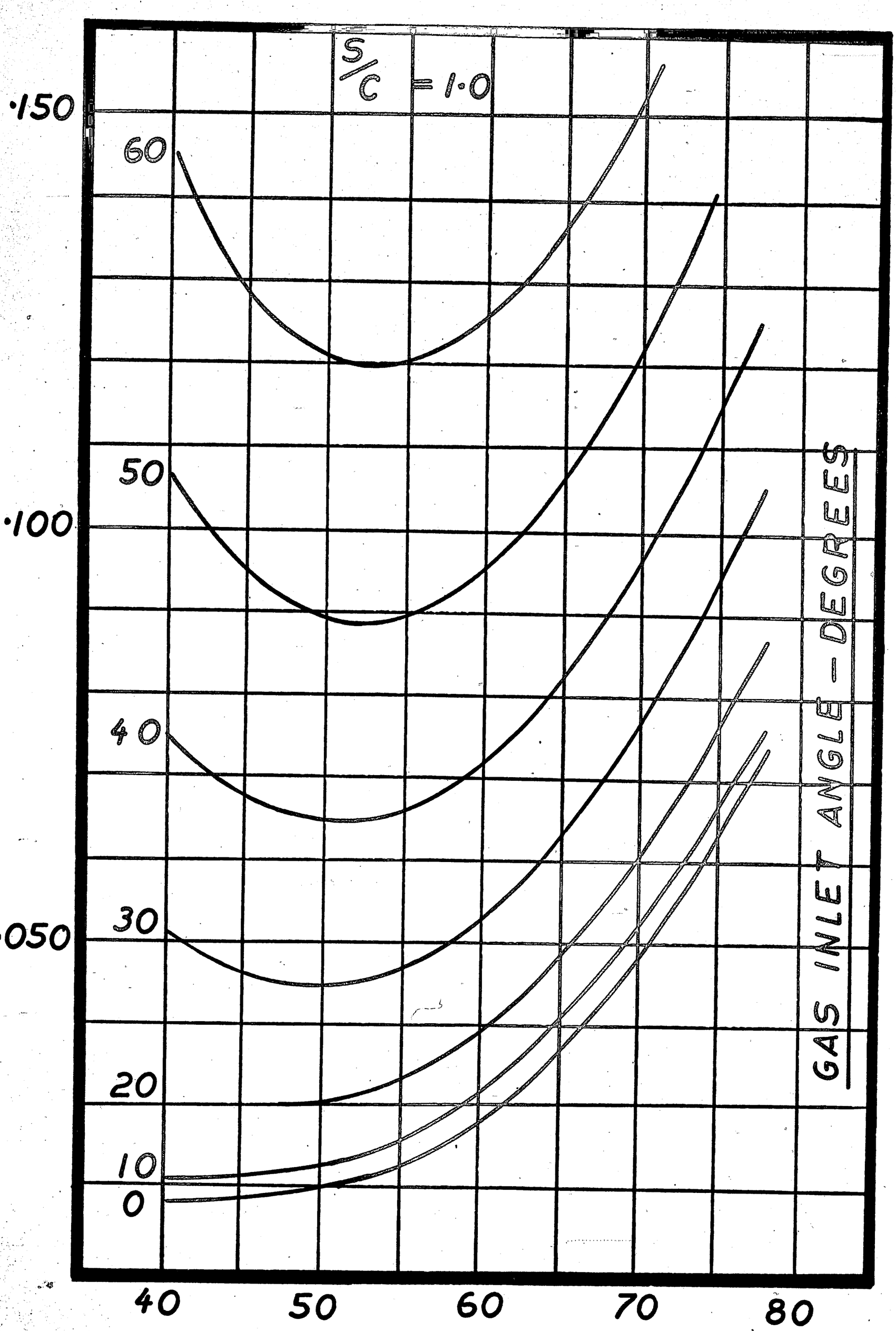
S/C = 1·0
60
50
40
30
20
10
0
·150
·100
·050
PROFILE LOSS COEFFICIENT Y_P
40
50
60
70
80
GAS INLET ANGLE - DEGREES
GAS OUTLET ANGLE DEGREES

FIGURE 2·12

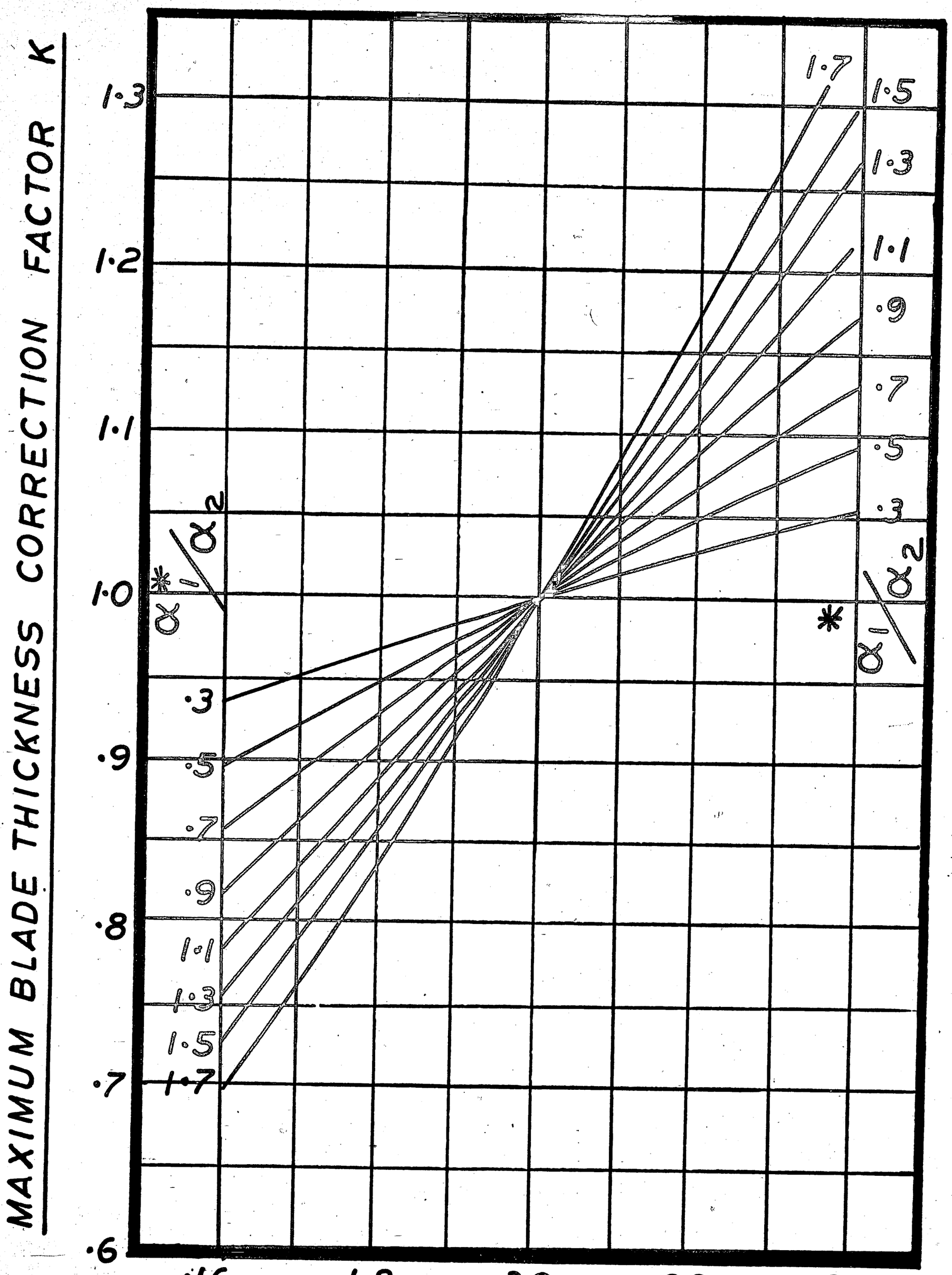
MAXIMUM BLADE THICKNESS CORRECTION FACTOR K
1·3
1·2
1·1
1·0
·9
·8
·7
·6
·16
·18
·20
·22
·24
t/c
1·7
1·5
1·3
1·1
·9
·7
·5
·3
α1*/α2
α1/α2*
·3
·5
·7
·9
1·1
1·3
1·5
1·7

Optimum Spacing

The selection of the pitch chord ratio is important since too many blades cause high friction losses while too few blades cause even higher separation losses. Figure 2.13 is a plot of the optimum space chord ratio against gas inlet and outlet angles. This curve was obtained by cross plotting the profile loss coefficient from Ainley's correlation against space chord ratio for constant values of blade inlet and outlet angles. The optimum space chord ratio is that at which the minimum profile loss occurs. Ainley's analysis, however, does not permit the prediction of space chord ratio for negative blade inlet angles. For a mean section design this usually does not cause any embarrassment since blade loadings are such that a positive inlet angle results. When three dimensional considerations are taken into account, however, the resulting flow is such that negative angles are usually obtained at the blade tip sections. In addition to Ainley's correlation, therefore, three curves have been plotted on figure 2.13. These curves are taken from reference 2, and are for blade inlet angles of 0, -10, and

FIGURE 2·13

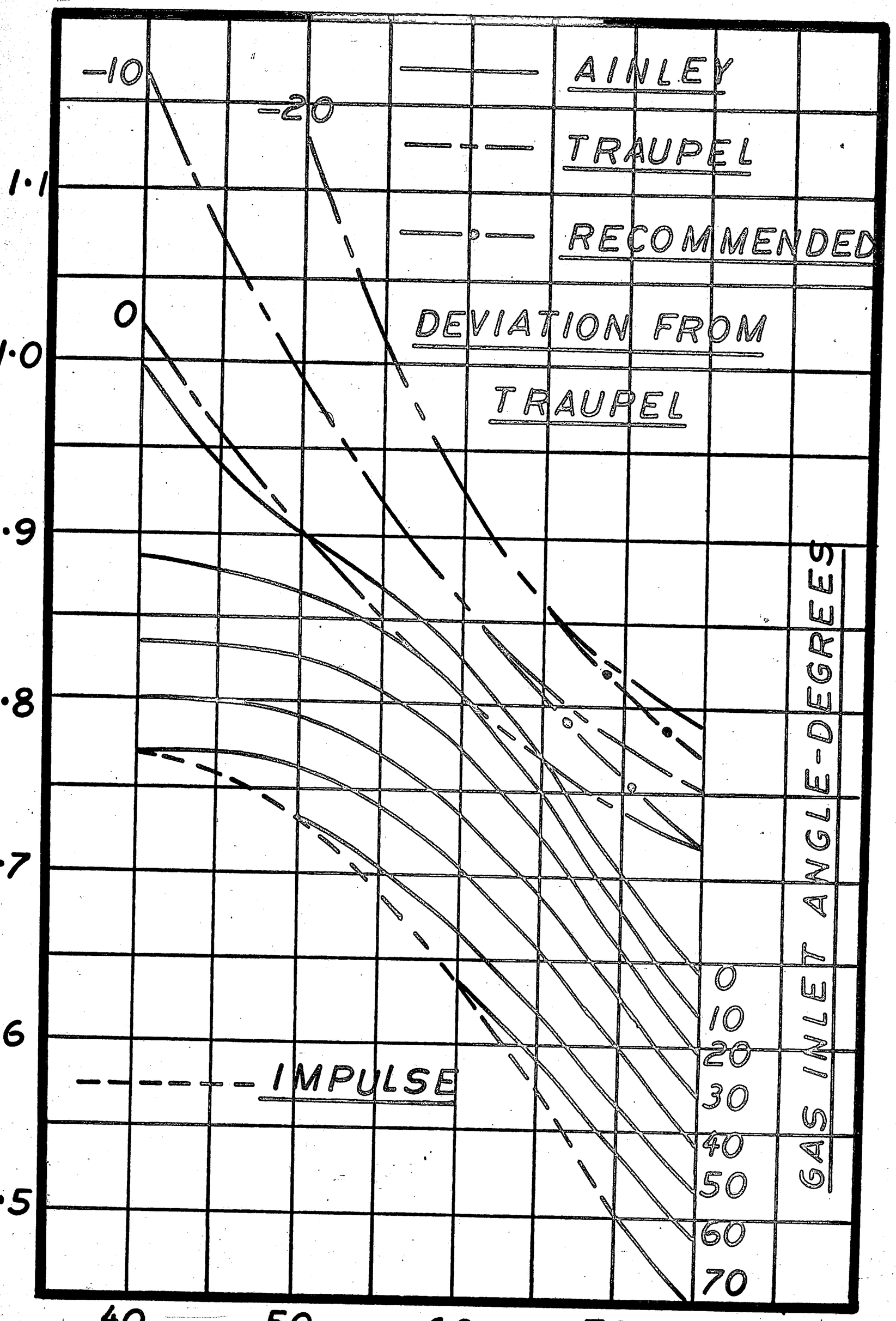
-10
-20
AINLEY
TRAUPEL
RECOMMENDED
DEVIATION FROM
TRAUPEL
1·1
1·0
·9
·8
·7
·6
·5
OPTIMUM SPACE CHORD RATIO
IMPULSE
0
10
20
30
40
50
60
70
GAS INLET ANGLE-DEGREES
40
50
60
70
GAS OUTLET ANGLE DEGREES

-20 degrees. The zero degree curve is included for comparison purposes. As can be seen from examination of figure 2.13 the maximum deviation between Ainley's correlation and that of reference 2 occurs at blade exit angles above 70 degrees, and it is recommended that the curves of reference 2 be modified as shown by the dotted lines on figure 2.13. The reason for reducing the optimum spacing values of reference 2 is that in addition to bringing the curves in line with the recommendations of Ainley, the design of a blade section is a compromise between the required inlet and outlet angles, the blade chord, the section area, the section center of gravity, the section stiffness, and the line up of the leading and trailing edges. It is therefore necessary to put a maximum and minimum tolerance on the blade chord since it is not possible to optimize all of the above parameters at the same time. The tolerance values chosen as acceptable are $\pm$ 5% at the mean section, and $\pm$ 10% at the tip and root section. In the course of a blade design, therefore, a blade chord of up to 10% smaller than the desired optimum may result.

O. Zweifel, reference 3, has obtained a correlation for blade spacing using a load coefficient Ψ_A which is defined as the ratio $\frac{\text{Actual lift}}{\text{ideal lift}}$ where the ideal lift corresponds to an ideal pressure distribution over the blade. For a value of Ψ_A of .9 Zweifel's correlation appears to match that of Ainley's exactly for all values of blade inlet angles occurring at a blade outlet angle of 65°. At angles below 65° Zweifel's correlation gives a smaller value of S/C than that of Ainley's, while above 65° it gives a larger value. Since $\Psi_A \cdot$ S/C approaches zero as the gas outlet angle approaches 90° Zweifel's correlation should be used with caution for high blade outlet angles.

In an aero engine blade weight affects disk weight, which in turn affects shaft weight, the shaft in turn affecting support weight. The selection of the space chord ratio is therefore extremely important, and has a pronounced effect on overall engine weight. As stated previously, for an outlet angle above 65°, Zweifel's correlation would give blades with smaller chords, however, a fair amount of experience and judgement is required to determine

the areas of validity, and it is recommended that for industrial engines where weight is relatively of less importance Ainley's correlation be used as plotted on figure 2.13. Where minimum weight is desirable figure 2.13 may be used for the initial selection of space chord ratio. With the aid of figures 2.5 to 2.11 the penalty incurred by increasing the space chord ratio above the optimum may then be assessed in terms of pressure loss coefficient. In the areas of normal blade loading quite a large reduction in blade chord can be effected for a modest increase in pressure loss coefficient.

Although Zweifel's correlation is not in general recommended, since it is mentioned in the above discussion it is considered appropriate to derive his expression for the optimum spacing of blades.

The tangential force on each blade is the product of the mass flow through each channel and the change in tangential velocity.

Referring to figure 2.14

$$F_\theta = \rho_m C_A \left[C_{\theta 2} + C_{\theta 1} \right] s \qquad 2.1$$

Where ρ_m is the density at the mean velocity condition C_m, and S is the blade pitch. For convenience we will assume the blade angles to be positive as drawn in figure 2.14.

Assuming $C_{A1} = C_{A2} = C_m = C_A$, then the axial force on each blade is given as follows:

$$F_A = \left[P_1 - P_2 \right] S \qquad \text{---------- 2.2}$$

Further, the change in static pressure may be approximated by the following equation

$$P_1 - P_2 = \frac{\rho_m}{2} \left| C_2^2 - C_1^2 \right| + \Delta P_{OL} \qquad \text{---- 2.3}$$

Where ΔP_{OL} is the loss of total pressure across the blade row.

Substituting equation (2.3) into (2.2), we get:

$$F_A = \frac{\rho_m}{2} \left(C_2^2 - C_1^2 \right) S + \Delta P_{OL} \cdot S \qquad \text{---------- 2.4}$$

FIGURE 2·14

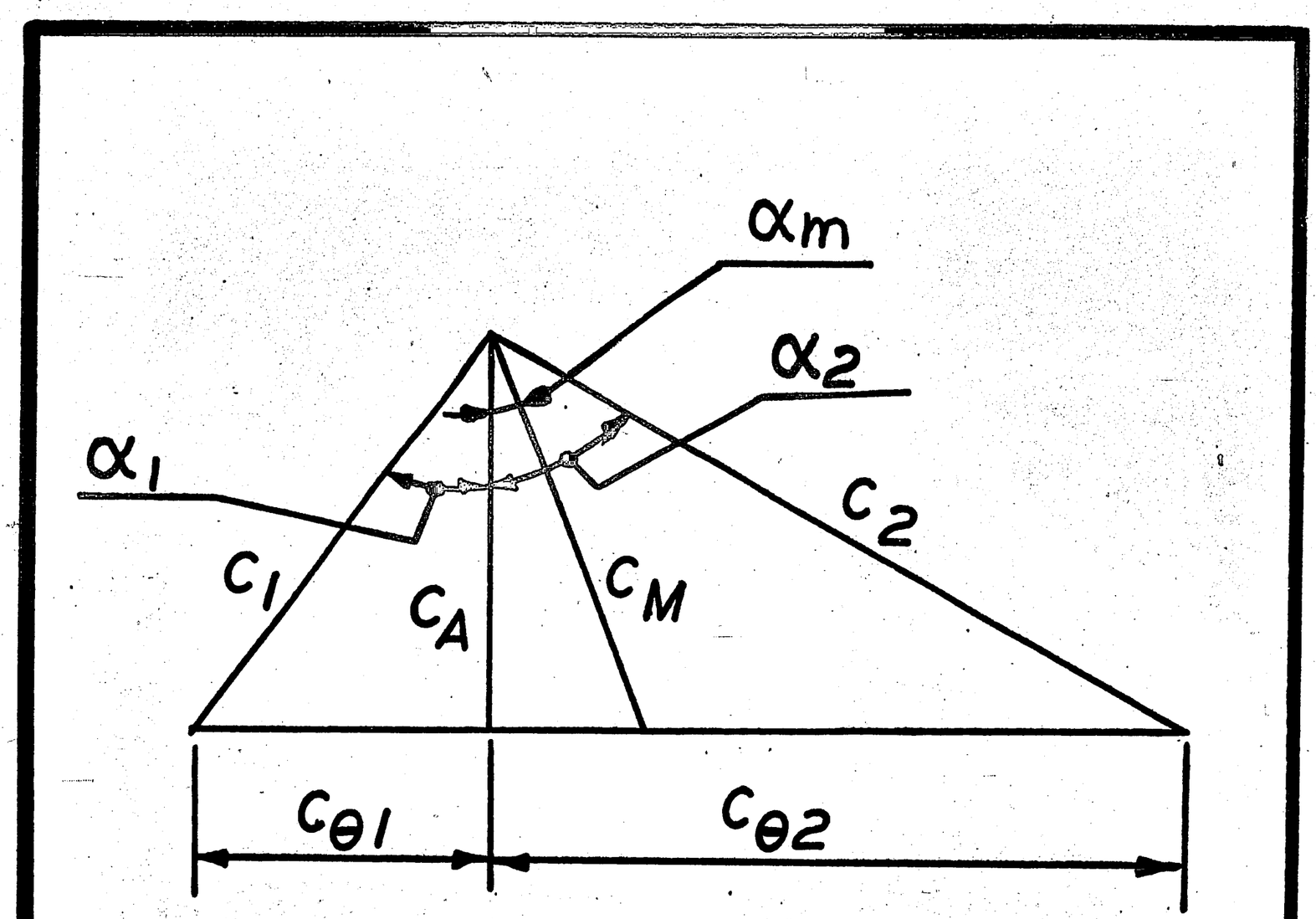

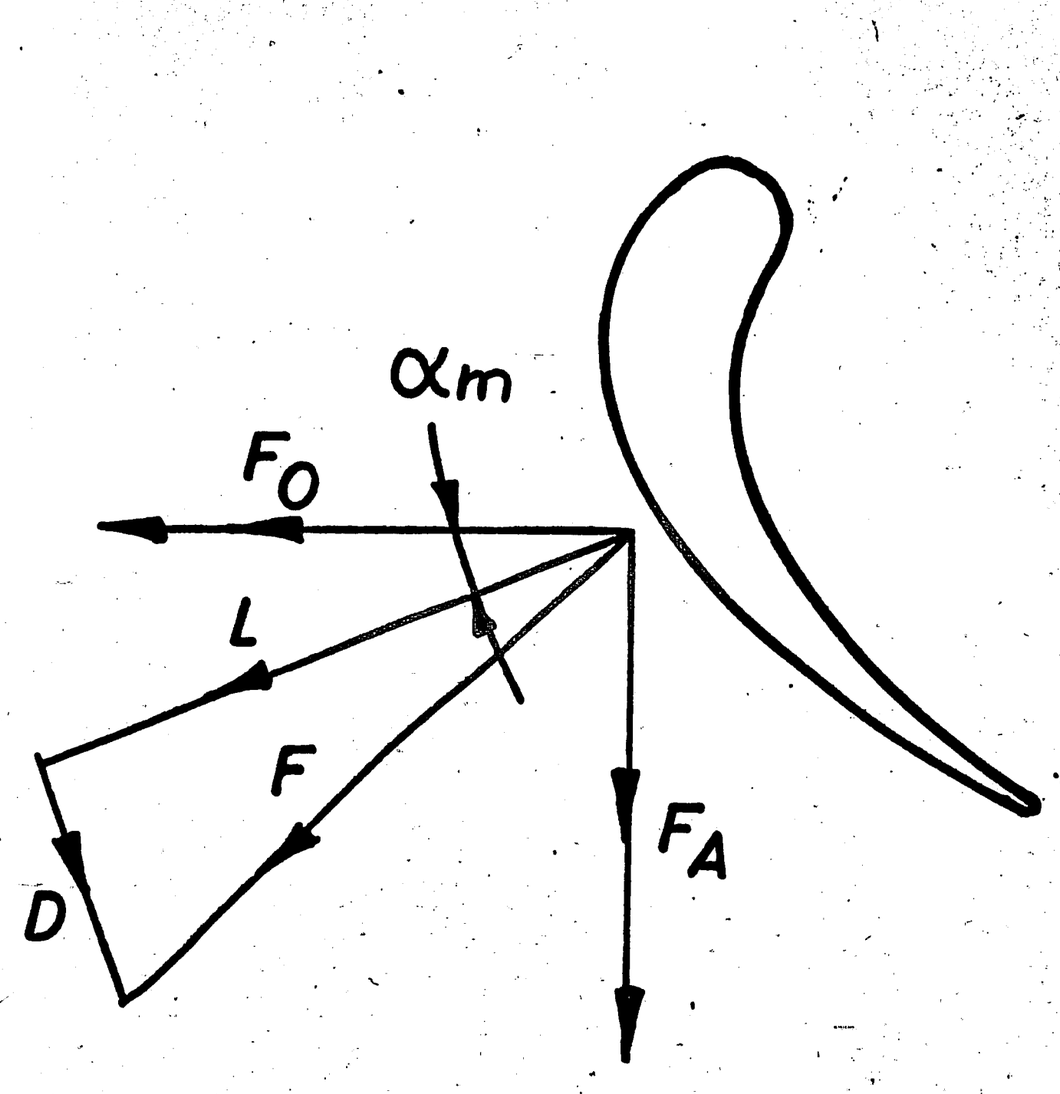

Now $$C_2^2 = C_{\theta 2}^2 + C_A^2$$
$$C_1^2 = C_{\theta 1}^2 + C_A^2$$ } ——— 2.5

and $$C_{\theta 2} = C_A \, TAN \, \alpha_2$$
$$C_{\theta 1} = C_A \, TAN \, \alpha_1$$ } ——— 2.6

Substituting equations (2.5) and (2.6) into (2.4) we get:

$$F_A = S \frac{\rho_m}{2} C_A^2 \left| TAN\alpha_2 + TAN\alpha_1 \right| \cdot \left| TAN\alpha_2 - TAN\alpha_1 \right| + \Delta P_{OL} \cdot S \quad — 2.7$$

and since

$$TAN\alpha_m = \frac{TAN\alpha_2 - TAN\alpha_1}{2}$$

equation (2.7) becomes

$$F_A = S \frac{\rho_m}{2} C_A^2 \, TAN\alpha_m \left| TAN\alpha_2 + TAN\alpha_1 \right| + \Delta P_{OL} \cdot S \quad — 2.8$$

The lift force perpendicular to the mean velocity.

vector C_m is obtained as follows:

$$\begin{aligned} L &= F_\theta \cdot COS\alpha_m + F_A \, SIN\alpha_m \\ &= S \cdot \rho_m \cdot C_A \left| C_{\theta 2} + C_{\theta 1} \right| COS\alpha_m \\ &\quad + S \cdot \rho_m \cdot C_A^2 \, TAN\alpha_m \left| TAN\alpha_2 + TAN\alpha_1 \right| SIN\alpha_m \\ &\quad + \Delta P_{OL} \cdot S \cdot SIN\alpha_m \end{aligned} \quad ——— 2.9$$

FIGURE 2·15

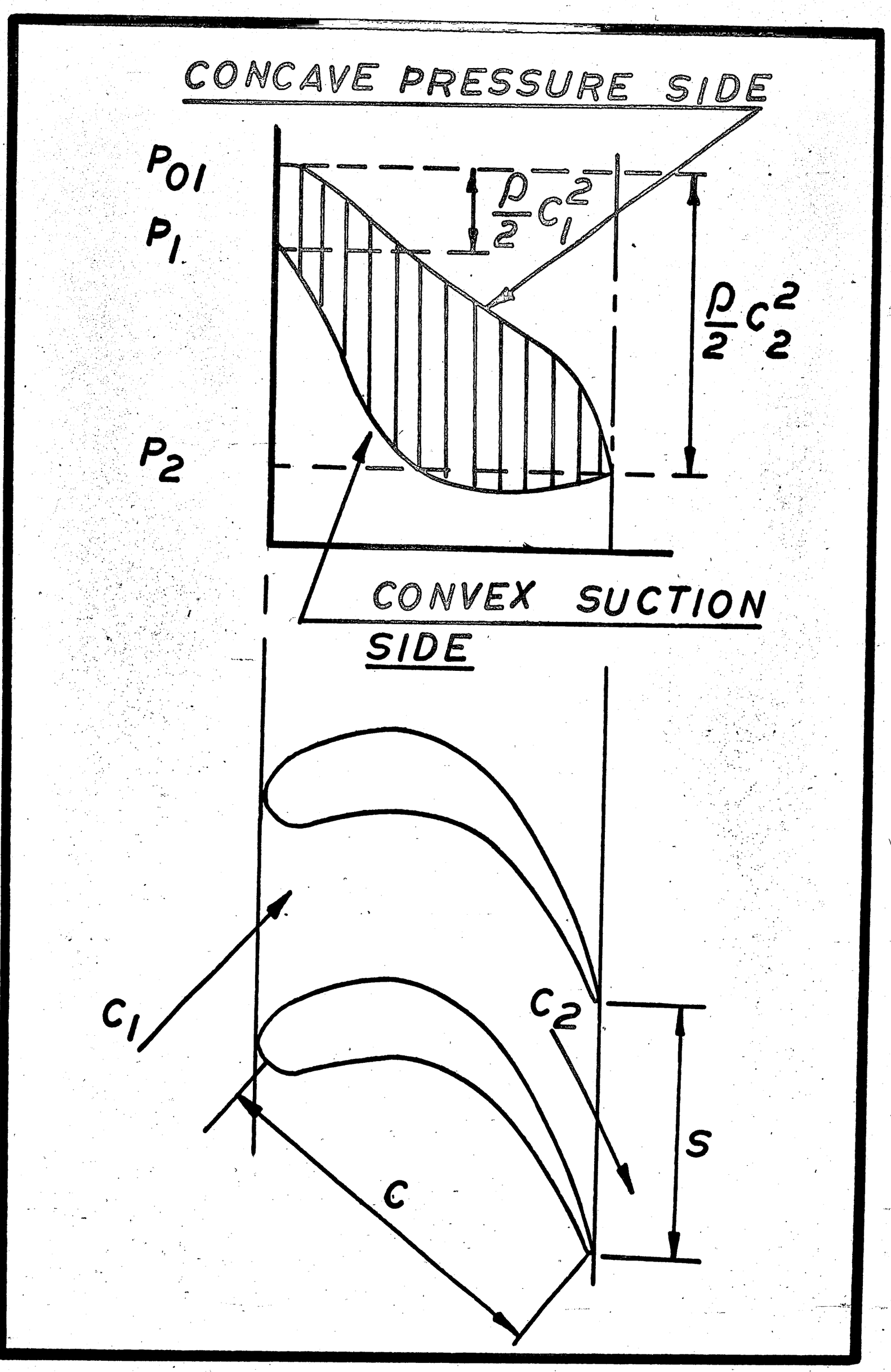
CONCAVE PRESSURE SIDE
P_{01}
P_1
P_2
$\frac{\rho}{2}c_1^2$
$\frac{\rho}{2}c_2^2$
CONVEX SUCTION SIDE
c_1
c_2
c
s

Substituting equations (2.5) and (2.6) into (2.9) we get:

$$L = S \cdot \rho_m \cdot C_A^2 \left| TAN\alpha_2 + TAN\alpha_1 \right| SEC\alpha_m + \Delta P_{OL} \cdot S \cdot SIN\alpha_m \quad \text{——— 2.10}$$

The drag force parallel to the mean velocity vector C_m is obtained as follows:

$$\begin{aligned} D &= F_A \cdot COS\alpha_m - F_\theta \cdot SIN\alpha_m \\ &= S \cdot \rho_m \cdot C_A^2 SIN\alpha_m \left| TAN\alpha_2 - TAN\alpha_1 \right| \\ &\quad + \Delta P_{OL} \cdot S \cdot SIN\alpha_m \\ &\quad - S \cdot \rho_m \cdot C_A \left| C_{\theta 2} + C_{\theta 1} \right| SIN\alpha_m \quad \text{——— 2.11} \end{aligned}$$

Substituting equation (2.6) into (2.11) we get:

$$D = S \cdot \Delta P_{OL} \cdot SIN\alpha_m \quad \text{——— 2.12}$$

Substituting equation (2.12) into (2.10) we get:

$$L = S \cdot \rho_m \cdot C_A^2 \left| TAN\alpha_2 + TAN\alpha_1 \right| SEC\alpha_m + D \quad \text{— 2.13}$$

For zero drag equation (2.13) becomes

$$L = S \cdot \rho_m \cdot C_A^2 \left| TAN\alpha_2 + TAN\alpha_1 \right| SEC\alpha_m \quad \text{——— 2.14}$$

Zweifel defines the aerodynamic load factor Ψ_A as the ratio $\frac{L}{\text{ideal lift}}$ where the ideal lift corresponds to an ideal pressure distribution which can never be realized. Referring to figure 2.15 this ideal pressure distribution assumes the pressure P_{TOT} on the concave pressure side of the blade remains constant over the whole blade, while on the convex suction side of the blade the pressure drops instantaneously to P_{2S} at the leading edge, where P_{2S} is the static pressure at the trailing edge and corresponds to C_2 the exit velocity.

This gives an ideal lift, as follows:

$$L_{ideal} = \frac{\rho_m}{2} \cdot C_2^2 \cdot C \qquad \text{2·15}$$

Where C = blade chord.

Substituting equations (2.5) and (2.6) into (2.15), we get:

$$L_{ideal} = \frac{\rho_m}{2} \cdot C_A^2 \cdot SEC^2\alpha_2 \cdot C \qquad \text{2·16}$$

The load coefficient Ψ_A then becomes

$$\Psi_A = 2\frac{S}{C}\left(TAN\alpha_2 + TAN\alpha_1\right)\frac{COS^2\alpha_2}{COS\,\alpha_m} \qquad \text{2·17}$$

Zweifel has shown that in applying the above method to experimental data obtained by Christiani and Keller, and by the Brown Boveri Company, Ψ_A is practically constant at 0.9 for cascades with optimum spacing, whether the flow is accelerating or decelerating, and whether the deflection is large or small.

Figure 2.16 is a plot of equation (2.17) for $\Psi_A = 0.9$.

2.2 Secondary and leakage loss coefficient

Ainley has shown that the secondary losses may be expressed by an equation of the form

$$C_{DS} = \lambda C_L^2 / (S/C)$$

Where λ is dependent primarily upon the degree of acceleration of the gas through the blade row. Similarly it may be shown that tip clearance losses may be expressed by

$$C_{DK} = B \left(\frac{K}{H}\right) C_L^2 / (S/C)$$

Where B is a constant depending upon whether the blades are shrouded or unshrouded. C_{DS} and C_{DK} are the secondary and leakage drag coefficients respectively.

Since the equations for secondary and tip losses are similar in form it is convenient to treat them together. Converting the drag coefficients into loss coefficients, the sum of the secondary and tip clearance losses are given by Ainley as follows:

$$Y_S + Y_K = \left[\lambda + B\left(\frac{K}{H}\right)\right]\left[\frac{C_L^2}{S/C}\right]^2\left[\frac{\cos^2\alpha_2}{\cos^3\alpha_m}\right] - 2.18$$

Where Y_S = Secondary loss coefficient

Y_K = Leakage loss coefficient

C_L = Lift coefficient

S/C = Space/chord ratio

α_m = Mean efflux angle of mean velocity vector C_m

B = Constant = 0.5 for row with radial tip clearance.

= 0.25 for row with shroud seal

k = Radial tip clearance

H = Annulus height (equals blade height if radial tip clearance is zero)

α_2 = Blade outlet angle

λ = Function of $\left(\frac{A_1}{A_2}\right)^2 \Big/ \left(1 + \frac{ID}{OD}\right)$

$$A_1 = A_{n1} \cos \alpha_1^*$$

$$A_2 = A_{n2} \cos \alpha_2$$

A_n = Annulus area

Ainley recommends restricting the range of equation (2.18) to $-1.5 < i/i_s < 1.0$

Where i_s is the stalling incidence.

For values of i/i_s less than -1.5 or greater than 1.0 it is recommended that the losses be maintained constant at those values for -1.5 and 1.0 respectively.

In order to reduce the time required to estimate the secondary and leakage loss coefficients equation (2.18) has been written in the form

$$Y_S + Y_K = \left[\lambda + B\left(\frac{K}{H}\right)\right]\bar{\mu} \qquad 2.19$$

Where

$$\bar{\mu} = \left[\frac{C_L}{S/C}\right]^2 \left[\frac{\cos^2\alpha_2}{\cos^3\alpha_m}\right] \qquad 2.20$$

The term $\left[\frac{C_L}{S/C}\right]$ is obtained as a function of the inlet and outlet gas angles as follows:

From equation (2.14)

$$L = S \cdot \rho_m \cdot C_A^2 \left| TAN\alpha_2 + TAN\alpha_1 \right| SEC\alpha_m$$

The lift coefficient is defined in terms of $\frac{1}{2} \rho_m C_m^2 C$

i.e.

$$C_L = \frac{L}{\frac{1}{2} \rho_m C_m^2 C}$$

$$= 2 \frac{S}{C} \frac{C_A^2}{C_m^2} \left[TAN\alpha_2 + TAN\alpha_1 \right] SEC\alpha_m$$

——— 2.21

and since $C_m = \frac{C_A}{COS\alpha_m}$ equation (2.21) becomes

$$C_L = 2 \frac{S}{C} \left[TAN\alpha_2 + TAN\alpha_1 \right] COS\alpha_m$$

or

$$\left[\frac{C_L}{S/C} \right]^2 = 4 \left| TAN\alpha_2 + TAN\alpha_1 \right|^2 \frac{COS^2\alpha_m}{1} \quad — 2.22$$

Substituting equation (2.22) into (2.20), we get:

$$\bar{\mu} = 4 \left| TAN\alpha_2 + TAN\alpha_1 \right|^2 \frac{COS^2\alpha_2}{COS\,\alpha_m} \quad ——— 2.23$$

Figure 2.17 is a plot of equation (2.23), and figure 2.18 is a plot of the parameter λ as a function of

$$\left(\frac{A_2}{A_1}\right)^2 \Big/ \left(1 + \frac{ID}{OD}\right)$$

In order to determine secondary and leakage loss coefficients the values of $\bar{\mu}$ and λ are obtained from figures 2.17 and 2.18, which together with a knowledge of the blade height, tip clearance, and the constant B provides all the information for the solution of equation (2.19).

Finally, having obtained the profile loss coefficient as shown in section 2.1, and the secondary and leakage loss coefficients as shown in this section, the total loss coefficient Y_T is the sum of the profile, secondary and leakage loss coefficients, i.e.

$$Y_T = Y_P + Y_S + Y_K$$

As stated previously all the loss correlations assume a trailing edge thickness of 2% of the blade pitch. Figure 2.19 provides a correction factor to be applied to the total loss coefficient Y_T where the trailing edge thickness of the blade is other than 2% of the pitch.

FIGURE 2·16

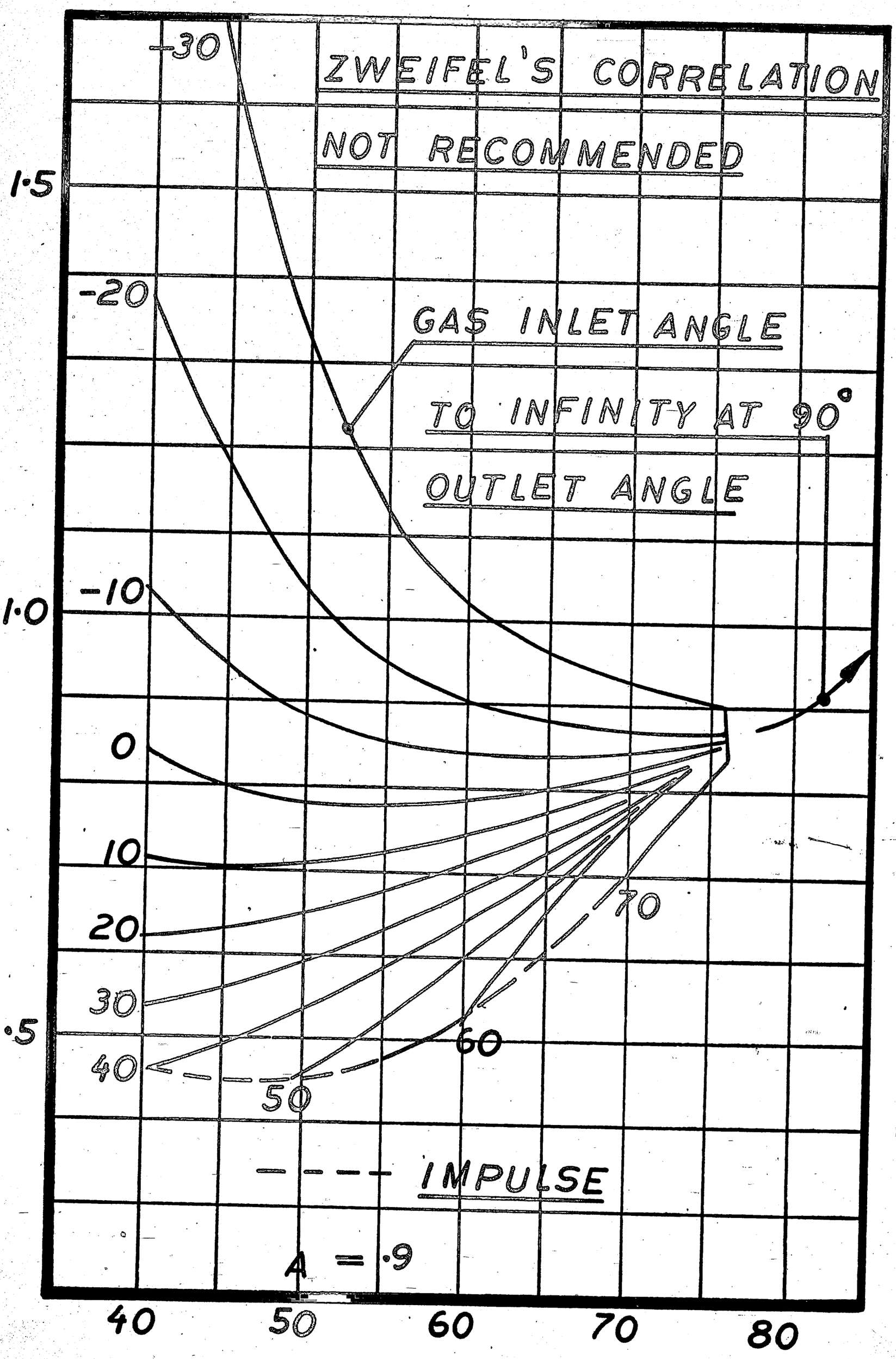
ZWEIFEL'S CORRELATION
NOT RECOMMENDED
GAS INLET ANGLE
TO INFINITY AT 90°
OUTLET ANGLE
-30
-20
-10
0
10
20
30
40
50
60
70
1·5
1·0
·5
OPTIMUM SPACE CHORD RATIO
IMPULSE
A = ·9
40
50
60
70
80
GAS OUTLET ANGLE DEGREES

FIGURE 2·17

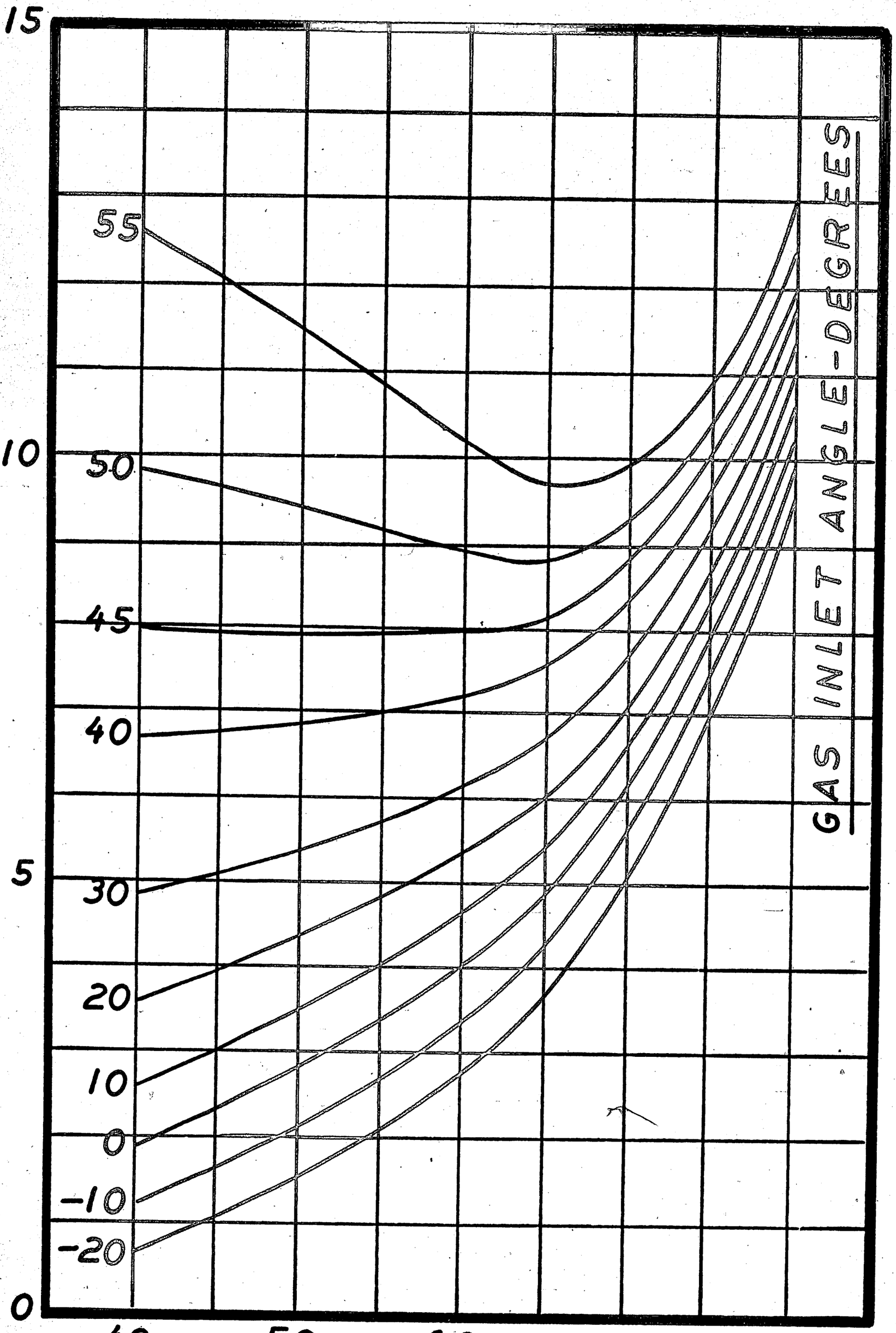
15
10
5
0
$\mu = \left[\frac{C_L/S_{/C}}{\cos^3 \alpha_m}\right]^2 \left[\frac{\cos^2 \alpha_2}{\cos^3 \alpha_m}\right]$
55
50
45
40
30
20
10
0
-10
-20
40
50
60
70
80
GAS INLET ANGLE-DEGREES
GAS OUTLET ANGLE DEGREES

FIGURE 2·18

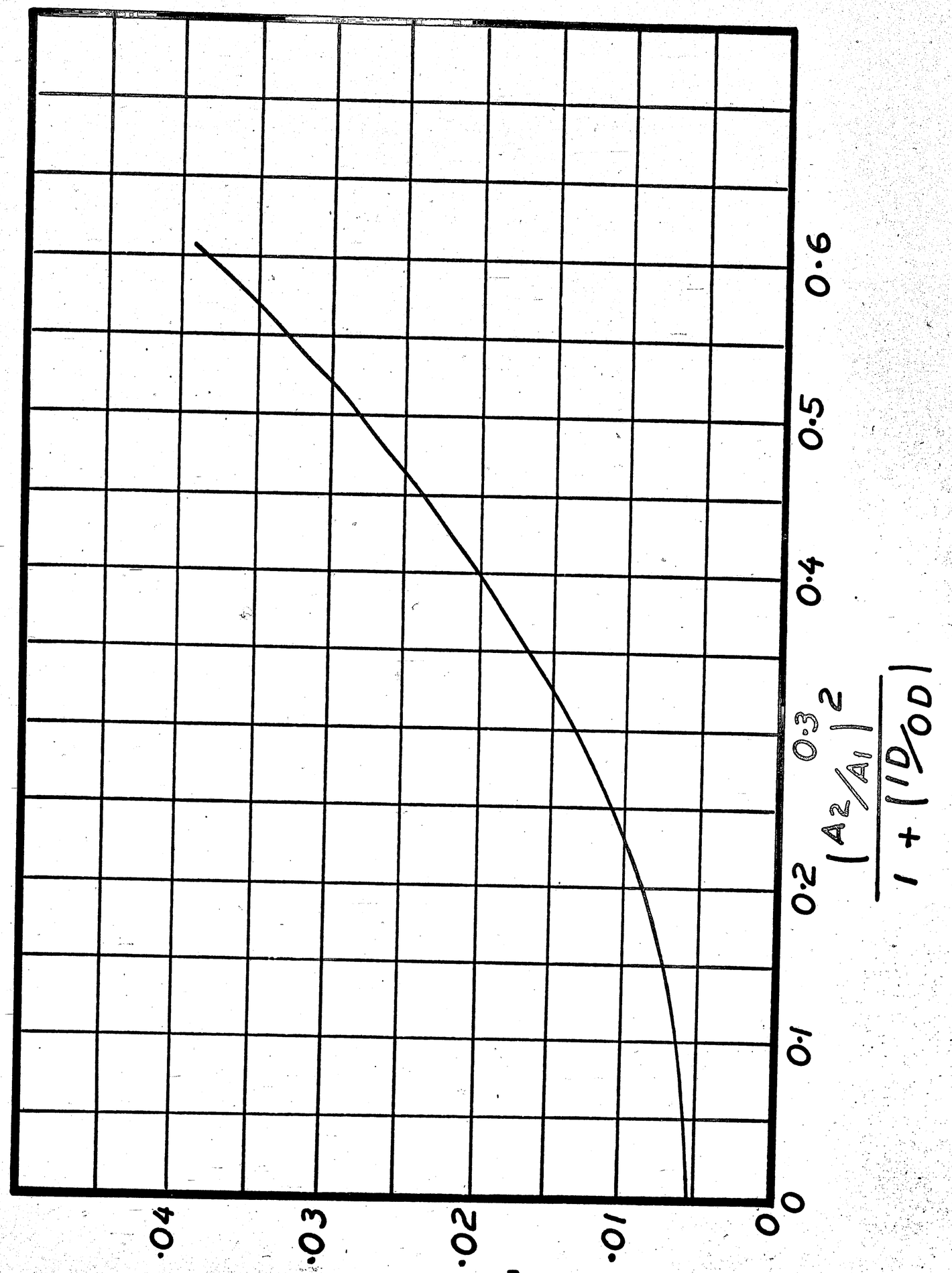
0
.01
.02
.03
.04
$\gamma = \frac{C_{DS}}{C_L^2} \cdot \frac{S}{C}$
0
0.1
0.2
0.3
0.4
0.5
0.6
$\frac{(A_2/A_1)^2}{1 + (1D_{OD})}$

FIGURE 2·19

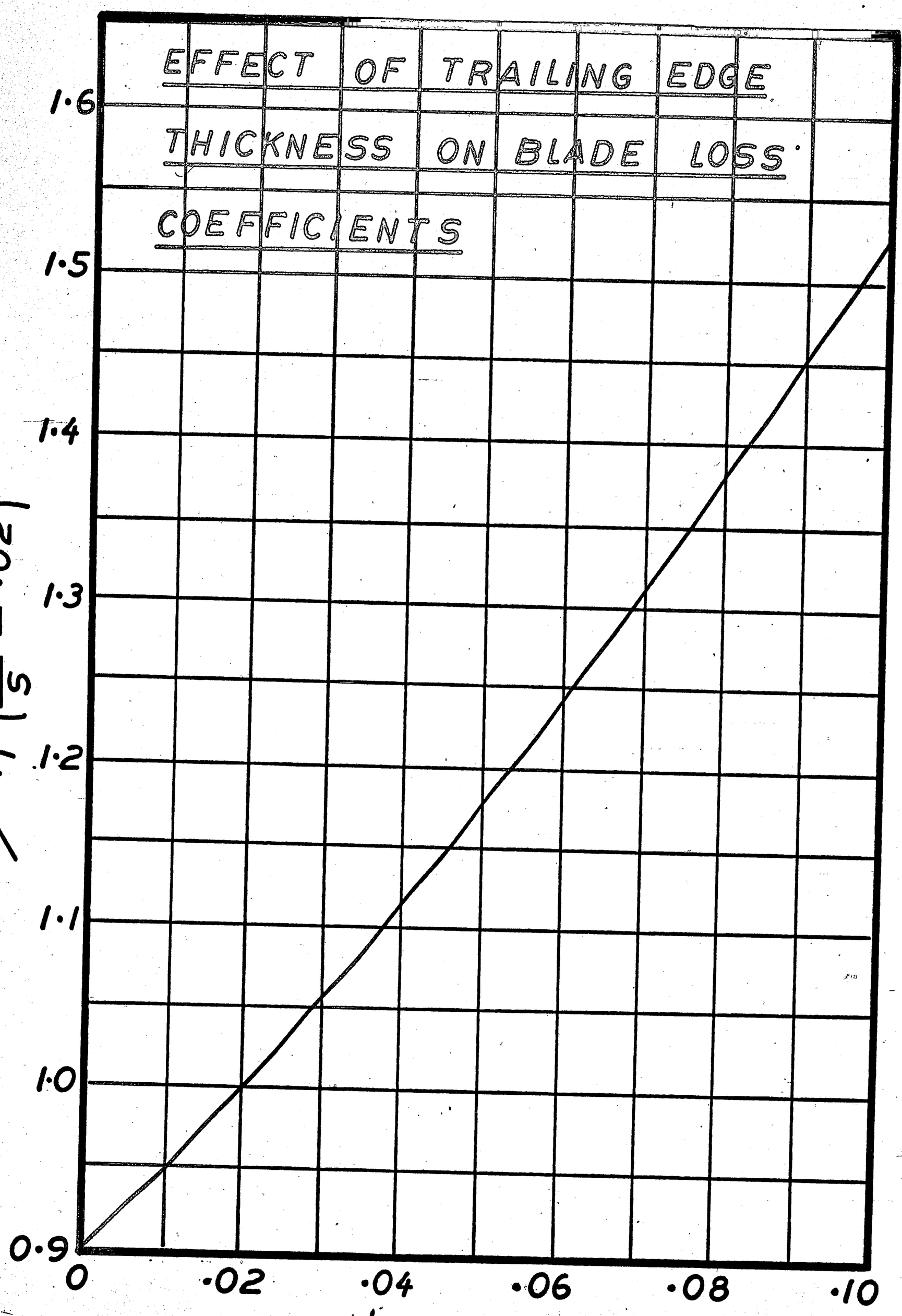
EFFECT OF TRAILING EDGE
THICKNESS ON BLADE LOSS
COEFFICIENTS
1·6
1·5
1·4
1·3
1·2
1·1
1·0
0·9
$Y_T / Y_T \left(\frac{te}{s} = .021\right)$
0
·02
·04
·06
·08
·10
$\frac{te}{s}$

2.3 Three Dimensional Considerations

The previous sections have been concerned with the estimation of optimum parameters, and with the prediction of efficiency based upon gas angles and blade losses estimated at the mean diameter. The purpose of this section is to define velocity components, pressure, and density throughout the flow field assuming the mean diameter velocity diagram is given together with a prescribed variation of peripheral velocity component with radius. This will enable the velocity diagrams to be defined at all radii, which in turn will enable blade profiles to be designed to produce the required deflection to the flow. Obtaining the above description of the flow field requires the solving of the Navier-Stokes equations for compressible, unsteady, viscous flow with turbulence, however, it has been found possible to introduce simplifying assumptions which greatly reduce the complexity of the problem while still enabling a reasonably accurate prediction of efficiency and capacity to be made.

Neglecting turbulence and assuming the usual boundary layer approximation that away from solid surfaces the flow

is inviscid, Newtons second law of motion may be stated as follows

$$\frac{D\bar{C}}{Dt} = \bar{F} - \frac{1}{\rho}\nabla P \qquad 2.24$$

and the continuity equation may be stated

$$\frac{D\rho}{Dt} + \rho \nabla \cdot \bar{C} = 0 \qquad 2.25$$

Where $\bar{C}$ = absolute vector velocity of gas

t = time

$\bar{F}$ = force acting on gas particles by blade per unit mass of gas.

ρ = mass density

p = static pressure

Consider a rotor blade. At the blade surfaces on opposite sides of a blade the relative velocities must in general be different from each other in order to produce the resultant blade force necessary for a change in energy level. Hence the flow cannot be axisymmetric everywhere. Also, stationary blade rows are used to change the direction of the flow which induces velocity changes in

the peripheral direction across the blade channel, and therefore the stator flow cannot be axisymmetric either. The assumption that the flows in both stators and rotors are steady is not in agreement with reality since a steady relative flow at the exit of a rotor row produces a non-steady flow in the following stator row. For the case of an axial flow turbine with normal stage loading it is possible to simplify the problem by reducing the three dimensional problem to that of two 2-Dimensional problems. Normal blade loading is defined here as a stage in which $\frac{K_p \Delta T}{U^2} < 2.0$ and/or the included annulus flare angle is less than 35°. The two dimensional problems to be solved are:

(a) The axisymmetric flow solution.

(b) The blade to blade solution.

An axisymmetrical flow is defined as a flow in which the stream surfaces are surfaces of revolution. Further, radial stream surfaces are assumed to coincide with blade surfaces. As the number of blades in a blade row is increased the actual flow approaches that of an axisymmetrical flow, and hence axisymmetric flow is

sometimes called the "infinite number of blades" solution.

To a first approximation it may be assumed that the flow has not only axisymmetric stream surfaces, but that the fluid motion on these surfaces is also axisymmetric.

This approximation allows the relative motions to be analysed in an absolute coordinate system since the flows relative to the rotor now coincide with the absolute flows (i.e. the flow is assumed steady).

With the above assumptions equation (2.24) may be written as follows

$$\frac{\partial \bar{C}}{\partial t} + \bar{C} \cdot \nabla \bar{C} = \bar{F} - \frac{1}{\rho} \nabla P \qquad 2.26$$

and since we are assuming steady flow $\frac{\partial \bar{C}}{\partial t} = 0$

Therefore $$\bar{C} \cdot \nabla \bar{C} = \bar{F} - \frac{1}{\rho} \nabla P \qquad 2.27$$

In cylindrical co-ordinates (r, θ, a), equation (2.27) becomes

$$C_r \frac{\partial C_r}{\partial r} + \frac{C_\theta}{r} \frac{\partial C_r}{\partial \theta} + C_a \frac{\partial C_r}{\partial a} - \frac{C_\theta^2}{r} = F_r - \frac{1}{\rho} \frac{\partial P}{\partial r}$$

$$C_r \frac{\partial C_\theta}{\partial r} + \frac{C_\theta}{r} \frac{\partial C_\theta}{\partial \theta} + C_a \frac{\partial C_\theta}{\partial a} + \frac{C_r C_\theta}{r} = F_\theta - \frac{1}{\rho} \frac{\partial P}{\partial \theta}$$

$$C_r \frac{\partial C_a}{\partial r} + \frac{C_\theta}{r} \frac{\partial C_a}{\partial \theta} + C_a \frac{\partial C_a}{\partial a} = F_a - \frac{1}{\rho} \frac{\partial P}{\partial a}$$

} 2.28

In the r, θ and a directions respectively.

Now since we are assuming axisymmetric flow $\frac{\partial}{\partial \theta}$ of all terms is negligible therefore equation (2.28) may be written:

$$C_r \frac{\partial C_r}{\partial r} + C_a \frac{\partial C_r}{\partial a} - \frac{C_\theta^2}{r} = F_r - \frac{1}{\rho} \frac{\partial P}{\partial r}$$

$$C_r \frac{\partial C_\theta}{\partial r} + C_a \frac{\partial C_\theta}{\partial a} + \frac{C_r C_\theta}{r} = F_\theta$$

$$C_r \frac{\partial C_a}{\partial r} + C_a \frac{\partial C_a}{\partial a} = F_a - \frac{1}{\rho} \frac{\partial P}{\partial a}$$

} 2.29

Equation (2.25) may be re-written as follows:

$$\frac{\partial \rho}{\partial t} + \bar{C} \cdot \nabla \rho + \rho \nabla \cdot \bar{C} = 0 \qquad 2.30$$

or

$$\frac{\partial \rho}{\partial t} + \nabla \cdot \left| \rho \bar{c} \right| = 0 \qquad \text{——— 2.31}$$

and since we are assuming steady flow $\frac{\partial \rho}{\partial t} = 0$

Therefore, $\nabla \cdot \left| \rho \bar{c} \right| = 0$ ——— 2.32

In cylindrical co-ordinates (r, θ, a), equation (2.32) becomes,

$$\frac{\partial \left| \rho_r c_r \right|}{\partial r} + \frac{1}{r} \frac{\partial \left| \rho_r c_\theta \right|}{\partial \theta} + \frac{\partial \left| \rho_r c_a \right|}{\partial a} = 0 \qquad \text{——— 2.33}$$

and since we are assuming axial symmetry the term $\frac{1}{r} \frac{\partial \left| \rho_r c_\theta \right|}{\partial \theta}$ is negligible and therefore equation (2.33) becomes:

$$\frac{\partial \left| \rho_r c_r \right|}{\partial r} + \frac{\partial \left| \rho_r c_a \right|}{\partial a} = 0 \qquad \text{——— 2.34}$$

Limiting the investigation to the flow between blade rows, and neglecting the effects of any interference, equation (2.29) becomes:

$$\left.\begin{aligned} C_r\frac{\partial C_r}{\partial r} + C_a\frac{\partial C_r}{\partial a} - \frac{C_\theta^2}{r} &= -\frac{1}{\rho}\frac{\partial P}{\partial r} \\ C_r\frac{\partial C_\theta}{\partial r} + C_a\frac{\partial C_\theta}{\partial a} + \frac{C_r C_\theta}{r} &= 0 \\ C_r\frac{\partial C_a}{\partial r} + C_a\frac{\partial C_a}{\partial a} &= -\frac{1}{\rho}\frac{\partial P}{\partial a} \end{aligned}\right\} 2.35$$

Considering the radial flow equation of equations (2.36)

i.e.

$$C_r\frac{\partial C_r}{\partial r} + C_a\frac{\partial C_r}{\partial a} - \frac{C_\theta^2}{r} = -\frac{1}{\rho}\frac{\partial P}{\partial r} \quad 2.36$$

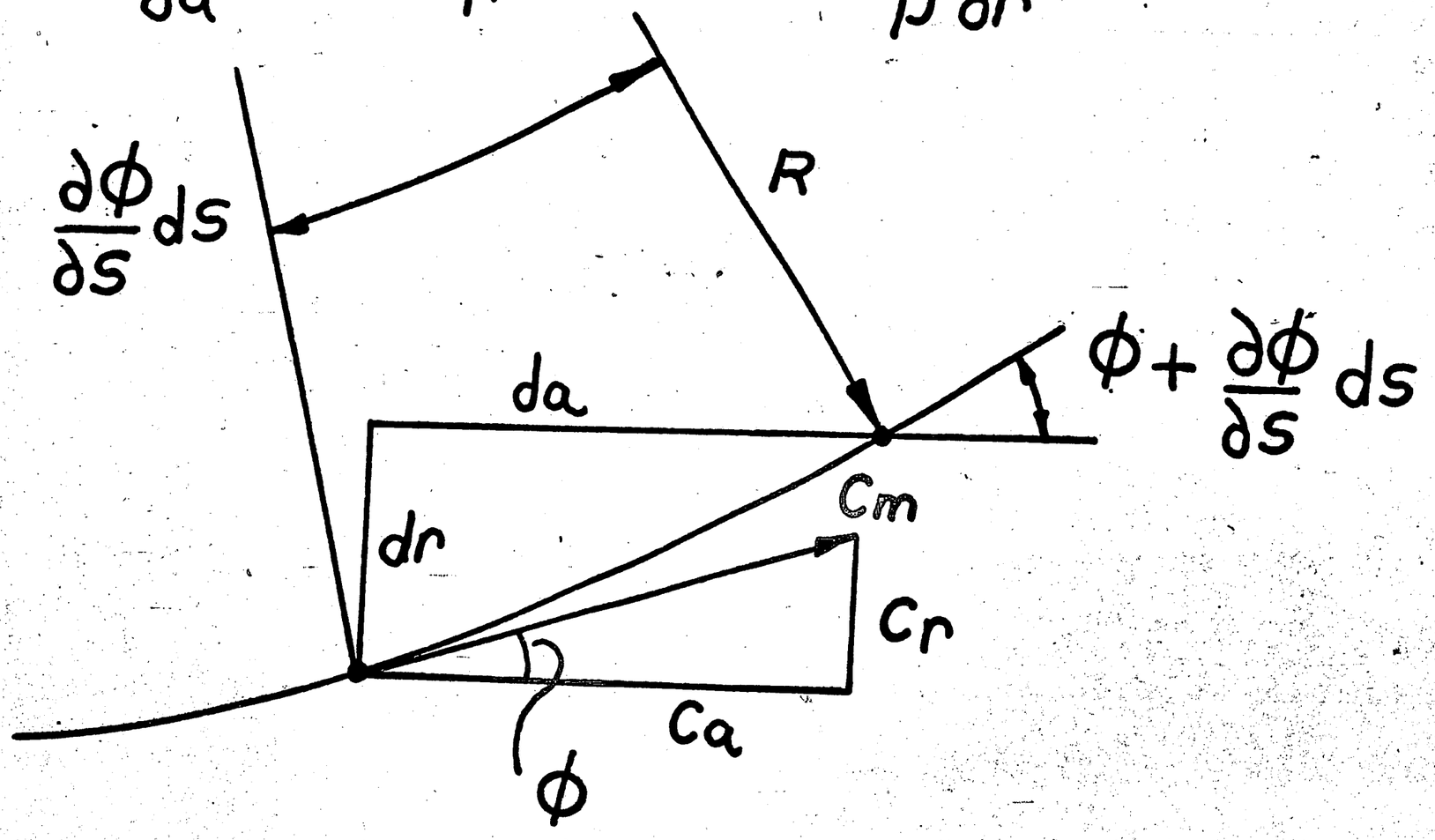

FIGURE 2·20

Referring to figure 2.20

$$C_r \frac{\partial C_r}{\partial r} + C_a \frac{\partial C_r}{\partial a} = \frac{dr}{dt} \cdot \frac{\partial C_r}{\partial r} + \frac{da}{dt} \cdot \frac{\partial C_r}{\partial a}$$

$$OR \quad C_r \frac{\partial C_r}{\partial r} + C_a \frac{\partial C_r}{\partial a} = \frac{1}{dt}\left[\frac{\partial C_r}{\partial r} dr + \frac{\partial C_r}{\partial a} da\right]$$

$$= \frac{1}{dt} \frac{\partial C_r}{\partial s} ds \qquad \text{——— 2·37}$$

and since

$$\frac{1}{dt} \frac{\partial C_r}{\partial s} ds = \frac{ds}{dt} \frac{\partial C_r}{\partial s}$$

$$= C_m \frac{\partial C_r}{\partial s} \qquad \text{——— 2·38}$$

$$C_r \frac{\partial C_r}{\partial r} + C_a \frac{\partial C_r}{\partial a} = C_m \frac{\partial C_r}{\partial s} \qquad \text{——— 2·39}$$

Now

$$C_r = C_m \, SIN \, \phi$$

and

$$\frac{\partial C_r}{\partial s} = SIN \, \phi \frac{\partial C_m}{\partial s} + C_m \cos \phi \frac{\partial \phi}{\partial s} \qquad \text{— 2·40}$$

Substituting equation (2.40) into (2.39), we get:

$$C_r \frac{\partial C_r}{\partial r} + C_a \frac{\partial C_r}{\partial a} = C_m \, SIN\phi \frac{\partial C_m}{\partial s}$$

$$+ C_m^2 \cos\phi \frac{\partial \phi}{\partial s} \quad \text{—2.41}$$

Now

$$ds = \frac{\partial \phi}{\partial s} ds \, R$$

or

$$\frac{\partial \phi}{\partial s} = \frac{1}{R} \quad \text{R = radius of curvature of streamline} \quad \text{—2.42}$$

Substituting equation (2.42) into (2.41), we get:

$$C_r \frac{\partial C_r}{\partial r} + C_a \frac{\partial C_r}{\partial a} = C_m \frac{\partial C_m}{\partial s} SIN\phi + \frac{C_m^2}{R} \cos\phi \quad \text{—2.43}$$

and substituting (2.43) into equation (2.36), we get:

$$-\frac{1}{\rho} \frac{\partial P}{\partial r} = -\frac{C_\theta^2}{r} + C_m \frac{\partial C_m}{\partial s} SIN\phi$$

$$+ \frac{C_m^2}{R} \cos\phi \quad \text{—2.44}$$

In an axial flow turbine ϕ is normally small, therefore, it may be assumed that

$$SIN\,\phi = 0$$

$$COS\,\phi = 1$$

Equation (2.44) then becomes

$$\frac{1}{\rho}\frac{\partial P}{\partial r} = \frac{C_\theta^2}{r} + \frac{C_m^2}{R} \qquad 2\,45$$

If we further assume the radius of curvature of the streamlines to be large equation (2.45) reduces to the so-called simple radial equilibrium equation.

i.e. $$\frac{\partial P}{\partial r} = \frac{\rho C_\theta^2}{r} \qquad 2.46$$

In section 1.5 equations were derived which enabled a preliminary mean section design to be checked at the root section for rotor divergence and Mach number. The basic assumptions used in deriving these equations were:

1. Equation 2.46 was assumed to apply before and after the blade row.
2. The tangential velocity distribution was such that

$$rC_\theta = \text{constant.}$$

With the above assumptions the flow solution used in section 1.4 may also be obtained as follows:-

First the partial differential equation 2.46 becomes an ordinary differential equation since conditions vary with r only i.e.

$$\frac{dP}{dr} = \frac{\rho C_\theta^2}{r} \qquad 2.47$$

Stagnation enthalpy is defined as

$$h_o = \frac{c^2}{2} + h$$

$$= \frac{C_a^2 + C_\theta^2 + C_r^2}{2} + h$$

$$= \frac{C_a^2 + C_\theta^2}{2} + h \qquad 2.48$$

since $C_r = 0$

Differentiating with respect to r equation 2.48 becomes:

$$\frac{dh_o}{dr} = \frac{d(C_a^2)}{2\,dr} + \frac{d(C_\theta^2)}{2\,dr} + \frac{dh}{dr} \qquad 2.49$$

Gibb's relation derived from the second law of thermodynamics is

$$T\,dS = dh - \frac{1}{\rho}\,dP \qquad 2.50$$

Dividing by dr

$$T\frac{dS}{dr} = \frac{dh}{dr} - \frac{1}{\rho}\frac{dP}{dr} \qquad 2.51$$

Substituting equation (2.51) into (2.49), we get:

$$\frac{dh_o}{dr} = \frac{d\left[C_a^2\right]}{2\,dr} + \frac{d\left[C_\theta^2\right]}{2\,dr} + T\frac{dS}{dr} + \frac{1}{\rho}\frac{dP}{dr}$$

or

$$\frac{dh_o}{dr} - T\frac{dS}{dr} = \frac{d\left[C_a^2\right]}{2\,dr} + \frac{d\left[C_\theta^2\right]}{2\,dr} + \frac{1}{\rho}\frac{dP}{dr} \qquad 2.52$$

Assuming no change of entropy or enthalpy with radius equation (2.52) becomes:

$$\frac{d\left[C_a^2\right]}{2\,dr} + \frac{d\left[C_\theta^2\right]}{2\,dr} + \frac{1}{\rho}\frac{dP}{dr} = 0 \qquad 2.53$$

Substituting equation (2.47) into (2.53), we get:

$$\frac{d\left[C_a^2\right]}{dr} + \frac{d\left[C_\theta^2\right]}{dr} + \frac{2\,C_\theta^2}{r} = 0 \qquad 2.54$$

or

$$\frac{d(Ca^2)}{dr} + \frac{1}{r^2}\frac{d(rC_\theta)^2}{dr} = 0 \qquad \text{——— 2·55}$$

If we now assume simple radial equilibrium i.e.

$$rC_{\theta 1} = CONSTANT, \quad rC_{\theta 2} = CONSTANT$$

then from equation (2.55) Ca is constant both after stator and rotor and we arrive at the solution given on page 40

The general form of the radial equilibrium equation, neglecting streamline curvature may be written as follows:

$$2\left[\frac{dh_o}{dr} - T\frac{dS}{dr}\right] = \frac{d(Ca^2)}{dr} + 2\frac{C_\theta}{r}\frac{d(rC_\theta)}{dr} \qquad \text{— 2·56}$$

In the calculations which follow it will be assumed that, at each axial station, there is no variation of total enthalpy or entropy with radius. Assuming that ahead of the first stage the flow is homenergic, then, the condition of constant enthalpy will be met if the rotor blades of the stages are designed such that each fluid particle undergoes the same change in energy.

Regarding the condition of constant entropy, assuming that ahead of the first stage the flow is homentropic then constant entropy implies that each fluid particle undergoes the same change of entropy. In general since blade losses will not be constant with radius, then the condition of constant entropy will not be realized, however, experience has shown that in calculating the performance of a turbine entropy gradients can be neglected in most cases since they are usually small. Further, even if entropy gradients become comparatively large, the effect of assuming no gradient may still be small since the maximum errors occur at the tip and root, and are consequently masked by secondary effects. Also, the main effects as far as efficiency is concerned will be the introduction of blade incidence. Because of the relative insensitivity of turbine blading to incidence the effect on efficiency will be small.

In view of the above comments equation (2.56) reduces to the following:

$$\frac{d\left[C_a^2\right]}{dr} = -2\frac{C_\theta}{r}\frac{d\left[rC_\theta\right]}{dr} \qquad 2.57$$

Although the above equation is valid only for cylindrical stream surfaces between blade rows, its use is not restricted only to stages with cylindrical annulus walls, and it may be used for stages with conical walls. In this case, however, it becomes necessary to define the streamlines across the blade row. It will be shown in section 4.0 that simple assumptions may be made regarding streamline positions, with no loss of accuracy. In the design of blading only two solutions to equation 2.57 will be considered. The first solution is the so-called free vortex solution already given on page 40. The second is the constant nozzle efflux angle solution, the purpose of which simplify the manufacture of the stator blades by enabling them to be produced from constant section bar stock. The difference in the variation of degree of reaction along the blade length between a constant nozzle outlet angle design and a free vortex design is small, consequently for reasons of simplicity and ease of manufacture the constant nozzle outlet angle design should be given serious consideration in preference to a free vortex design since all other things being equal, the

efficiency of either design will not differ by any significant amount.

To arrive at a solution for the constant nozzle outlet angle design we proceed as follows:

Referring to figure 1.1 page 16

$$C_{\theta 2} = C_{a2} \, TAN\alpha_2 \qquad \text{——————} \quad 2.58$$

Now equation 2.57 may be written as follows:

$$C_{a2} \frac{dC_{a2}}{dr_2} + C_{\theta 2} \frac{dC_{\theta 2}}{dr_2} + \frac{C_{\theta 2}^2}{r_2} \qquad \text{——————} \quad 2.59$$

For convenience the subscript on α_2 will be dropped.

Substituting equation 2.58 into 2.59, we obtain

$$C_{a2} \frac{dC_{a2}}{dr_2} + C_{a2} TAN\alpha \frac{dC_{a2} TAN\alpha}{dr_2} + \frac{C_{a2}^2 TAN^2\alpha}{r_2} = 0$$

and since we are assuming α is constant

$$C_{a2} \frac{dC_{a2}}{dr_2} + C_{a2} TAN^2\alpha \frac{dC_{a2}}{dr_2} + \frac{C_{a2}^2 TAN^2\alpha}{r_2} = 0$$

rearranging we get

$$\frac{dC_{a2}}{dr_2} \cdot \frac{1}{SIN^2\alpha} + \frac{dr_2}{r_2} = 0 \qquad \text{——————} \quad 2.60$$

Integrating equation (2.60), we get:

$$\frac{1}{SIN^2\alpha} \cdot LOG_e C_{a2} + LOG_e r = C_1$$

or

$$C_{a2} r_2^{SIN^2\alpha} = \text{CONSTANT} \qquad 2.61$$

Substituting equation (2.61) into (2.58) gives

$$C_{\theta 2} r_2^{SIN^2\alpha} = \text{CONSTANT} \qquad 2.62$$

Now

$$q J C_p \Delta T = U_{m2} C_{\theta 2m} + U_{m3} C_{\theta 3m}$$

and since we are assuming that each fluid particle undergoes the same change of enthalpy

$$U_{m2} C_{\theta m2} + U_{m3} C_{\theta 3m} = U_2 C_{\theta 2} + U_3 C_{\theta 3}$$

or

$$C_{\theta m2} + \frac{r_{3m}}{r_{2m}} C_{\theta m3} = \frac{r_2}{r_{2m}} C_{\theta 2} + \frac{r_3}{r_{2m}} C_{\theta 3} \qquad 2.63$$

For a particular design

$$C_{\theta m2} + \frac{r_{3m}}{r_{2m}} C_{\theta m3} = \text{CONSTANT, A} \qquad 2.64$$

Substituting equation (2.64) into (2.63), we obtain:

$$\frac{r_2}{r_{2m}} C_{\theta 2} + \frac{r_3}{r_{2m}} C_{\theta 3} = A' \qquad 2.65$$

If we now let

$$\frac{r_2}{r_{2m}} = \bar{X} \qquad 2.66$$

substituting the above into equation (2.65), we obtain:

$$\bar{X} C_{\theta 2} + \frac{r_3}{r_{2m}} C_{\theta 3} = A' \qquad 2.67$$

We will now consider a turbine blade with a conical hub and shroud.

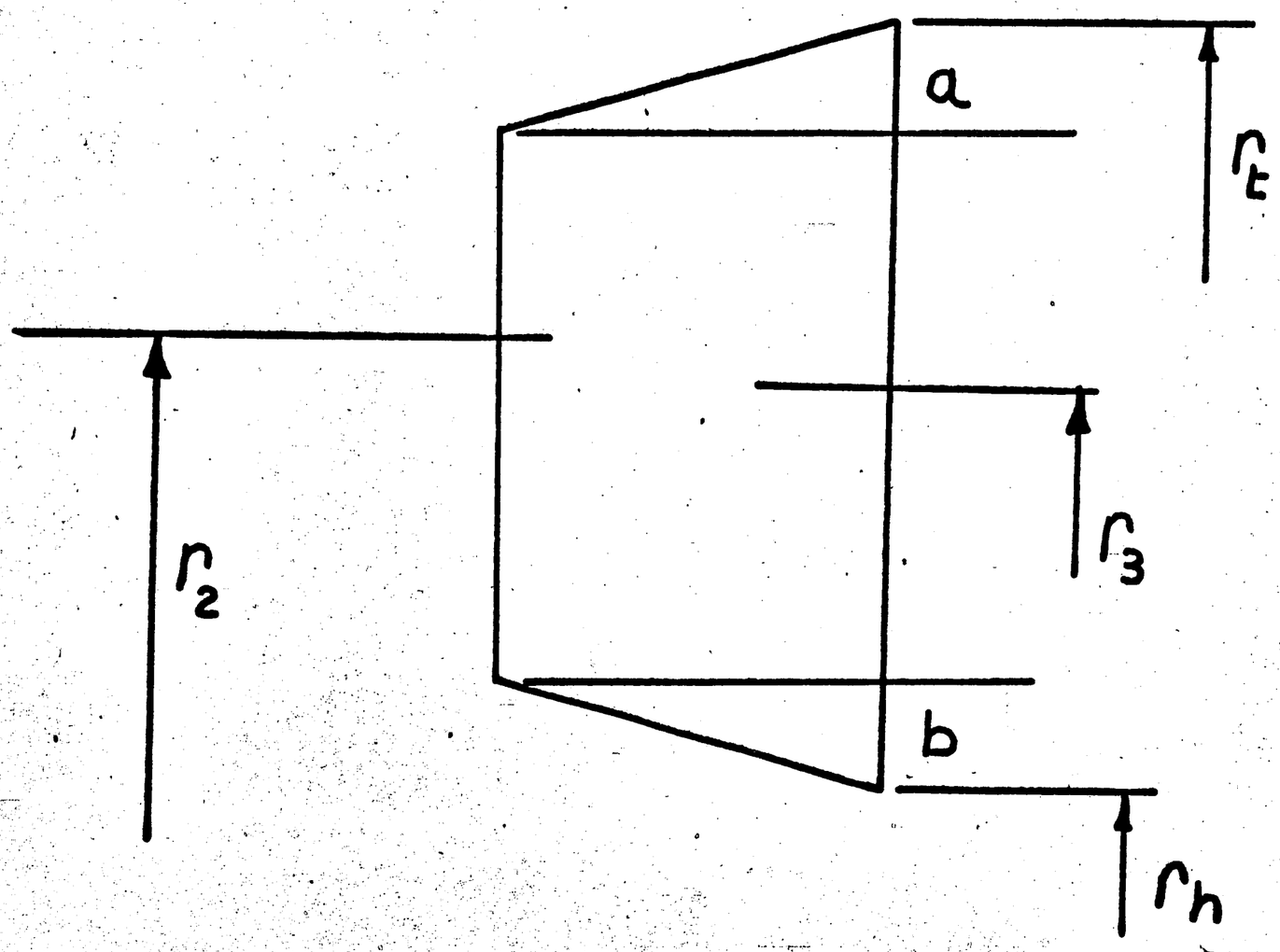

FIGURE 2.21

Referring to figure 2.21 the displacement of the stream-lines across the blade will assume to be governed by the following equations:

$$r_3 = r_2 + \Delta r \qquad 2.68$$

$$\Delta r = C_1 + C_2 r_3 \qquad 2.69$$

To find the constants C_1 and C_2 we substitute the following boundary conditions

$$\left.\begin{aligned} \text{when } r_3 &= r_h \,,\ \Delta r = -b \\ r_3 &= r_t \,,\ \Delta r = a \end{aligned}\right\} \qquad 2.70$$

Substituting equation (2.70) into (2.69), we obtain the following values for C_1 and C_2

$$C_1 = -\left|\frac{a r_h + b r_t}{r_t - r_h}\right| \qquad 2.71$$

$$C_2 = \frac{a + b}{r_t - r_h} \qquad 2.72$$

Substituting equation (2.71) and (2.72) into (2.69) we obtain

$$\Delta r = \frac{a + b}{r_t - r_h} r_3 - \frac{a r_h + b r_t}{r_t - r_h} \qquad 2.73$$

Substituting equation (2.73) into (2.68), we get:

$$r_3 = \frac{r_2(1-h)r_t - (ah+b)r_t}{(1-h)r_t - (a+b)} \qquad 2.74$$

Where $h = \frac{r_h}{r_t}$

Dividing equation (2.74) by r_{2m}, we get:

$$\frac{r_3}{r_{2m}} = \frac{\bar{x}(1-h)r_t - (ah+b)\frac{r_t}{r_{2m}}}{(1-h)r_t - (a+b)} \qquad 2.75$$

Substituting equation (2.75) into (2.67), we get:

$$A' = \bar{x}C_{\theta 2} + \left[\frac{\bar{x}(1-h)r_t - (ah+b)\frac{r_t}{r_{2m}}}{(1-h)r_t - (a+b)}\right]C_{\theta 3} \qquad 2.76$$

Now from equation (2.62)

$$C_{\theta 2} r_2^{SIN^2\alpha} = CONSTANT$$

or

$$C_{\theta 2} = C_{\theta 2m}\,\bar{x}^{-SIN^2\alpha} \qquad 2.77$$

Substituting equation (2.77) into (2.76)

$$C_{\theta 3} = \frac{A' - C_{\theta 2m}\bar{x}^{1-SIN^2\alpha}}{\bar{x}\left|1-h\right|r_t - \left|a+b\right|\frac{r_t}{r_{2m}}}\left[\left|1-h\right|r_t - \left|a+b\right|\right] \text{-----2.78}$$

Now equation (2.57) may be written

$$\frac{d\left|C_{a3}\right|^2}{dr_3} + \frac{d\left|C_{\theta 3}\right|^2}{dr_3} + \frac{2C_{\theta 3}^2}{r_3} - 0$$

Integrating we get

$$C_{a3}^2 + C_{\theta 3}^2 + 2\int \frac{C_{\theta 3}^2}{r} dr_3 = K_1 \text{----------2.79}$$

From equation (2.74)

$$dr_3 = \frac{dr_2\left|1-h\right|r_t}{\left|1-h\right|r_t - \left|a+b\right|} \text{----------2.80}$$

and from equation (2.66)

$$dr_2 = r_{2m}\, d\bar{x} \text{----------2.81}$$

Substituting equation (2.81) into (2.80), we obtain:

$$dr_3 = \frac{r_{2m}\left|1-h\right|r_t}{\left|1-h\right|r_t - \left|a+b\right|} d\bar{x} \text{----------2.82}$$

considering the integral

$$\int \frac{c_{\theta 3}^2}{r_3} dr_3$$

substituting equations (2.74), (2.78), and (2.82) into the above we obtain,

$$\int \frac{c_{\theta 3}^2}{r_3} dr_3 =$$

$$\int \frac{\left[A' - c_{\theta 2m} \bar{x}^{1-SIN^2\alpha}\right]^2}{\left[\bar{x}(1-h)r_t - (ah+b)\frac{r_t}{r_{2m}}\right]^3} \left[(1-h)r_t - (a+b)\right]^2 (1-h) r_t \, d\bar{x} \qquad \text{——— 2.83}$$

Substituting equation (2.83) into (2.79) we get:

$$c_{a3}^2 + c_{\theta 3}^2 + 2\int \frac{\left[A' - c_{\theta 2m} \bar{x}^{1-SIN^2\alpha}\right]^2 \left[(1-h)r_t - (a+b)\right]^2 (1-h) r_t \, d\bar{x}}{\left[\bar{x}(1-h)r_t - (ah+b)\frac{r_t}{r_{2m}}\right]^3} = K_1 \qquad \text{——— 2.84}$$

The integral in equation (2.84) cannot be integrated in closed form, therefore it is necessary to solve this equation numerically for each design. However, if the cone angles of shroud and platform are small, then

$$a \simeq b \simeq 0, \quad r_{2m} \simeq r_{3m}$$

With these conditions applied to equation (2.84), we obtain:

$$C_{a3}^2 + C_{\theta 3}^2 + 2\int \frac{\left[A' - C_{\theta 2m}\bar{X}^{1-SIN^2\alpha}\right]^2}{\bar{X}^3} d\bar{X} = K_1$$

——————2·85

Integrating equation (2.85) and substituting in equation (2.78), we obtain:

$$C_{a3}^2 = \left|1 - SIN^2\alpha\right|\left[\frac{C_{\theta 2m}^2}{\bar{X}^{2SIN^2\alpha}} \cdot \frac{1}{SIN^2\alpha} - \frac{2A'C_{\theta 2m}}{\left|1+SIN^2\alpha\right|\bar{X}^{1+SIN^2\alpha}}\right] + K_2$$

——————2·86

Equation (2.86) gives the variation of C_{a3} with radius in terms of the known mean diameter design for constant nozzle efflux design.

The final case to be considered is that of a free vortex design with conical annulus walls.

Equation (2.57) may be written

$$C_a \frac{dC_a}{dr} + \frac{1}{r^2}\frac{d(rC_\theta)^2}{dr} = 0$$

——————2·87

Considering the case of free vortex after the stator, then,

$$r_2 C_{\theta 2} = C_1 \qquad \text{2·88}$$

Substituting equation (2.88) into (2.87) gives

$$C_{a2} = CONSTANT$$

If we again let $\frac{r_2}{r_{2m}} = \bar{X}$, then for a particular design with conical annulus walls equations (2.67) and (2.75) apply. Substituting equations (2.88) and (2.75) into (2.67), we get:

$$\frac{C_1}{r_{2m}} + \frac{\bar{X}|1-h|r_t - |ah+b|\frac{r_t}{r_{2m}}}{|1-h|r_t + |a+b|} C_{\theta 3} = A'$$

or

$$C_{\theta 3} = \frac{[A' - C_1/r_{2m}][|1-h|r_t - |a+b|]}{\bar{X}|1-h|r_t - |ah+b|\frac{r_t}{r_{2m}}} \qquad \text{2·89}$$

Equation (2.57) may be written

$$\frac{dC_{a3}^2}{dr_3} + \frac{dC_{\theta 3}^2}{dr_3} + \frac{2C_{\theta 3}^2}{r_3} = 0$$

or integrating,

$$C_{a3}^2 + C_{\theta 3}^2 + K + 2\int \frac{C_{\theta 3}^2}{r_3} dr_3 = 0 \qquad \text{---------- 2.90.}$$

Substituting equations (2.89) and (2.75) into (2.90)

$$C_{a3}^2 + C_{\theta 3}^2 + K +$$

$$\left[A' - \frac{C_1}{r_{2m}}\right]^2 \left[(1-h)r_t - (a+b)\right]^2 \left[(1-h)r_t\right]^2 2\int \frac{d\bar{x}}{\left[\bar{x}(1-h)r_t - (ah+b)\frac{r_t}{r_{2m}}\right]^3} = 0$$

Integrating we get,

$$C_{a3}^2 = -C_{\theta 3}^2 + \frac{\left[A' - \frac{C_1}{r_{2m}}\right]^2 \left[(1-h)r_t - (a+b)\right]^2}{\left[\bar{x}(1-h)r_t - (ah+b)\frac{r_t}{r_{2m}}\right]^2} + K_3 \qquad \text{---------- 2.91}$$

Substituting equation (2.89) into (2.91) we obtain,

$$C_{a3}^2 = \frac{\left[A' - \frac{C_1}{r_{2m}}\right]^2 \left[(1-h)r_t - (a+b)\right]^2 - \left[A' - \frac{C_1}{r_{2m}}\right]^2 \left[(1-h)r_t - (a+b)\right]^2}{\left[\bar{x}(1-h)r_t - (ah+b)\frac{r_t}{r_{2m}}\right]^2}$$

Therefore

$$C_{a3} = K_4 \qquad \text{---------- 2.92}$$

The conclusion of the above is that whether the annulus walls are cylindrical or conical the axial velocity from the rotor will be constant with radius providing that each fluid particle undergoes the same change of enthalpy and entropy.

Continuity

In applying the above equations it is still necessary to adjust the blade height at the outlet of each row for continuity.

For continuity the following equation applies

$$W = 2\pi \int \rho C_a r \, dr \qquad 2.93$$

2.4 Stage Thermodynamic Calculations

The pressure loss coefficient defined by Ainley is as follows:

$$Y_{TS} = \frac{P_{01} - P_{02}}{P_{02} - P_2} \qquad 2.94$$

$$Y_{TR} = \frac{P_{02R} - P_{03R}}{P_{03R} - P_3} \qquad 2.95$$

Rearranging equations (2.94) and (2.95), we get:

$$\frac{P_{02}}{P_{01}} = \frac{1}{1 + Y_{TS}\left(1 - 1/\frac{P_{02}}{P_2}\right)} \qquad 2.96$$

$$\frac{P_{03R}}{P_{02R}} = \frac{1}{1 + Y_{TR}\left(1 - 1/\frac{P_{03R}}{P_3}\right)} \qquad 2.97$$

The above equations relate the total to total, and total to static pressure ratios with the total pressure loss coefficients obtained from section 2.0.

Referring to figure 1.1 page 16, the mean section calculations proceed as follows, assuming the total pressure loss coefficients have already been obtained for stator and rotor.

$$T_{01} = T_{02} \qquad 2.98$$

and therefore,

$$T_2 = T_{02} - C_2^2/2K_p$$

$$= T_{01} - C_2^2/2K_p \qquad 2.99$$

From known inlet conditions we can thus obtain a value for T_2 from equation (2.99).

Now $$\frac{P_{02}}{P_2} = \left[\frac{T_{02}}{T_2}\right]^{\frac{\gamma}{\gamma-1}} \qquad 2.100$$

Since T_{01} and T_2 are known we can obtain a value for the ratio P_{02}/P_2 which when substituted into equation (2.96) together with a value for Y_{TS} gives a value for P_{02}/P_{01} and since P_{01} is known (i.e. turbine inlet conditions) we obtain a value for P_{02}. Substitution of P_{02} into equation (2.100) gives a value for P_2.

Now $$T_{02R} = T_2 + \frac{W_2^2}{2K_p} \qquad 2.101$$

From the relationship $$\frac{P_{02R}}{P_2} = \left[\frac{T_{02R}}{T_2}\right]^{\frac{\gamma}{\gamma-1}} \qquad 2.102$$

we can find a value for P_{02_R}. Since,

$$T_{02R} = T_{03R} \qquad 2.103$$

Then

$$T_3 = T_{03R} - \frac{W_3^2}{2K_p} \qquad 2.104$$

and we can obtain a value for T_3.

Now $$\frac{P_{03R}}{P_3} = \left[\frac{T_{03R}}{T_3}\right]^{\frac{\gamma}{\gamma-1}} \qquad 2.105$$

From equation (2.105) we can obtain a value for the ratio P_{03_R}/P_3 which substituted into equation (2.97) together with a value for Y_{TR} gives a value for the ratio P_{03_R}/P_2. Since we know P_{02_R} we can obtain a value for P_{03_R} and hence obtain a value of P_3 from equation (2.105).

Now $$T_{03} = T_3 + \frac{C_3^2}{2K_p} \qquad 2.106$$

From which we can obtain a value for T_{03}

Now $$\frac{P_{03}}{P_3} = \left[\frac{T_{03}}{T_3}\right]^{\frac{\gamma}{\gamma-1}} \qquad 2.107$$

Since the only unknown in equation (2.107) is P_{03} we can now obtain it's value.

Equations (2.94) to (2.107) enable the temperatures and pressures to be established at the mean section at all points in the flow path.

Efficiency

The two efficiencies of importance in turbine design are given on page 22. The total to total efficiency is known as the blading efficiency and assumes recovery of the outlet velocity in later stages. The total to static efficiency, sometimes referred to as the work ratio, is a comparison of the actual work from a stage to the ideal available energy. This efficiency assumes the outlet velocity to be lost.

3.0 Relating Thermodynamic Calculations to Blade Profiles

The previous sections have covered the estimation of optimum parameters, the mean section design of a turbine stage, and the application of radial equilibrium. When the above calculations have been completed on a particular design the thermodynamic properties will have been estimated at all points in the flow field between blade rows. The problem now arises of specifying a blade shape which will give the required amount of work. This in turn requires specifying the velocity magnitude and direction throughout the passages, and the blade surface velocities. The solution to this problem is referred to as the blade to blade solution of the quasi three dimensional flow problem. The classical methods of solution are based upon potential flow theories and conformal transformation methods, however, since the flow through a turbine blade row is predominantly an accelerating one, the blade surface boundary layers are generally thin, and high efficiency blading may be designed without detailed analytical study. It has been found that the

methods given in Section 2.0 for determination of pressure loss coefficient are sufficiently accurate to enable a blade row efficiency to be estimated to within ± 2.0% even though the pressure loss coefficient is based upon blade gross parameters. A plausible explanation for this experimental fact is that even if the blade shape is such that velocity gradients are induced of a magnitude which result in flow separation since the flow is predominantly an accelerating one re-attachment occurs some short distance downstream of separation. The problem which remains is that of determining the fluid efflux angle from the blade row, and the mass flow passed by a given throat. In reality the solution to this complex problem requires a knowledge of the throat boundary layer thickness together with a knowledge of the velocity profile across the throat, the total throughflow then being obtained by integration. In the solution of this problem the method used by reference 1 is to assume one dimensional flow at the throat and then select the axial position of the station between stages such that the correct flow magnitude through the throat is obtained.

The fluid efflux angle is obtained from experimental correlations. The degree of accuracy that may be expected from the above simplification is a prediction of mass flow to within ± 3.0%.

3.1 Efflux Angle Prediction from a Blade Row

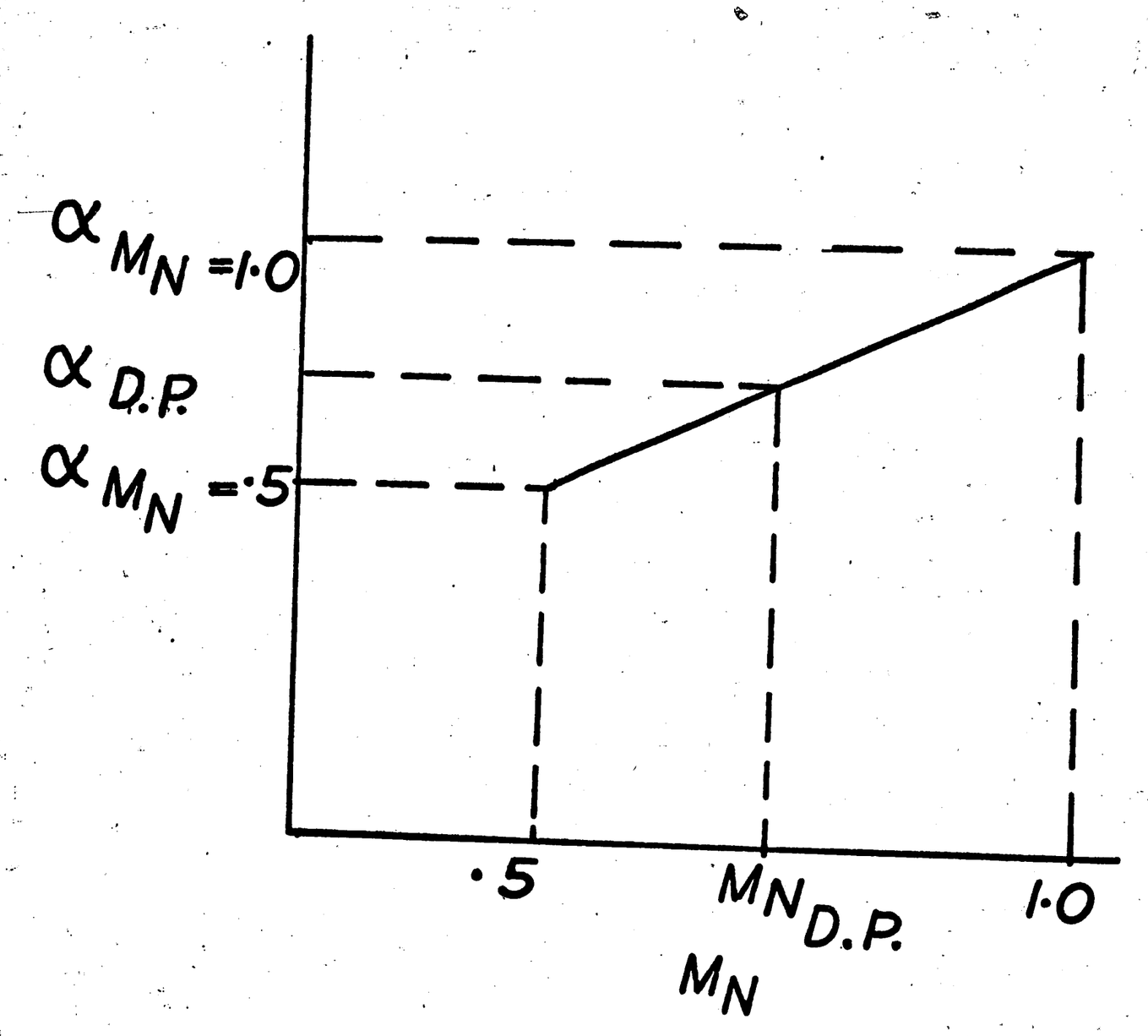

FIG 3.1

Referring to figure 3.1, between a Mach number of 0 and .5 the gas efflux angle from a blade row is assumed to be constant, and between a Mach number of .5 and 1.0 the

efflux angle is assumed to vary linearly.

The problem is to determine that value of o/s which gives the outlet angles at Mach numbers of .5 and 1.0 such that for the design efflux Mach number the design efflux angle is obtained.

The following correlations are from the Ainley and Mathieson report (reference 1).

Considering first the stator the correlation between the outlet angle at Mach number 1.0 and o/s is given by the following equations.

$$A'_{t_2} = \frac{o/s\,|5A_{n2} + A_{n1}|}{6} \qquad 3.1$$

where A'_{t_2} is the stator throat area with zero tip clearance.

Now $$A_{t2} = A'_{t2}\left|1 - \frac{K}{H}\right| + A_{K2} \qquad 3.2$$

Substituting 3.2 into 3.1

$$A_{t2} = \frac{o/s\left|5A_{n2} + A_{n1}\right|\left|1 - \frac{K}{H}\right|}{6} + A_{K2} \qquad 3.3$$

Dividing by A_{n2} we obtain

$$\frac{A_{t2}}{A_{n2}} = \frac{O/S\left(5 + \frac{A_{n1}}{A_{n2}}\right)\left(1 - \frac{K}{H}\right)}{6} + \frac{A_{K2}}{A_{n2}} \qquad 3.4$$

Now
$$\left.\begin{aligned} A_K &= \pi d_t K \\ A_{n2} &= \pi d_m H \end{aligned}\right\} \qquad 3.5$$

Substituting 3.5 into 3.4 we obtain

$$\frac{A_{t2}}{A_{n2}} = \frac{O/S\left(5 + \frac{A_{n1}}{A_{n2}}\right)\left(1 - \frac{K}{H}\right)}{6} + \frac{d_t K}{d_m H} \qquad 3.6$$

If we let

$$\left.\begin{aligned} \bar{a} &= \frac{\left(5 + \frac{A_{n1}}{A_{n2}}\right)\left(1 - \frac{K}{H}\right)}{6} \\ \bar{b} &= \frac{d_t}{d_m} \cdot \frac{K}{H} \end{aligned}\right\} \qquad 3.7$$

Then

$$\frac{At_2}{An_2} = \bar{a}\,\%s + \bar{b} \qquad \text{---------- 3.8}$$

and

$$\alpha_{2(M_N - 1)} = \cos^{-1}\frac{At_2}{An_2} \qquad \text{---------- 3.9}$$

The correlation between o/s and efflux angle at Mach number .5 is obtained as follows:

$$\alpha_2' = \bar{\alpha}_2^* - 4\left(\frac{s}{e}\right) \qquad \text{---------- 3.10}$$

where α_2' is the gas efflux angle with zero tip clearance

$$\bar{\alpha}_2^* = f(\cos^{-1}\%s)$$

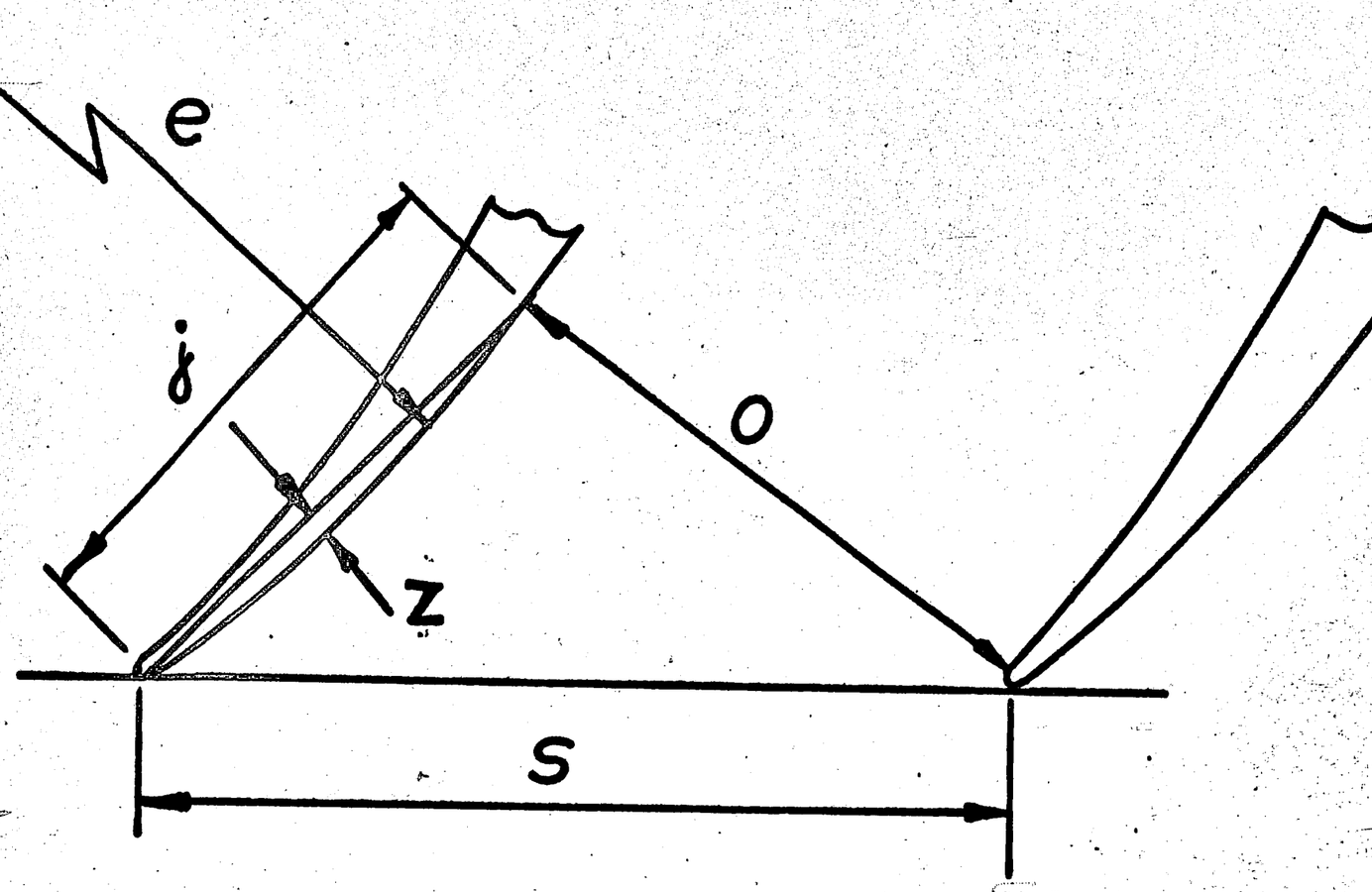

FIG 3·2

Figure 3.2 shows the back radius value "e" to be used in equation 3.10. If the value of e is unknown it may be approximated as follows:

$$e = \frac{8j^2}{Z} \qquad 3\cdot11$$

Figure 3.3 is a curve of the functional relationship between $\bar{\alpha}_2^*$ and o/s to be used in equation 3.10.

Now $\alpha_{2(M_N=.5)}$ is given by reference 1 as follows:

$$\alpha_{2(M_N=.5)} = TAN^{-1}\left[\left(1-\frac{XK}{H}\left|\frac{\cos\alpha_1^*}{\cos\alpha_2'}\right|\right)TAN\alpha_2' + \frac{XK}{H}\left|\frac{\cos\alpha_1^*}{\cos\alpha_2'}\right| TAN\alpha_1^*\right] \qquad 3.12$$

If we let

$$\left.\begin{aligned}\frac{XK}{H}\cos\alpha_1^* &= \bar{m}\\ \text{and}\quad \frac{XK}{H}\sin\alpha_1^* &= \bar{n}\end{aligned}\right\} \qquad 3.13$$

we get

$$\alpha_{2(M_N=.5)} = TAN^{-1}\left[\left(1-\frac{\bar{m}}{\cos\alpha_2'}\right)TAN\alpha_2' + \frac{\bar{n}}{\cos\alpha_2'}\right] \qquad 3.14$$

Equations 3.9 and 3.14 give the relationship between stator blade geometry and gas efflux angles at Mach numbers 1.0 and .5 respectively. In order to obtain the correct value of o/s for a given design gas outlet angle at a given Mach number it is necessary to iterate. The above procedure is repeated for the rotor.

Having obtained a value of o/s from the above equations which satisfies the requirements the problem is now to define a suitable blade shape. Considering the conflicting requirements when designing blade profiles the following method of specifying blade shapes has been found to give satisfactory results and to be acceptable compromise.

The main criteria in the attainment of high efficiency subsonic profiles appear to be:

(a) Uniformly converging passage from inlet to throat.

(b) Avoidance of pure impulse or rotor blade recompression.

(c) Thin trailing edges.

The conflicting requirements in profile design are:

(1) Required inlet angle

(2) Required o/s

(3) Required blade chord

(4) Required section area

(5) Required position of section center of gravity.

The most rapid way to produce blade sections to meet the above requirements is the circular arc method, the general parameters of which are given in figure 3.4. Profiles drawn to these parameters have in general been found to give satisfactory efficiencies while still enabling a

blade to be designed in a reasonably short period of time. The procedure is that each blade section is drawn independently to meet the requirements of o/s, blade chord, inlet angle and required section area. The sections are then stacked and individual sections modified where necessary to give the desired leading and trailing edge line up and position of center of gravity. The required variation of section area is, of course, known from previously determined stress requirements.

FIGURE 3·3

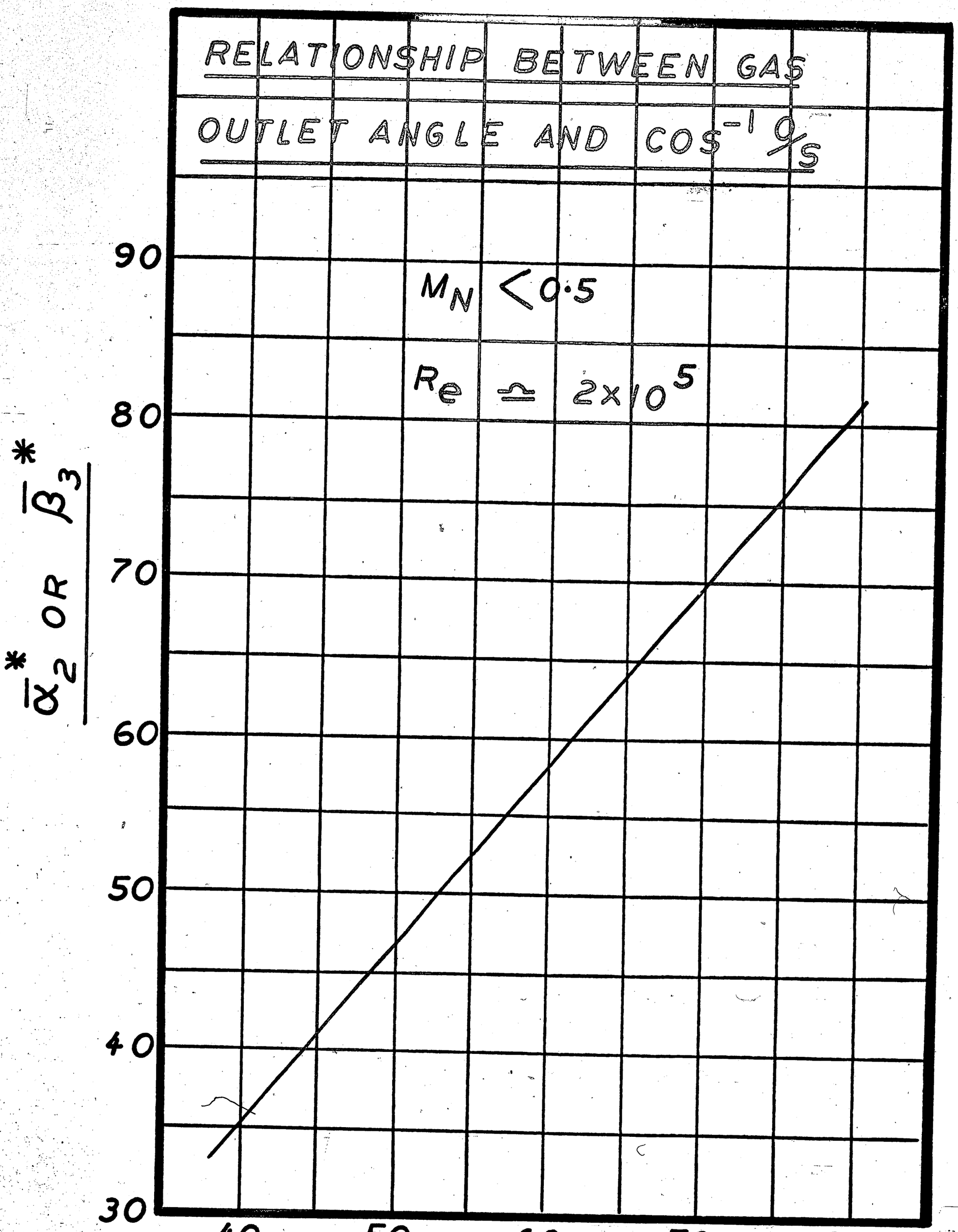
RELATIONSHIP BETWEEN GAS
OUTLET ANGLE AND COS⁻¹ θ/S
$M_N < 0.5$
$Re \simeq 2 \times 10^5$
$\bar{\beta}_3^* / \bar{\alpha}_2^*$ OR $\bar{\beta}_3^*$
90
80
70
60
50
40
30
40
50
60
70
80
$\cos^{-1} \theta/s$ - DEGREES

FIGURE 3.4

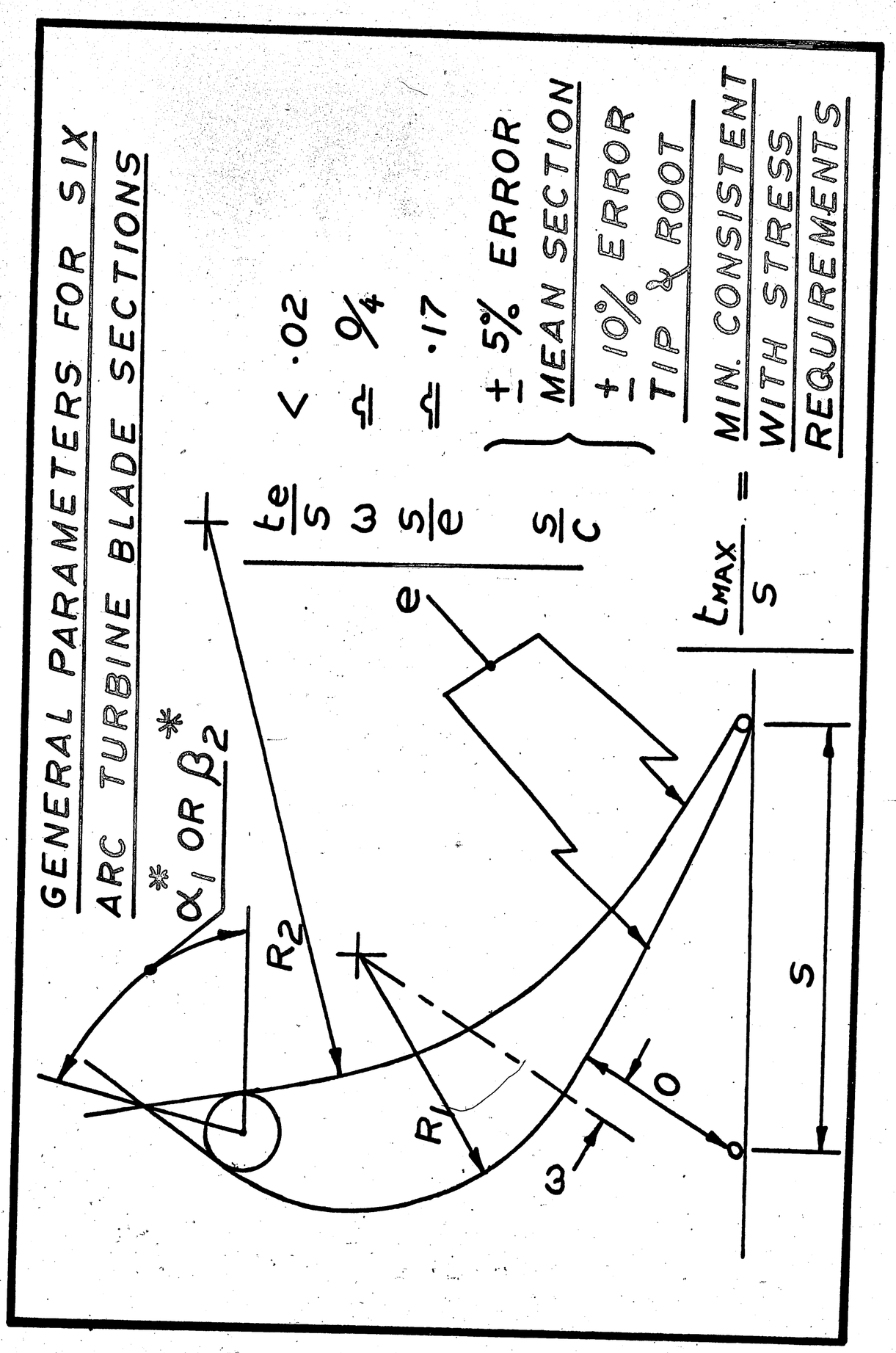

GENERAL ARC TURBINE BLADE SECTIONS

GEOMETRICAL PARAMETERS FOR SIX

4.0 Design Example

A turbine is required to deliver shaft power by expanding the products of combustion from the inlet conditions given below to a static pressure of 14.3 p.s.i.a.

Inlet total pressure	=	33.49 p.s.i.a.
Inlet total temperature	=	1425 °R.
Mass flow	=	151.1 lbs/sec.

The inlet configuration to the turbine has already been determined from other considerations, and the required speed of the turbine to match the driven machine is 5250 R.P.M. With the above given information the design approach is first to select optimum parameters and then carry out a detailed thermodynamic design as follows.

4.1 Selection of Parameters

In order to estimate approximately the optimum parameters it is first necessary to assume a turbine efficiency. The value assumed is only important to the degree that it is used to obtain the general work parameter level upon which the optimization is based.

Usually with experience of the type of turbine to be designed a good initial guess can be made. If, however, the efficiency obtained after optimization is different from the one assumed by more than two or three points the procedure should be iterated. Usually one iteration will be sufficient.

Initial assumed efficiency $\eta_s = 83\%$

Turbine expansion Ratio $= \frac{33.49}{14.3}$

$= 2.34$

Average gas properties are

$\gamma = 1.35$

$c_p = .246$

$R = 53.3$

Now

$$\Delta T = \eta_s T_{01}\left[1 - \left(\frac{P_3}{P_{01}}\right)^{\frac{\gamma-1}{\gamma}}\right]$$

$$= .83 \times 1425\left[1 - \left(\frac{1}{2.34}\right)^{.259}\right]$$

$$= \underline{233^\circ F}$$

$$T_{03} = 1425 - 233$$

$$= \underline{1192^{\circ} R}$$

Since the exhaust velocity must be low from an industrial type turbine we can approximate the fluid outlet density using total temperature i.e.

Approximate outlet fluid density

$$= \frac{144 \times 14.3}{53.3 \times 1192} = .0324 \text{ lbs/cubic ft.}$$

Now $K_p \Delta T = 32.2 \times 778 \times .264 \times 233$

$= 1{,}540{,}000$

For economic reasons it is desirable to use as few stages as possible therefore as a first assumption we will consider a single stage turbine. The blade root stress is to be limited to a value of less than 33,000 pounds per square inch. This value takes into consideration blade configuration, material, and blade temperature. The method of determining stress magnitude is beyond the scope of this thesis and it will be assumed that the above value is given.

From equation 1.73 Page 62.

$$\sigma = \frac{N^2 An}{1.14} \times 10^{-6} \qquad \text{1.73}$$

Substituting the known values of stress and speed into the above equation we obtain a maximum permissible value for rotor blade outlet annulus area, and since this is an industrial turbine where the outlet kinetic energy is lost the maximum permissible outlet area is the one most desirable.

i.e. $A_{n3} = \frac{33500 \times 1.14 \times 10^6}{5250^2}$

$$= \underline{1390 \text{ square inches}} \qquad \text{4.1}$$

Now

$$W = \rho_3 C_{A3} A_{n3}$$

or

$$C_{A3} = \frac{W}{\rho_3 A_{n3}}$$

$$= \frac{151.1 \times 144}{.0324 \times 1390}$$

$$= \underline{490 \text{ FT/SEC}} \qquad \text{4.2}$$

With known values of $K_p \Delta T$ and C_{A3}

i.e. $$K_p \Delta T = 1{,}540{,}000$$

$$C_{A3} = 490 \text{ ft/sec.}$$

The problem resolves itself into one of finding a value of blade speed to give the maximum efficiency.

With the aid of the following equations table 4.1 was compiled.

$$U_m = \frac{d_m N}{229} \qquad 4.3$$

$$l = \frac{A_{n3}}{\pi d_m} \qquad 4.4$$

$$\frac{h}{t} = \frac{d_m - l}{d_m + l} \qquad 4.5$$

$$d_{disk} - d_m - l \qquad 4.6$$

Column 9 was obtained from figure 1.8 and column 8 from figure 1.10

Column 10 was obtained by deducting an allowance for leakage loss, of 3 points, from column 9. The loss due to leakage is a function how close it is possible

to run the turbine rotor blade tips to the casing and whether the blading is shrouded or unshrouded. In this case it was decided to go with unshrouded blades and the assumed leakage loss is an approximation based upon experience with this size of turbine.

Figures 4.1, 4.2, and 4.3 are plots of the data in table 4.1 and it should be remembered that the basic assumptions in the plotting of these curves are a speed of 5250 R.P.M. and a blade root stress of 33,500 pounds per square inch. With these curves together with other information of an economic nature it is possible to arrive at a set of design parameters.

First examination of Figure 4.3 reveals that with simple radial equilibrium and axial outlet it is not possible to design the turbine with a blade speed of below about 1085 without obtaining recompression at the root. Further, for economic reasons the disk forging should be made as small as possible and for competitive reasons the turbine total to static efficiency should be in the order of 83%.

With the above limitations the following design parameters were selected:

$K_p \Delta T / U^2$ ≏ 1.2

C_{A3} / U ≏ .43

Disk Diameter ≏ 41 inches

Mean Diameter ≏ 50 inches

Blade Length ≏ 9 inches

Total to Static Efficiency ≏ 83.5

h/t ≏ .7

h/t_{MIN} ≏ .62

With the above relationship between hub tip ratio and minimum hub tip ratio about 5 to 10 percent reaction may be expected at the root. It now remains to check the stator root Mach number before commencing with the detail design.

Now $\frac{Um}{\sqrt{T_{01}}} = \frac{1145}{\sqrt{1425}} = \underline{30.4}$

From equation 1.68

$\zeta_2 = 2.43 \times 1.2$

$= \underline{2.92}$

From figure 1.12

$$\mathcal{J}_2 = \underline{1.52}$$

From equation 1.72

$$\frac{C_{2hub}}{\sqrt{T_{01}}} = \frac{U_m}{\sqrt{T_{01}}} \times \mathcal{J}_2$$

$$= 30.4 \times 1.52$$

$$= \underline{46.2}$$

From figure 1.14 the outlet Mach Number from the stator root will be approximately 1.05 and since this will be the maximum value of Mach Number within the stage it is acceptable. With the above parameters it is now possible to commence the detail design.

U_m	$\frac{K_p \Delta T}{U_m^2}$	$\frac{C_{A3}}{U_m}$	d_m	BLADE LENGTH l	$\frac{h}{t}$	DISK DIA.	$\frac{h}{t}_{MIN}$	η_s	η_s INCL. LEAK.
1	2	3	4	5	6	7	8	9	10
900	1·900	·545	39·3	11·25	·555	28·05	·95	·82	·79
1000	1·540	·490	43·6	10·15	·622	33·45	·78	·846	·816
1100	1·271	·445	48	9·24	·675	38·76	·66	86	83
1200	1·070	·407	52·4	8·46	·722	43·94	·58	·87	·84

TABLE 4·1

FIGURE 4.1

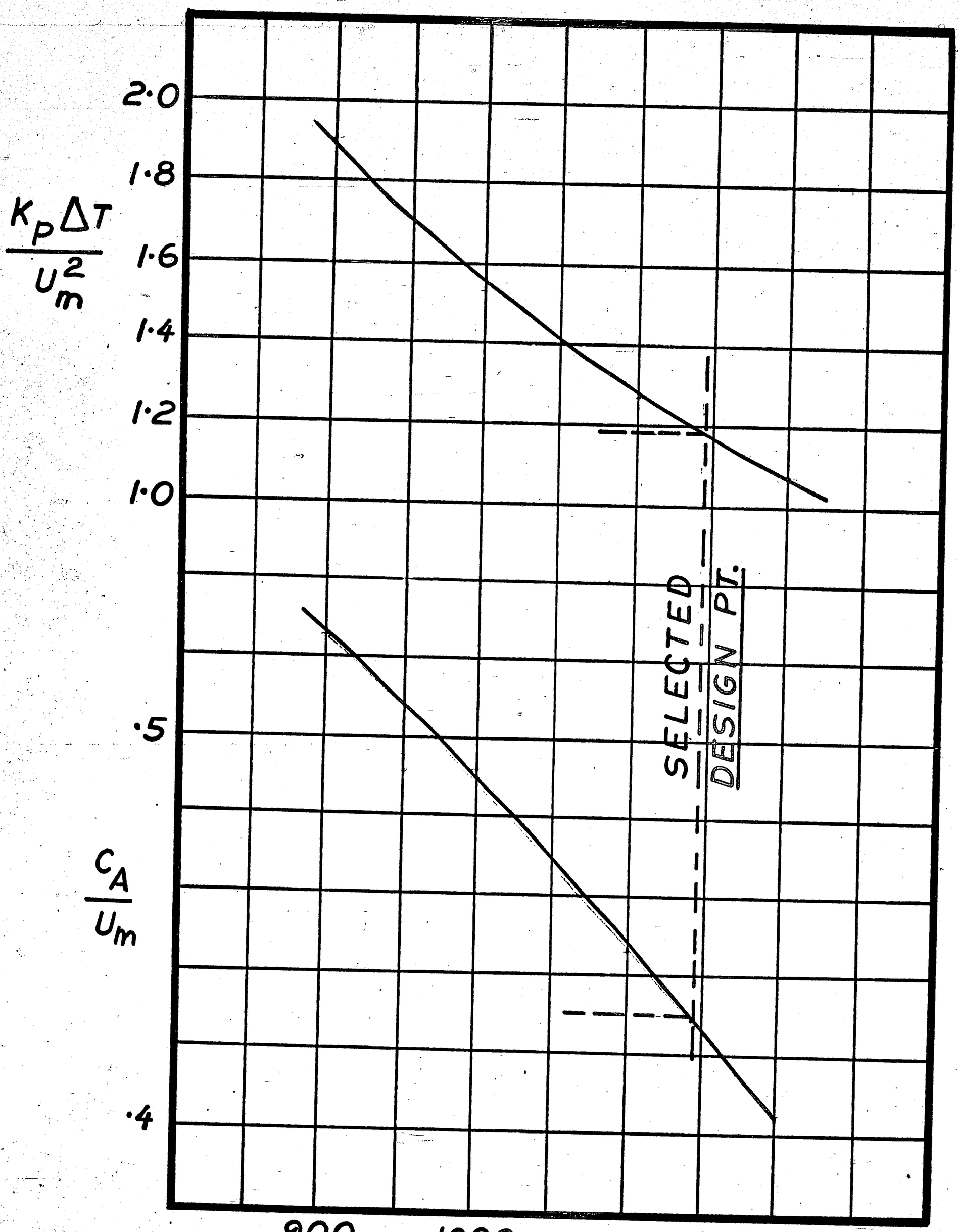
2.0
1.8
$\frac{K_p \Delta T}{U_m^2}$
1.6
1.4
1.2
1.0
.5
$\frac{C_A}{U_m}$
.4
SELECTED
DESIGN PT.
900
1000
1100
1200
U_m FT/SEC

FIGURE 4·2

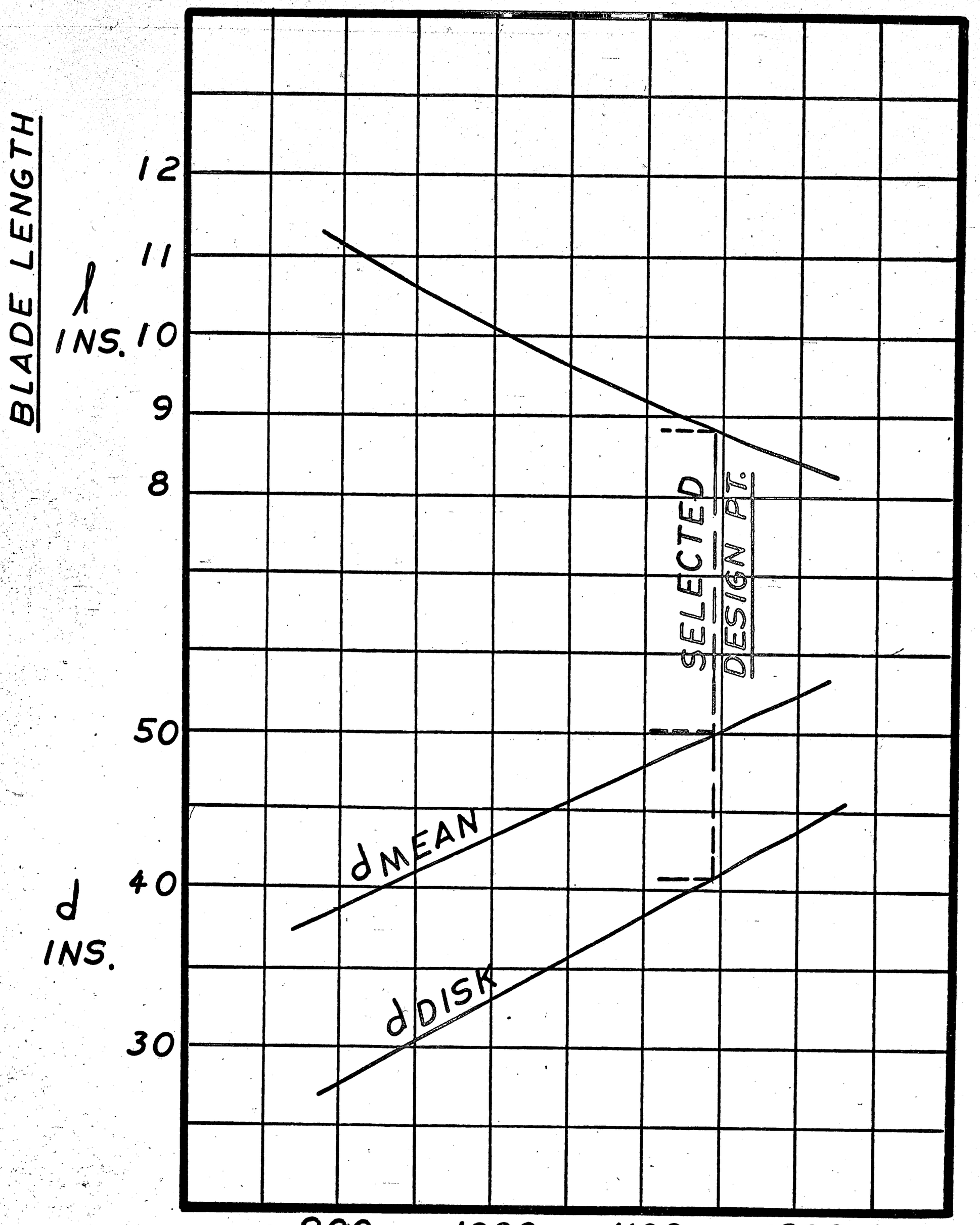
BLADE LENGTH
l
INS.
12
11
10
9
8
d
INS.
50
40
30
SELECTED DESIGN PT.
dMEAN
dDISK
900
1000
1100
1200
Um FT/SEC.

FIGURE 4·3

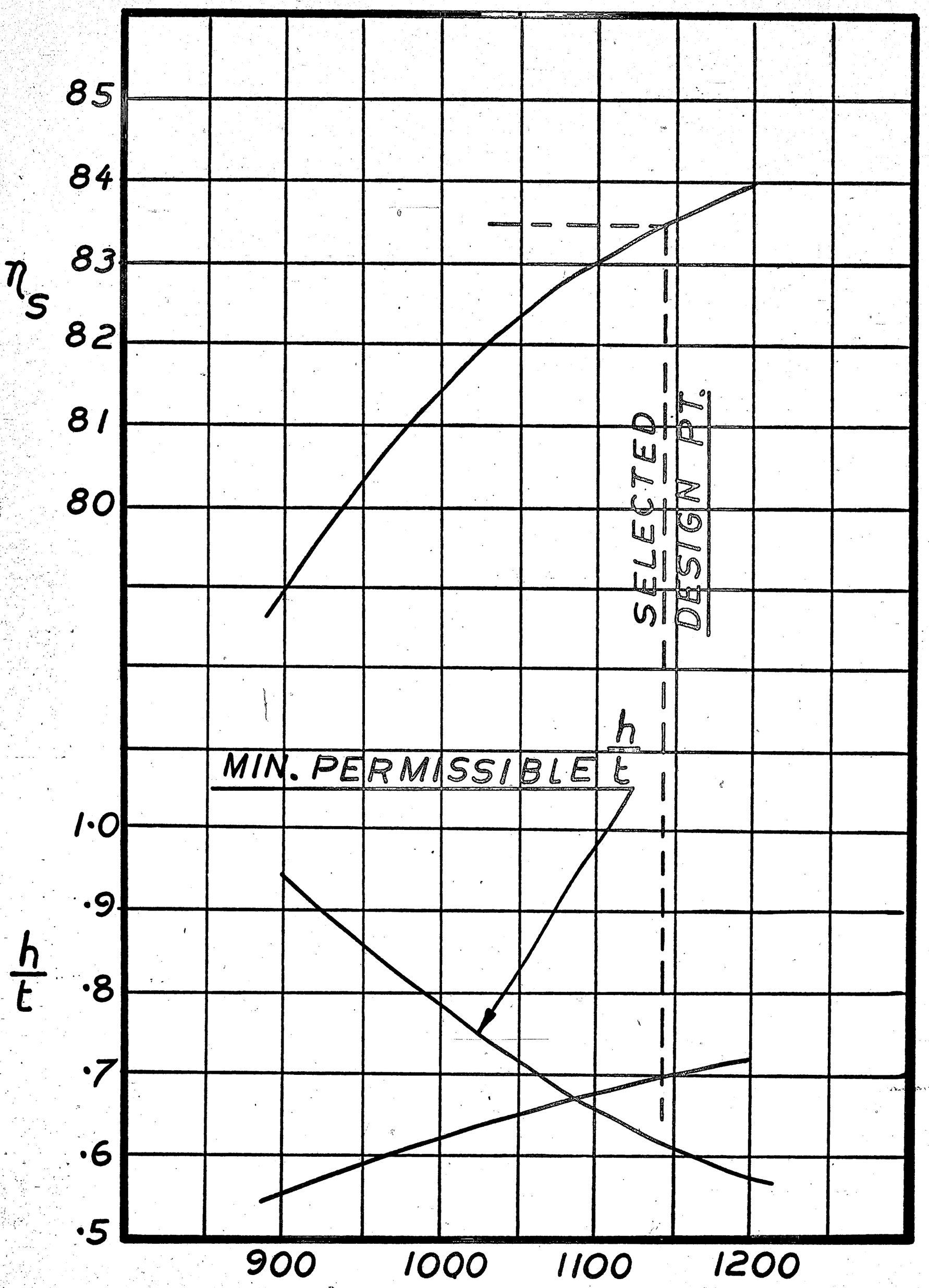
85
84
83
82
81
80
η_s
SELECTED DESIGN PT.
MIN. PERMISSIBLE $\frac{h}{t}$
$\frac{h}{t}$
1·0
·9
·8
·7
·6
·5
900
1000
1100
1200
U_m FT./SEC.

4.2 Detailed Thermodynamic Design

From the given conditions and the parametric study the following information is available.

P_{o1} = 33.49 lbs/square inch

T_{o1} = 1425°R

W = 151.1 lbs/sec.

N = 5250 R.P.M.

d_m = 50 inches

It has previously been decided that the turbine will be a single stage turbine with axial outlet. The procedure is to first calculate conditions at the mean section and then to apply some form of radial equilibrium to obtain the variation of parameters along the blade length.

Proceeding with the mean section calculations it is necessary to first guess a temperature or enthalpy drop across the stage and then to iterate in order to match the stage discharge pressure. In the following calculations the correct temperature obtained from previous iterations will be used as a first assumption in order to reduce calculation length.

Assumed Stage ΔT total = 238°F

Also, from previous iterations the axial velocities from the stator and rotor have been fixed at 450 and 475 ft/sec. respectively. The exit velocity from the rotor was determined from stress considerations and that from the stator was found to be necessary in order to obtain a smooth annulus from stage inlet to outlet. With the above information it is possible to calculate the work parameter and flow coefficient.

$$U_m = \frac{d_m N}{229} = \frac{50 \times 5250}{229}$$

$$= \underline{1145 \text{ ft/sec.}}$$

Therefore

$$\frac{K_p \Delta T}{U_m^2} = \frac{32.2 \times 778 \times .264 \times 238}{1145^2} \qquad \text{——— 4·8}$$

$$= \underline{1.1998}$$

and

$$\left.\begin{aligned} \frac{C_{A2}}{U_m} &= \frac{450}{1145} = .3929 \\ \frac{C_{A3}}{U_m} &= \frac{475}{1145} = .4147 \end{aligned}\right\} \qquad \text{——— 4·9}$$

From equation 1.6, since $\alpha_3 = 0$

$$TAN\alpha_2 = \frac{1.1998}{.3929} = 3.05392$$

$$= \underline{71° \quad 52.14} \qquad 4.10$$

Referring to Figure 1.1

$$TAN\beta_2 = TAN\alpha_2 - \frac{U}{C_{A2}}$$

$$= 3.05392 - 2.545269 \qquad 4.11$$

$$= \underline{.508651}$$

$$\beta_2 = \underline{26° \quad 57.612}$$

$$TAN\beta_3 = 2.411307$$

$$\beta_3 = \underline{67° \quad 28.535} \qquad 4.12$$

α_3 is, of course, equal to zero. Figure 4.4 is the stage velocity diagram drawn from the above information. Again from previous iterations approximate values are available for A_{n1}, A_{n2}, A_{n3} Stator ID/OD and Rotor ID/OD. These values are used to approximate secondary and leakage pressure loss coefficients.

A_{n1} = 773 square inches

A_{n2} = 1121 square inches

A_{n3} = 1384 square inches

Stator $\frac{ID}{OD}$ = .773

Rotor $\frac{ID}{OD}$ = .706

4.13

At this point it is convenient to carry out the calculations in table form. Table 4.2 is a listing of the information available at the start of the calculations. Table 4.3 is the stator pressure loss calculation and Table 4.4 is the rotor blade pressure loss coefficient calculation. Table 4.5 is a tabulation of the stage thermodynamics.

From Table 4.5 the turbine efficiency and horsepower may be calculated as follows:

$$\eta_s = \frac{1 - \frac{T_{03}}{T_{01}}}{1 - \left(\frac{P_3}{P_{01}}\right)^{\frac{\gamma-1}{\gamma}}}$$

$$\eta_s = \frac{1 - \frac{1187}{1425}}{1 - \left(\frac{14.3}{33.49}\right)^{.2592}}$$

$$= \frac{.84}{} \qquad 4.14$$

$$\text{Horse Power} = \frac{151.1 \times 238 \times .264 \times 778}{550}$$

$$= \frac{13,465}{} \qquad 4.15$$

Comparing equation 4.14 with equation 4.1, it will be observed that the preliminary estimate of efficiency differs from that obtained from the detailed stage calculations by approximately half a point.

Having completed the mean section design the next step is to apply radial equilibrium in order to obtain the variation of parameters with blade length. The decision made in this case was to assume free vortex and, further,

since the included angle of the annulus is less than 30° a further assumption made is that of cylindrical streamlines. With these assumptions the following equations result from the application of Section 3.

$$\left.\begin{aligned} C_{\theta 2} &= \text{Constant} \\ C_{\theta 3} &= \text{Constant} \end{aligned}\right\} \quad \text{4.16}$$

$$\left.\begin{aligned} C_{A2} &= \text{Constant} \\ C_{A3} &= \text{Constant} \end{aligned}\right\} \quad \text{4.17}$$

$$U\left(C_{\theta 2} + C_{\theta 3}\right) = K_p \Delta T \qquad \text{4.18}$$

Equations 4.16 and 4.17 are obtained from the application of free vortex radial equilibrium, and equation 4.18 when applied to each radius satisfies the condition of constant enthalpy with radius. In applying equations 4.16, 4.17 and 4.18 we obtain Table 4.6 which is a tabulation of angles and velocity components for velocity diagrams at selected radii. The selected radii were chosen to obtain the thermodynamic parameters at five equally spaced sections.

With the above information it is now possible to calculate the thermodynamic parameters at each radii similar to the calculations carried out for the mean section. For these calculations the pressure loss coefficient is assumed to be constant with radius. The results of these calculations are given in Table 4.7 and from this data sufficient information can be extracted to enable blade sections to be drawn.

The optimum S/C for each section can be obtained from Figure 2.13, the required O/S can be obtained from the required gas outlet angle and Mach number as described in Section 3. At this point it is necessary to fix certain blade geometry such as S/e and aspect ratio. With this information together with a known area distribution determined by stress requirements the blade sections can be drawn and stacked.

Tables 4.8 and 4.9 show the stator and rotor blade deviations as determined by the calculation methods of Section 3. The actual drawing of the blade sections is a trial and error process to obtain the thermodynamic and stress requirements with a minimum of compromise.

FIGURE 4.4

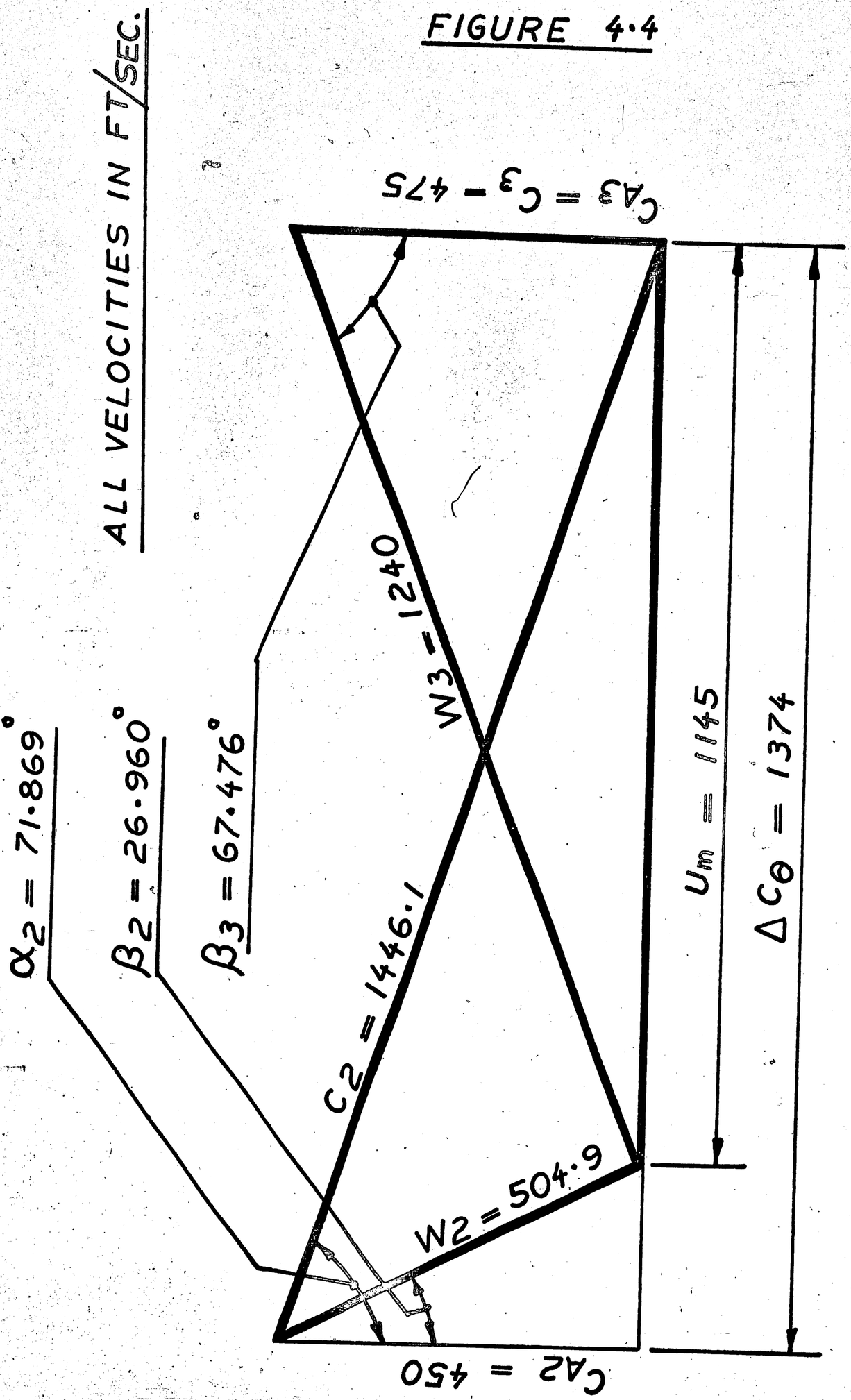
ALL VELOCITIES IN FT/SEC.
$\alpha_2 = 71.869^\circ$
$\beta_2 = 26.960^\circ$
$\beta_3 = 67.476^\circ$
$C_{A3} = C_3 - 475$
$W_3 = 1240$
$C_2 = 1446.1$
$W_2 = 504.9$
$C_{A2} = 450$
$U_m = 1145$
$\Delta C_\theta = 1374$
MEAN DIAMETER VELOCITY DIAGRAM
DRAWN APPROXIMATELY TO SCALE

TABLE 4.2

GIVEN PARAMETERS

1	$K_P \Delta T / U^2$	1.19984	14	C_1	450
2	C_{A2} / U	.39288	15	C_2	1446.1
3	C_{A3} / U	.41471	16	W_2	504.9
4	α_1	0°	17	W_3	1240
5	α_2	71.869	18	C_3	475
6	β_2	26.960	19	dm	50.
7	β_3	67.476	20	An1	773
8	α_3	0	21	An2	1.121
9	$\cos \alpha_1$	1	22	An3	1384
10	$\cos \alpha_2$	.31119	23	C_{A2}	450
11	$\cos \beta_2$	.89132	24	C_{A3}	475
12	$\cos \beta_3$	.38308	25	U_2	1145.4
13	$\cos \alpha_3$	1	26	U_3	1145.4

VELOCITIES — FT/SEC

ANGLES — DEGREES

AREAS — SQUARE INS.

DIA. — INS.

TABLE 4·3

CALCULATION FOR STATOR PRESSURE LOSS COEFFICIENT

TIP CLEARANCE	1	K	·100
FROM FIG. 2·13	2	S/C	·69
$1/$BLADE HEIGHT	3	K/H	·0156
GIVEN	4	t_{max}/C	·2
"	5	te/S	·02
"	6	A_2	348·8
"	7	A_1	773
$\lvert 6/7 \rvert^2$	8	$\lvert A_2/A_1 \rvert^2$	·2036
GIVEN	9	$1 + ID/OD$	1·773
8/9	10	$\lvert A_2/A_1 \rvert^2/1+\frac{ID}{OD}$	·1148
FROM FIG. 2·18	11	λ_S	·0065
0·5 × 3	12	$B\lvert K/H \rvert_S$	·0078
FROM FIG. 2·17	13	μ_S	6·6
11 + 12	14	$\lambda_S + B\frac{K}{H}$	·0143
13 × 14	15	$Y_S + Y_K$	·09438
FROM FIGS. 2·5 – 2·11	16	Y_P	·039
GIVEN	17	α_1/α_2	0
FROM FIG 2·12	18	K	1
18 × 16	19	KY_P	·039
19 + 15	20	$KY_P + Y_S + Y_K$	·1334
FROM FIG 2·19	21	$Y_t/Y_t(\frac{te}{S}=.02)$	1
20 × 21	22	Y_{TS}	·1334

TABLE 4.4

CALCULATION FOR ROTOR PRESSURE LOSS COEFFICIENT

TIP CLEARANCE	1	K	.100
FROM FIG. 2.13	2	S/C	.69
$1/$ BLADE HEIGHT	3	K/H	.0116
GIVEN	4	t_{max}/C	.2
"	5	te/S	.02
"	6	A_2	530.18
"	7	A_1	999.2
$\lvert 6/7 \rvert^2$	8	$\lvert A_2/A_1 \rvert^2$	.2806
GIVEN	9	$1 + ID/OD$	1.706
$8/9$	10	$\lvert A_2/A_1 \rvert^2/1+\frac{ID}{OD}$	.1645
FROM FIG. 2.18	11	λ_R	.0076
0.5 X 3	12	$B\lvert K/H \rvert_R$	.0058
FROM FIG. 2.17	13	μ_R	6.9
11+12	14	$\lambda_R + B\frac{K}{H}$	.0134
13X14	15	$Y_S + Y_K$	.09246
FROM FIGS. 2.5-2.11	16	Y_P	.0505
GIVEN	17	β_2/β_3	.3995
FROM FIG. 2.12	18	K	1
18X16	19	KY_P	.0505
19+15	20	$KY_P + Y_S + Y_K$	.14296
FROM FIG 2.19	21	$Y_t/Y_t\left(\frac{te}{S}=.02\right)$	1
20X21	22	Y_{TR}	.14296

TABLE 4·5

STAGE THERMODYNAMICS

MEAN DIAMETER

GAS TABLES	1	C_p	·264
"	2	γ	1·350
$2g_J C_p$	3	$2K_p$	13227
$C_1^2 / 2K_p$	4	θC_1	15·309
$C_2^2 / 2K_p$	5	θC_2	158·09
$W_2^2 / 2K_p$	6	θW_2	19·27
$W_3^2 / 2K_p$	7	θW_3	116·24
$C_3^2 / 2K_p$	8	θC_3	17·06
GIVEN	9	T_{01}	1425
9 — 5	10	T_2	1266·9
$9/10$	11	T_{02}/T_2	1·1248
$(11)\gamma/\gamma-1$	12	P_{02}/P_2	1·5739
$1/12$	13	$1/P_{02}/P_2$	·63537
1 — 13	14	$1-1/P_{02}/P_2$	·36463
14 × (22 TABLE 4·3)	15	$Y_{TS}\left(1-\frac{1}{P_{02}/P_2}\right)$	·0486
1 + 15	16	$1+Y_{TS}\left(1-\frac{1}{P_{02}/P_2}\right)$	1·0486
$1/16$	17	P_{02}/P_{01}	·9536
10 + 6	18	T_{02R}	1286·2
$18/10$	19	T_{02R}/T_2	1·01521
$(19)\gamma/\gamma-1$	20	P_{02R}/P_2	1·0599
18 — 7	21	T_3	1169·9
$18/21$	22	T_{03R}/T_3	1·0994

TABLE 4.5 CONTINUED

$(22)^{\gamma}/_{\gamma-1}$	23	P_{O3R}/P_3	1.441
$1/23$	24	$1/P_{O3R}/P_3$	.6939
$1 - 24$	25	$1 - 1/P_{O3R}/P_3$	.3061
$25 \times (22.\ \text{TABLE } 4.4)$	26	$Y_{TR}\left(1 - 1/P_{O3R}/P_3\right)$	.0437
$1 + 26$	27	$1 + Y_{TR}\left(1 - 1/P_{O3R}/P_3\right)$	1.0437
$1/27$	28	P_{O3R}/P_{O2R}	.9581
$21 + 8$	29	T_{O3}	1187
$29/21$	30	T_{O3}/T_3	1.0146
$(30)^{\gamma}/_{\gamma-1}$	31	P_{O3}/P_3	1.0574
GIVEN	32	P_{O1}	33.49
32×17	33	P_{O2}	31.94
$33/12$	34	P_2	20.29
34×20	35	P_{O2R}	21.51
35×28	36	P_{O3R}	20.61
$36/23$	37	P_3	14.3
37×31	38	P_{O3}	15.12
$W \times 144 / 43 \times C_{A2}$	39	An_2	1117
$W \times 144 / 44 \times C_{A3}$	40	An_3	1387
$\sqrt{\frac{2}{\gamma-1}\left(\frac{T_{O2}}{T_2} - 1\right)}$	41	Mn_2	.845
$\sqrt{\frac{2}{\gamma-1}\left(\frac{T_{O3R}}{T_3} - 1\right)}$	42	Mn_3	.754
$144 \times 34 / R_G \times 10$	43	P_2	.0433
$144 \times 37 / R_G \times 21$	44	P_3	.033
$\lvert T_2 - T_3 \rvert / \lvert T_{O1} - T_{O3} \rvert$	45	R	.4

TABLE 4·6

VELOCITY TRIANGLE DATA AT VARIOUS RADII

DIA.	41	45·5	50	54·5	59
α_1	0	0	0	0	0
α_2	74·97	73·41	71·87	70·37	68·87
β_2	58·58	46·17	26·96	1·57	−22·56
β_3	63·17	65·50	67·48	69·17	70·64
α_3	0	0	0	0	0
C_{A2}	450	450	450	450	450
C_{A3}	475	475	475	475	475
U_2	939·2	1042·3	1145·4	1248·4	1351·5
U_3	939·2	1042·3	1145·4	1248·4	1351·5
$\cos\alpha_1$	1	1	1	1	1
$\cos\alpha_2$	·25932	·28557	·31119	·33615	·36042
$\cos\beta_2$	·52126	·69319	·89132	·99962	·92351
$\cos\beta_3$	·45131	·41469	·38308	·35560	·33157
$\cos\alpha_3$	1	1	1	1	1
C_1	450	450	450	450	450
C_2	1735·3	1575·8	1446	1338·7	1248·5
W_2	863·29	649·17	504·86	450·17	487·27
W_3	1052·5	1145·4	1239·9	1335·7	1432·5
C_3	475	475	475	475	475

TABLE 4·6

VELOCITY TRIANGLE DATA AT VARIOUS RADII

DIA.	41	45·5	50	54·5	59
α_1	0	0	0	0	0
α_2	74·97	73·41	71·87	70·37	68·87
β_2	58·58	46·17	26·96	1·57	−22·56
β_3	63·17	65·50	67·48	69·17	70·64
α_3	0	0	0	0	0
C_{A2}	450	450	450	450	450
C_{A3}	475	475	475	475	475
U_2	939·2	1042·3	1145·4	1248·4	1351·5
U_3	939·2	1042·3	1145·4	1248·4	1351·5
$\cos\alpha_1$	1	1	1	1	1
$\cos\alpha_2$	·25932	·28557	·31119	·33615	·36042
$\cos\beta_2$	·52126	·69319	·89132	·99962	·92351
$\cos\beta_3$	·45131	·41469	·38308	·35560	·33157
$\cos\alpha_3$	1	1	1	1	1
C_1	450	450	450	450	450
C_2	1735·3	1575·8	1446	1338·7	1248·5
W_2	863·29	649·17	504·86	450·17	487·27
W_3	1052·5	1145·4	1239·9	1335·7	1432·5
C_3	475	475	475	475	475

TABLE 4·7

STAGE THERMODYNAMIC PARAMETERS AT VARIOUS RADII

DIA.	41	45·5	50	54·5	59
θC_1	15·309	15·309	15·309	15·309	15·309
θC_2	227·65	187·73	158·09	135·48	117·85
θW_2	56·343	31·860	19·270	15·321	17·950
θW_3	83·745	99·189	116·237	134·893	155·155
θC_3	17·057	17·057	17·057	17·057	17·057
T_{01}	1425	1425	1425	1425	1425
T_2	1197·3	1237·3	1266·9	1289·5	1307·1
T_{02R}	1253·7	1269·1	1286·18	1304·8	1325
T_3	1169·9	1169·9	1169·9	1169·9	1169·9
T_{03}	1187	1187	1187	1187	1187
P_{01}	33·49	33·49	33·49	33·49	33·49
P_2	16·06	18·37	20·29	21·84	23·13
P_{02R}	19·18	20·29	21·51	22·80	24·38
P_{03R}	18·56	19·53	20·60	21·74	23·12
P_3	14·22	14·27	14·3	14·27	14·3
P_{03}	15·03	15·09	15·1	15·08	15·12
Mn_2	1·042	·931	·844	·755	·718
Mn_3	·640	·690	·753	·812	·871
R	·075	·283	·407	·502	·576
ρ_2	·03626	·0402	·0433	·0458	·048
ρ_3	·033	·033	·033	·033	·033

TABLE 4.8

STATOR BLADE DEVIATION

DIA.	GAS EXIT ANGLE	REQU. O/S	DEVIATION $\alpha_2 - \cos^{-1} O/S$
41	74.97	.2645	.31
45.5	73.41	.2856	0
50	71.87	.3090	−.138
54.5	70.36	.3301	−.366
59	68.87	.3492	−.69

TABLE 4.9

ROTOR BLADE DEVIATION

DIA.	GAS EXIT ANGLE	REQU. O/S	DEVIATION $\beta_3 - \cos^{-1} O/S$
41	63.172	.4324	−1.21
45.5	65.5	.4011	−.85
50	67.476	.3755	−.47
54.5	69.17	.3528	−.17
59	70.64	.3316	− 0

4.3 Comparison of Design Prediction and Test Results

Using the methods of this thesis, together with additional data relating pressure loss coefficient to incidence, the part load characteristics have been estimated for the turbine.

Figures 4.5, 4.6 and 4.7 are plots of total efficiency, static efficiency, dimensionless mass flow and dimensionless horsepower versus total to static expansion Ratio for $\frac{N}{\sqrt{T_{01}}}$ = 100%, as calculated. The additional points shown are test results.

Examination of these curves show that the turbine total and static efficiencies are approximately within ± 1% while the turbine capacity is approximately within ± 2%.

In obtaining the test results a calibrated water brake was used to measure power and an A.S.M.E. calibrated nozzle used to measure flow, therefore the only thermodynamic measurements used in estimating turbine efficiency are inlet pressure and exhaust pressure and temperature. It is estimated that the test accuracy is in the order of ± 2%.

Using the methods of this thesis to design single and multi stage units of various sizes and horsepowers has resulted in similar correlations and it is therefore concluded that for subsonic turbines, within the limitations given in the body of this report, the simplifications used in describing the flow through a turbine stage are acceptable.

FIGURE 4·5

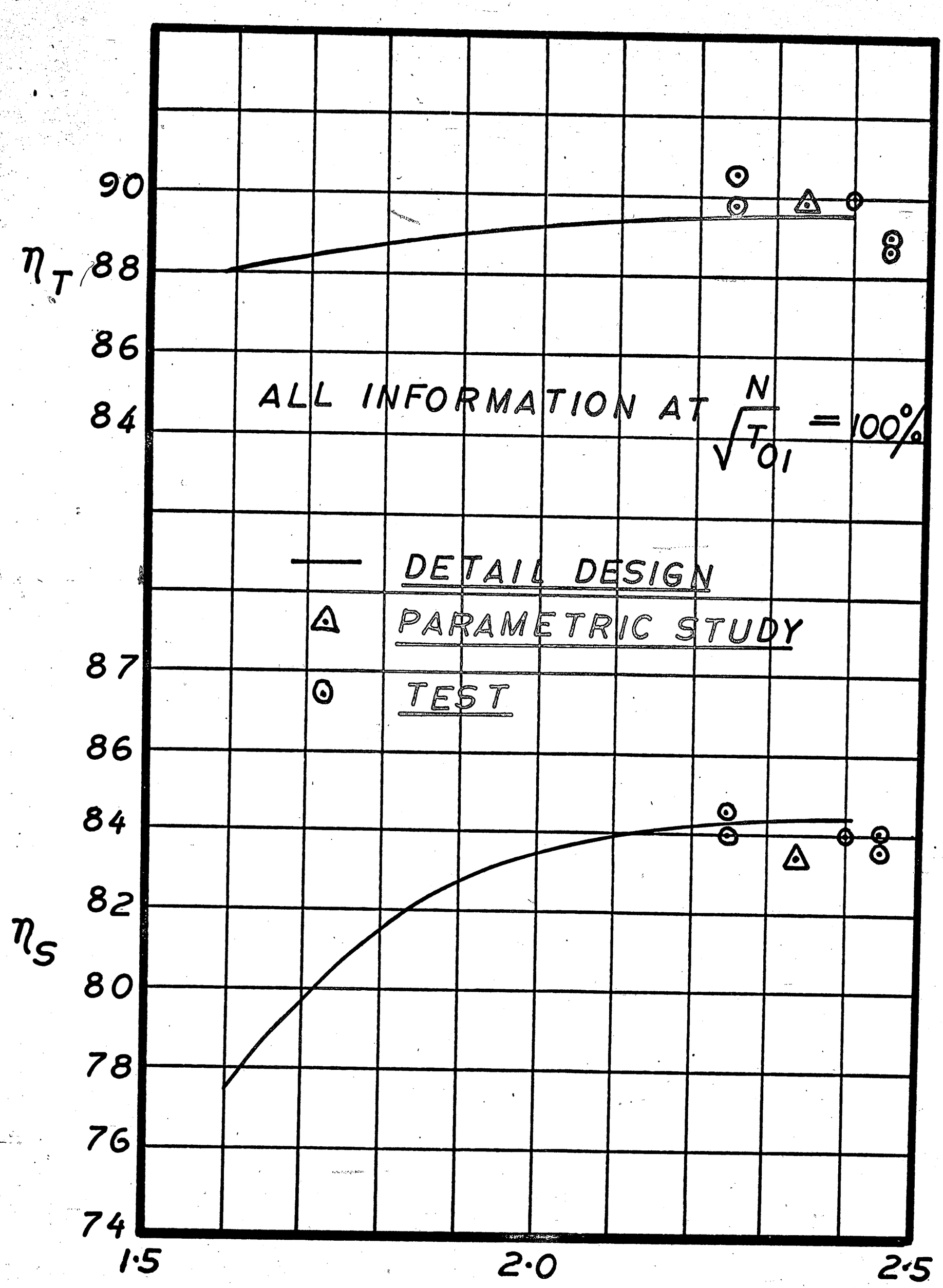
90
88
86
84
82
80
78
76
74
η_T
η_S
ALL INFORMATION AT $\frac{N}{\sqrt{T_{01}}} = 100\%$
DETAIL DESIGN
PARAMETRIC STUDY
TEST
8
1·5
2·0
2·5
$\frac{P_{01}}{P_3}$

FIGURE 4.6

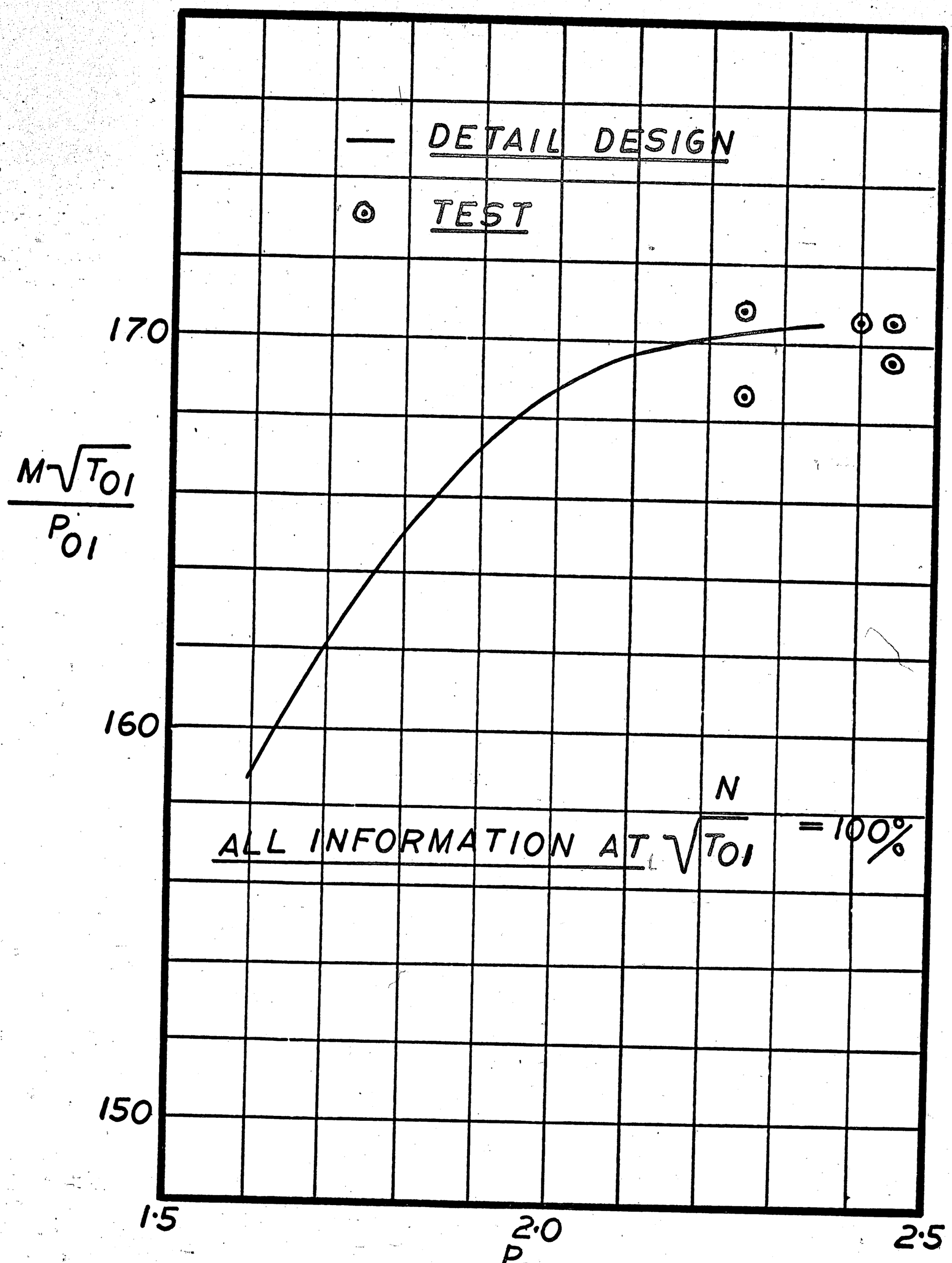
— DETAIL DESIGN
o TEST
170
160
150
$\frac{M\sqrt{T_{01}}}{P_{01}}$
ALL INFORMATION AT $\frac{N}{\sqrt{T_{01}}}$ = 100%
1·5
2·0
2·5
$\frac{P_{01}}{P_3}$

FIGURE 4·7

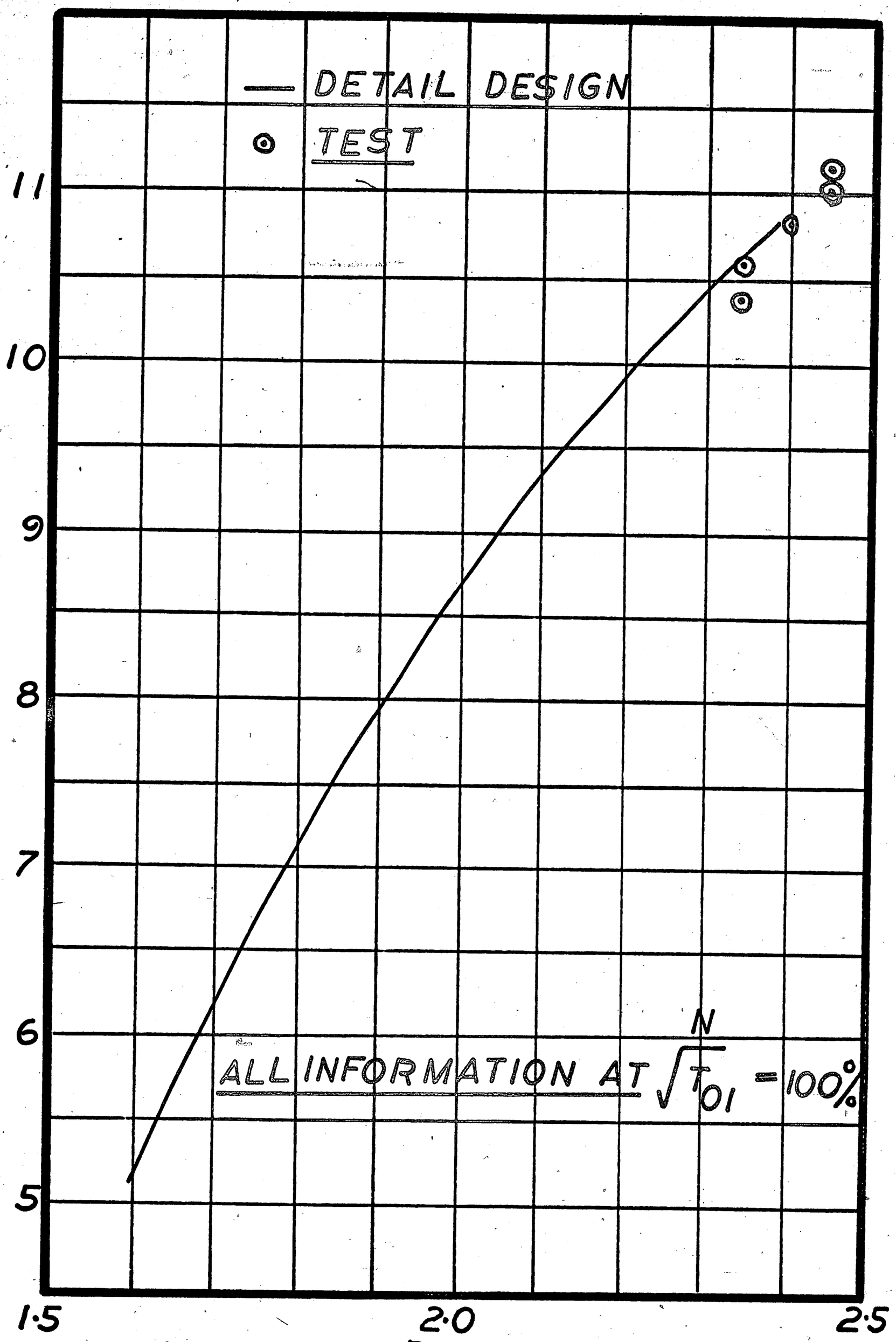
— DETAIL DESIGN
TEST
11
10
9
8
7
6
5
BHP / P01√T01
ALL INFORMATION AT √(T01/T01)N = 100%
1·5
2·0
2·5
P01 / P3

References

1. Ainley, D. G. & Mathieson, G.C.R. A Method of Performance Estimation for Axial Flow Turbines. Report No. R111. Pyestock, Hants, England: National Gas Turbine Establishment. December, 1951.

2. Vavra, M. H. Aero Thermodynamics and Flow in Turbomachines. New York, London: John Wiley & Sons, Inc., 1960.

3. Traupel, W. Thermische Turbomachinen. Berlin/ Gottingen/Heideiberg: Springer-Verlag, 1958.

4. Owczarek, J. A. Fundamentals of Gas Dynamics. Scranton, Pennsylvania: International Texbook Company, 1964.

5. Horlock, J. H. Axial Flow Turbines. London: Butterworths, 1966.

6. Golomb, M. & Shanks, M. Elements of Ordinary Differential Equations. New York: McGraw-Hill, Inc., 1965.

7. Stenning, A. H. Fluid Mechanics Applied to Turbo Machinery, Lecture Notes taken at Graduate Turbo Machinery Course delivered at Lehigh University, 1967.

8. Zweifel, O., The Spacing of Turbomachine Blading, Especially with Large Angular Deflection, Brown Boveri Review, 1945.

VITA

Born in Rochdale, England on April 15th, 1926, Leslie Fielding attended Derby Technical College, Wigan Technical College, and Wolverhampton and Staffordshire Technical College from which he was awarded the Higher National Certificate in Mechanical Engineering in 1950.

Upon leaving College Mr. Fielding was employed by Rolls Royce Ltd. as a gas turbine design engineer first on mechanical design and subsequently on turbine blading design. He performed further blade and disk design at Bristol Aero Engines Ltd.

In 1957 Mr. Fielding joined Clark Brothers, Olean, N.Y. as a gas turbine design engineer responsible for turbine hot end stressing and aerodynamics. He was promoted to head of the Stress Analysis and Dynamics Group in 1961.

In 1963 Mr. Fielding joined Ingersoll-Rand Company in the capacity of Senior Designer in a newly formed Gas Turbine Group where he was responsible for turbine thermodynamics and stress analysis. He was promoted to Supervisor of the Analytical Group in 1967.

Mr. Fielding is a member of the American Society of Mechanical Engineers, the Institution of Mechanical Engineers and the British Nuclear Energy Society. He is married to the former Ida Smith and they have three children, two boys and one girl.